

# POLITECNICO DI TORINO

## Automotive Engineering

### Master degree in Propulsion Systems Development

“Headform impact test” under ECE R043 regulation: analysis and processing of data on dedicated program developed to calculate the HIC index and several correlate results.



Academic Tutor: Prof. Belingardi Giovanni  
Company Tutors: Eng. Bocchino Marco  
Eng. Filippa Paolo

Candidate:  
Ricci Paolo

Date:

# CONTENTS

---

Abstract.....	9
1 INTRODUCTION.....	10
1.1 Automotive crash avoidance and crashworthiness .....	10
1.2 Consumer automotive safety information.....	10
1.3 Crash tests and the head injury criterion (HIC) .....	12
2 OVERVIEW OF THE HEAD INJURY CRITERIA.....	14
2.1 THIV – Theoretical Head Impact Velocity.....	15
2.2 PHD – Post-Impact Head Deceleration.....	15
2.3 ASI - Acceleration Severity Index .....	16
2.4 Relation between ASI, THIV, and PHD index .....	17
2.5 AIS - Abbreviated Injury Scale.....	18
2.6 GSI - Gadd Severity Index.....	20
2.7 WSTC – Wayne State Tolerance Curve.....	20
2.8 HIC – Head Injury Criterion .....	23
2.9 Correlation between HIC and AIS .....	25
2.10 Correlation between ASI and HIC .....	26
2.11 CLASSIFICATION BETWEEN THE PREVIOUS INDEXES.....	27
3 HEAD INJURY MECHANISM .....	29
3.1 Biomechanical principles .....	29
3.2 Injury mechanism.....	30
3.3 Analysis of experimental data on Brain and skull trauma .....	36
4 TESTS IN “CSI-SPA AUTOMOTIVE DIVISION” FACILITIES.....	41
4.1 General Test Conditions – ECE R043 Regulations .....	41
4.1.1 Apparatus .....	41
4.1.2 Test conditions.....	44
4.1.3 Adjustment and calibration.....	44
4.1.4 Supporting fixture for testing flat test pieces.....	48
4.1.5 Procedure .....	48
4.1.6 Evaluation .....	48
4.2 Results of headform calibration .....	49
4.3 Execution of Headform impact test.....	52

4.3.1	Explanation of HIC calculation through dedicated MATLAB program\code .....	52
4.4	results .....	56
4.4.1	Results of the tests on the first type of plastic compound glass .....	56
4.4.2	Results of the tests on the second type of plastic compound glass .....	69
4.5	Discussion of results .....	82
4.5.1	Analysis of first sample – type one .....	83
4.5.2	Analysis of second sample – type one .....	84
4.5.3	Analysis of third sample – type one .....	85
4.5.4	Analysis of first sample – type two .....	86
4.5.5	Analysis of second sample – type two .....	87
4.5.6	Analysis of third sample – type two .....	88
5	CONCLUSIONS .....	89
6	REFERENCES .....	93
7	APPENDIX .....	102
7.1	Matlab computation Code .....	102
7.2	Technical characteristic of the PCB accelerometer used in the tests .....	106

## List of Acronyms

- THIV : Theoretical Head Impact Velocity
- PHD: Post-Impact Head deceleration
- ASI : Acceleration Severity Index
- AIS : Abbreviated Injury Scale
- GSI : Gadd Severity Index
- WSTC: Wayne State Tolerance Curve
- HIC : Head Injury Criterion

## List of Figures

Figure 1: Example of Euroncap crash tests comparison.....	12
Figure 2: Example of crash test with dummies.....	13
Figure 3: Scheme of driver occupant position in a car .....	14
Figure 4: The scalp, skull, meninges and brain scheme .....	22
Figure 5: The Wayne state tolerance curve .....	22
Figure 6: Distorted waveform each of which have the same HIC.....	24
Figure 7: Correlation between HIC and AIS .....	25
Figure 8: Relation between HIC and ASI index .....	27
Figure 9: Injury criteria for assessing occupant injury risk for a motor vehicle crash test.....	27
Figure 10: Fracture mechanism of the base of the skull .....	29
Figure 11: Fracture mechanism of an impression fracture of the skull .....	30
Figure 12: Applied force on the fibres.....	31
Figure 13: Applied force in function of time .....	31
Figure 14: Illustration of mechanical properties: elasticity, viscosity, plasticity and visco-elasticity .....	31
Figure 15: Illustration of how the impact duration affects the peak acceleration necessary to induce a given amplitude level of response .....	33
Figure 16: Wayne State Tolerance Curve.....	34
Figure 17: Tolerance curve constructed from NASA .....	34
Figure 18: Mechanics of head injury .....	35
Figure 19: Skull fracture data .....	36
Figure 20: Brain damage data .....	37
Figure 21: Predicted cumulative distribution curves of threshold HIC values for cadaver skull fracture.....	39
Figure 22: Predicted cumulative distribution curves of threshold HIC values for cadaver brain damage. ....	40
Figure 23: 10 kg headform.....	41
Figure 24 : 10,2 kg headform used in the tests .....	43
Figure 25: Test apparatus for the headform experiment with deceleration measurement .....	44
Figure 26: Support for headform tests .....	45
Figure 27: Support for headform tests used.....	45
Figure 28: PCB triaxial accelerometer used in the tests .....	47
Figure 29: Results of 50mm drop height .....	49
Figure 30: Results of 150mm drop height .....	50
Figure 31: Results of 100mm drop height .....	50
Figure 32: Results of 254mm drop height .....	51
Figure 33: Deceleration curve along x axis .....	56
Figure 34: Deceleration curve along y axis .....	56
Figure 35: Deceleration curve along z axis .....	57
Figure 36: Total resultant deceleration curve .....	57

Figure 37: Head impact force .....	58
Figure 38: HIC vs (t2-t1) .....	58
Figure 39: HIC surface .....	59
Figure 40: HIC surface .....	59
Figure 41: Deceleration curve along x axis .....	60
Figure 42: Deceleration curve along y axis .....	60
Figure 43: Deceleration curve along z axis .....	61
Figure 44: Total resultant deceleration curve .....	61
Figure 45: Head impact force .....	62
Figure 46: HIC vs (t2-t1) .....	62
Figure 47: HIC surface .....	63
Figure 48: HIC surface .....	63
Figure 49: Deceleration curve along x axis .....	64
Figure 50: Deceleration curve along y axis .....	64
Figure 51: Deceleration curve along z axis .....	65
Figure 52: Total resultant deceleration curve .....	65
Figure 53: Head impact force .....	66
Figure 54: HIC vs (t2-t1) .....	66
Figure 55: HIC surface .....	67
Figure 56: HIC surface .....	67
Figure 57: Deceleration curve along x axis .....	69
Figure 58: Deceleration curve along y axis .....	69
Figure 59: Deceleration curve along z axis .....	70
Figure 60: Total resultant deceleration curve .....	70
Figure 61: Head impact force .....	71
Figure 62: HIC vs (t2-t1) .....	71
Figure 63: HIC surface .....	72
Figure 64: HIC surface .....	72
Figure 65: Deceleration curve along x axis .....	73
Figure 66: Deceleration curve along y axis .....	73
Figure 67: Deceleration curve along z axis .....	74
Figure 68: Total resultant deceleration curve .....	74
Figure 69: Head impact force .....	75
Figure 70: HIC vs (t2-t1) .....	75
Figure 71: HIC surface .....	76
Figure 72: HIC surface .....	76
Figure 73: Deceleration curve along x axis .....	77
Figure 74: Deceleration curve along y axis .....	77
Figure 75: Deceleration curve along z axis .....	78
Figure 76: Total resultant deceleration curve .....	78
Figure 77: Head impact force .....	79
Figure 78: HIC vs (t2-t1) .....	79
Figure 79: HIC surface .....	80
Figure 80: HIC surface .....	80

Figure 81: AIS and HIC correlation of the first sample - type one .....	83
Figure 82: ASI and HIC relation of the first sample - type one.....	83
Figure 83: AIS and HIC correlation of the second sample - type one.....	84
Figure 84: ASI and HIC relation of the second sample - type one.....	84
Figure 85: AIS and HIC correlation of the third sample - type one .....	85
Figure 86: ASI and HIC relation of the third sample - type one .....	85
Figure 87: AIS and HIC correlation of the first sample - type two .....	86
Figure 88: ASI and HIC relation of the first sample - type two .....	86
Figure 89: AIS and HIC correlation of the second sample - type two.....	87
Figure 90: ASI and HIC relation of the second sample - type two.....	87
Figure 91: AIS and HIC correlation of the third sample - type two .....	88
Figure 92: ASI and HIC relation of the third sample - type two .....	88
Figure 93: Distorted waveforms each of which have the same maximum HIC .....	90
Figure 94: Distorted waveforms each of which have the same maximum HIC .....	90
Figure 95: Illustration of the biomechanics of an oblique impact (lower), compared to a corresponding perpendicular one (upper), when impacted against the same padding using an identical initial velocity of 6.7 m/s.....	91

## List of Tables

Table 1: Tolerable acceleration limits .....	17
Table 2: Impact severity levels according to EN 1317 .....	18
Table 3: Abbreviated Injury Scale .....	19
Table 4: Head Injury Criterion Threshold related to time window and dummy type ..	24
Table 5: List of pieces for the 10kg headform.....	43
Table 6: Greatest deceleration $a_z$ as a multiple of acceleration due to gravity $g$ in function of the drop height.....	46
Table 7: Numerical results of headform calibration .....	51
Table 8: Numerical results of the three sample - type one .....	68
Table 9: Numerical results of the three sample - type two .....	81
Table 10: Technical characteristic of the PCB accelerometer used in the tests .....	106
Table 11: Technical characteristic of the PCB accelerometer used in the tests .....	107
Table 12: Technical characteristic of the PCB accelerometer used in the tests .....	108
Table 13: Technical characteristic of the PCB accelerometer used in the tests .....	109

# ABSTRACT

---

First of all, I would like to make a premise regarding the reasons that led me to choose the theme of my thesis. Let me start by explaining that I have a particular passion for what concerns the real world of automobiles and this led to the choice of my study at the Polytechnic of Turin in the specific field of automotive engineering.

I developed my master thesis thanks to an internship conducted at the company “CSI Automotive division”, an IMQ Group that allowed me to grow and immerse myself in the working world.

The analysis that I carried out at this company is the result of a discussion with the engineers of the CSI (Marco Bocchino and Paolo Filippa and subsequently approved by my academic tutor Giovanni Belingardi) regarding customer orders.

In particular, I conducted the test and successively an analysis of the headform impact test on two different types of plastic compound glass, directly in the CSI Automotive Division facilities.

Then, I developed a program with the MATLAB software to implement the data collected during the test in order to obtain the results requested by the client.

After the test, I tried to speed up and generalize the program in order to make it useful for different tests.

In conclusion, I compared and analysed the results of the program output.

# 1 INTRODUCTION

---

## 1.1 AUTOMOTIVE CRASH AVOIDANCE AND CRASHWORTHINESS

Automotive crashes are very complex events that result from the interaction of driver behaviour, the driving environment and vehicle design. Authorities agree that driver error or incorrect driver behaviour is the main factor affecting the probability of being in a crash. Human characteristics, such as age and state of health, also affect the possibility of surviving crash injuries. The predominance of the human factor in crash relationship does not reduce the important effect of vehicle design and safety features on crash likelihood. It must be said that drivers cannot change their age or control the driving behaviour of others, but they can decide which automobile to buy and try to select the safest vehicle that will meet their needs and minimize crash chance and injury potential.

The safety of the vehicle is affected in two ways:

- It helps the driver avoid a crash or recover from a driving error (crash avoidance);
- It provides protection from injury during a crash (crashworthiness);

Characteristics such as vehicle stability and braking performance affect the likelihood of being in a crash, all else being equal. However, the driver plays a more important role in determining the extent to which these crash avoidance features reduce crash possibility. During a crash, vehicle characteristics that contribute to crashworthiness, such as size and weight, how the vehicle absorbs energy, and restraint system characteristics, play a large role in determining the probability and degree of occupant injury.

Due to the close coupling of vehicle characteristics and vehicle crashworthiness, the automotive safety research program has given top priority to research on measures for improving vehicle crashworthiness. Many standards have been developed and injury moderation measures introduced, such as air bags, which have been incorporated into vehicles.

[1,2]

## 1.2 CONSUMER AUTOMOTIVE SAFETY INFORMATION

Significant information is available to consumers regarding vehicle safety. The agency with statutory authority to provide consumer automotive safety information, provides comparative data on the crashworthiness of vehicles in the same class from full-frontal crash tests conducted in its New Car Assessment Program; the insurance industry publishes information on injury complaint and death rates by vehicle brand and model

and provides relative data on vehicle crashworthiness. Therefore, some information on vehicle safety is available to help consumers compare products when shopping.

It is interesting to remark that current safety information has numerous limitations:

- The information is partial and hard for consumers to collect in any summary valuation and comparison of the performance of different vehicles.
- Results of crash test can be compared only among vehicles in the same size and weight class.
- The repeatability of crash test results is a problem. Only one test per vehicle is conducted because of the cost of testing. Thus, the range of variance in test scores is not well recognized.
- Crash tests that are focused on frontal impact cannot provide a comprehensive representation of vehicle crashworthiness given the real-world variation in crash configurations and speeds. In fact, crash test performance is highly correlated with real-world crash variants, which reflect driver characteristics and so, it is difficult to separate the vehicle from driver characteristics.

In conclusion, progress has been made in vehicle safety, in particular the behaviour of vehicles in accidents and the problems that cause injuries. Some of this information has been made available to consumers in a form that enables comparisons of vehicle safety performance and characteristics.



*Figure 1: Example of EURONCAP crash tests comparison*

[1,2]

### **1.3 CRASH TESTS AND THE HEAD INJURY CRITERION (HIC)**

Opportunely, nowadays many consumers pay more attention to the safety of their automobile and crash tests (Fig. 2) can give valuable indications on advantages or disadvantages of construction.

A index, called HIC, head injury criterion, is an analytical tool usually used in tests, reports and comparisons to evaluate the head injury risk. In crash situations, the load on the head results from too high negative acceleration (deceleration) values during the crash. Construction features such as collapse zones and airbags are employed to extend the period of braking on the driver's body and so decreasing the deceleration during the crash below dangerous threshold. The dummies used in crash tests have numerous sensors fixed to the head zone, which capture the value of the deceleration in function of time. So, the injury risks to the head in contact with various locations of the vehicle including the windscreen and its frame were studied on the basis of headform impact tests.

The injury value is calculated from measurements of accelerations obtained from humans and crash test dummies. Tests must be executed to validate and calibrate the

correlation between an injury index and the risk of an injury of a specified severity under certain experiment conditions.



*Figure 2: Example of crash test with dummies*

[3,4,11]

## 2 OVERVIEW OF THE HEAD INJURY CRITERIA

---



*Figure 3: Scheme of driver occupant position in a car*

Head injury is one of the most frequent causes of mortality and disability of users involved in road accidents. The occupants of a car involved in a crash, even if belted, could undergo oscillatory movements such as to push their head against the airbags, the dashboard, the uprights, the crystals, the roof.

In case of people investment, their head could initially impact the bonnet, the windshield, the uprights and subsequently, against the asphalt or other elements of the roadway.

The head is a very complex system consisting of three components such as the skull box, the skin and other soft tissues covering the skull. In particular, the skull performs the function of energy absorption as a natural mechanism, in fact, the creation of some small fracture of the skull does not cause brain injury and therefore its presence is precisely aimed at protecting the internal brain area by diffusing and dissipating energy shock.

The lesions to the box involve the breaking of one or more bones of the skull while those of the internal organs of the brain are the result of an impact of the head, of its abrupt movement or of a combination of the two processes. One must keep in mind that when

the head hits an obstacle, its movement stops, however, the organs inside it continue in their inertial movement, generating possible intracranial lesions.

Head injury can generally be defined as temporary or permanent damage to one or more components of the skull and brain system following a headshot. In general, four categories can be grouped under the heading of head injury, such as damage to the scalp, skull fracture, brain injury and neck injuries.

The biomechanical reconstruction of a harmful event must first determine the cause (from contact or acceleration) and the type of lesions. The different quantitative criteria for the performance of injuries have been developed to provide an answer, in terms of risk to life or injuries and using crash tests with anthropomorphic dummies.

[5,6,11]

## 2.1 THIV – THEORETICAL HEAD IMPACT VELOCITY

The index THIV (Theoretical Head Impact Velocity) represents the value of the theoretical velocity wherewith the head of the occupant collides against the first rigid element that is along its path in the cockpit.

This index is expressed by the relation:

$$THIV = \sqrt{V_x^2(t_1) + V_y^2(t_1)} \quad (1)$$

In which  $V_x$  and  $V_y$  are the components in the vehicle coordinate system of the head's velocity in the instant  $t_1$  in which the head hits against the nearest cockpit surface.

[7,8,9]

## 2.2 PHD – POST-IMPACT HEAD DECELERATION

The index PHD (Post-impact Head deceleration) represents the value of the maximum resultant deceleration in the origin of the local vehicle reference calculated as the average on 10 ms period of the two components  $\ddot{x}_c$  and  $\ddot{y}_c$  in the consecutive instants at time  $t_1$ .

This index is expressed by the relation:

$$PHD = MAX \left( \sqrt{(\ddot{x}_c(t))^2 + (\ddot{y}_c(t))^2} \right) \quad (2)$$

With  $t > t_1$ .

[1,2,9,10]

### 2.3 ASI - ACCELERATION SEVERITY INDEX

The Acceleration Severity Index (ASI) is used to calculate the potential risk for occupants in crash tests relating to the roadside safety.

Using measured vehicle information, the ASI index is computed with the following equation:

$$ASI(t) = \sqrt{\left(\frac{\bar{a}_x}{\hat{a}_x}\right)^2 + \left(\frac{\bar{a}_y}{\hat{a}_y}\right)^2 + \left(\frac{\bar{a}_z}{\hat{a}_z}\right)^2} \quad (3)$$

With  $\bar{a}_x$ ,  $\bar{a}_y$ ,  $\bar{a}_z$  :

$$\bar{a}_x = \frac{1}{\delta} \int_t^{t+\delta} a_x dt \quad (4)$$

$$\bar{a}_y = \frac{1}{\delta} \int_t^{t+\delta} a_y dt \quad (5)$$

$$\bar{a}_z = \frac{1}{\delta} \int_t^{t+\delta} a_z dt \quad (6)$$

With the time interval  $\delta = 50 \text{ ms}$ ,

And with  $\hat{a}_x$ ,  $\hat{a}_y$ ,  $\hat{a}_z$  equal to the corresponding accelerations limit for each component. The limits of the accelerations are 12 g, 9 g and 10 g for the longitudinal (x), lateral (y), and vertical (z) directions, respectively.

So the ASI index equation becomes:

$$ASI(t) = \sqrt{\left(\frac{\bar{a}_x}{12g}\right)^2 + \left(\frac{\bar{a}_y}{9g}\right)^2 + \left(\frac{\bar{a}_z}{10g}\right)^2} \quad (7)$$

It must be noted, that it uses only vehicle accelerations. The maximum ASI value during the duration of the vehicle deceleration gives a single measurement of crash severity that is supposed to be proportional to occupant risk. To offer an assessment of occupant probable risk, the ASI value for a given crash acceleration pulsation is related to established limit values.

The table below shows the tolerable acceleration limits in different restraint configurations:

Restraint	Maximum Acceleration (G)		
	Longitudinal	Lateral	Vertical
Unrestrained	7	5	6
Lap Belt Only	12	9	10
Lap and Shoulder Belt	20	15	17

*Table 1: Tolerable acceleration limits*

[8,9, 13-30, 116-126]

## 2.4 RELATION BETWEEN ASI, THIV, AND PHD INDEX

The EN 1317 is the official reference for testing and discriminant criteria of road restraint systems. Through the ASI, THIV and PHD index, it is possible to evaluate the differences of road restraint systems in respect to others and in particular, knowing the ASI index, it is possible to interpolate the crash tests to injury severity levels A or B as can be seen in table 2.

Impact severity level	Index values		
A	ASI $\leq$ 1,0	and	THIV $\leq$ 33 km/h PHD $\leq$ 20 g
B	ASI $\leq$ 1,4		
<p>Note 1: Impact severity level A affords a greater level of safety for the occupants of an errant vehicle than level B, and is preferred when other considerations are the same.</p> <p>Note 2: At specific hazardous locations where the containment of an errant vehicle (such as a heavy goods vehicle) is the prime consideration, a vehicle restraint system with no specific impact severity level may need to be adopted and installed.</p>			

*Table 2: Impact severity levels according to EN 1317*

[8,9, 13-30, 116-133]

## 2.5 AIS - ABBREVIATED INJURY SCALE

The AIS system was created from the need to standardize the description of the lesions, according to the classification system, and to graduate them on a certain gravity scale.

The guiding role in the creation and development of the system has been carried out by the American Association for the Advancement of the Automotive Medicine through its "Committee for the Graduation of Injuries". The latest version published in 1998 includes more than 1300 codes for the description of individual lesions.

The AIS is at the same time a dictionary of codes for the description of lesions and a scale of gravity. This system is based on anatomy and is the result of consensus among experts.

The lesions are then classified according to the body region and graded according to an ordinal gravity scale with relative scores.

It is worth noting that AIS is not a system of systematic evaluation of the traumatized, but takes into account only the severity of the individual lesions. Therefore, it is not able to take into account the combined effects of multiple injuries.

The AIS system is extremely expensive in terms of information requirements because it is based on the description of very detailed clinical conditions and requires that these are proven by clinical reports or specific investigations such as, for example, those of diagnostic imaging techniques. Furthermore, the coding of the lesions, since it requires precise knowledge of anatomy and physio-pathology, in addition to the knowledge of the coding rules of the system, must be carried out by specially trained qualified staff.

Table (3), shows the relation between AIS level, max linear acceleration, category of the injury and the description of the injuries.

<b>AIS level</b>	<b>Max linear acceleration</b>	<b>Category</b>	<b>Injuries description</b>
<b>0</b>	< 50 g	No injury	Light brain injuries with headache, vertigo, no loss of consciousness, light cervical injuries, whiplash, abrasion, contusion.
<b>1</b>	50 - 100 g	Minor	Concussion with or without skull fracture, less than 15 minutes unconsciousness, tiny corneal cracks, detachment of retina, face or nose fracture without shifting.
<b>2</b>	100 - 150 g	Moderate	Concussion with or without skull fracture, more than 15 minutes unconsciousness without severe neurological damages, closed and shifted or impressed skull fracture without unconsciousness or other injury indications in skull, loss of vision, shifted and/or open face bone fracture with antral or orbital implications, cervical fracture without damage to spinal cord.
<b>3</b>	150 – 200 g	Serious	Closed and shifted or impressed skull fracture with severe neurological injuries.
<b>4</b>	200 – 250 g	Severe	Concussion with or without skull fracture with more than 12 hours unconsciousness with haemorrhage in skull and/or critical neurological indications.
<b>5</b>	250 – 300 g	Critical	Death, partial or full damage of brainstem or upper part of cervical, due to pressure or disruption, fracture and/or wrench of upper part of cervical with injuries to spinal cord.
<b>6</b>	> 300 g	Non – survivable \ fatal	Light brain injuries with headache, vertigo, no loss of consciousness, light cervical injuries, whiplash, abrasion, contusion.

*Table 3: Abbreviated Injury Scale*

[23, 13-30, 116-125]

## 2.6 GSI - GADD SEVERITY INDEX

The first model used in practice to describe the risk of the injury in a crash through a number was the Gadd Severity Index GSI. By correlating the severity of injury with time and deceleration upon impact, it was able to produce a relatively simple formula to derive an index of survivability from head injuries. The deceleration was considered at a power  $n$ , whose value depended on the part of the body, based on empirical experience.

For the head,  $n = 2.5$  was selected.

In mathematical formulation, the GSI has been defined as :

$$GDI = \int_0^T a(t)^n dt \quad (8)$$

with  $n = 2.5$ , and with  $T$  equal to the total period of the deceleration that has an influence on the head. The confirmation of the model was not satisfactory for the comparison between different types of cars and different crash situations.

To overcome this problem, the HIC index was formulated, the Head Injury Criterion index.

[13-30,127]

## 2.7 WSTC – WAYNE STATE TOLERANCE CURVE

The origin of the head injury criterion (HIC) are based on the so-called "Wayne State University Cerebral Concussion Tolerance Curve" which delivered a boundary between a "safe" head response and an "unsafe" head response (figure 5). The curve was originally a plot of "effective head acceleration" in function of time duration.

The whole acceleration-time tolerance curve for cerebral concussion due to frontal impacts was constructed by combining data from various sources. Cadaver skull fracture data anchored the short duration end of the curve below 6 milliseconds. Some clinical experience had revealed that a modest concussion usually accompanies a linear skull fracture. On that basis, it had been rationalized that for the short time duration of the curve, cadaver skull fracture would be associated with living cerebral concussion.

Experimental concussion pressure-time relationships developed with dogs, along with head acceleration-pressure data obtained from a series of cadaver drop tests onto automobile dash panels. These were used to construct the intermediate time domain of the curve up to ten milliseconds.

The validity of this tolerance curve has been questioned on the following reasons:

- The ordinate's "effective" acceleration was not well defined. It is currently regarded as the time average acceleration.
- The head impact data is not applicable to blows other than those to which the experimental animals and cadavers were subjected.
- Some of the original data from which the curve was constructed was misplotted while other data points were simply omitted.
- The short time duration portion of the Wayne State curve was based upon the measurement of the acceleration of a point on the skull of a cadaver head opposite the forehead blow location.
- The Wayne State curve has never been verified for living human beings other than for the very long duration impulses by which volunteers have been subjected to sub-injurious events.

So, the factors that would appear to limit the applicability of the Wayne State tolerance curve are :

- It is not clear what the acceleration measurements were.
- The data even if unclear is applicable only to the experimental conditions under which the tests were conducted.
- The significant characteristics of the skull, sheds considerable doubt on the validity of acceleration measurements for pulses whose contact time is less than about 10 milliseconds.
- For pulses of longer duration (more than 15 milliseconds) the concussion aspect of the curve has been refuted by one of its principal proponents who considered it non reliable.

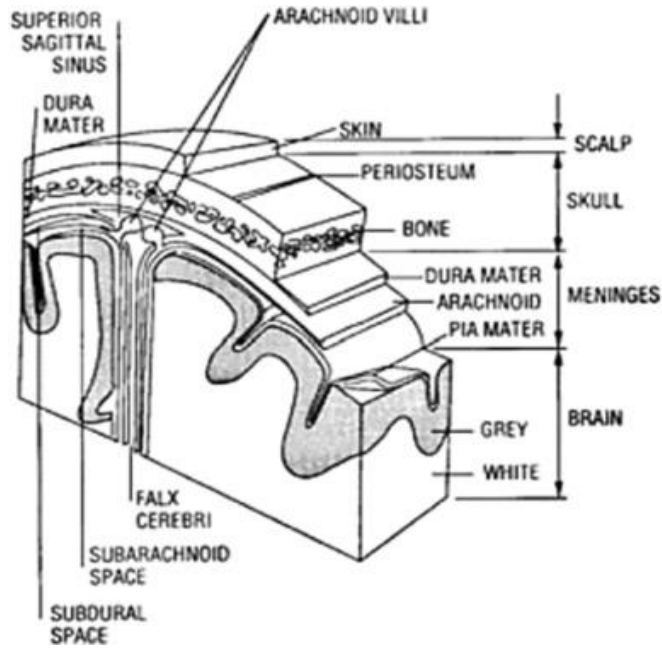


Figure 4: The scalp, skull, meninges and brain scheme

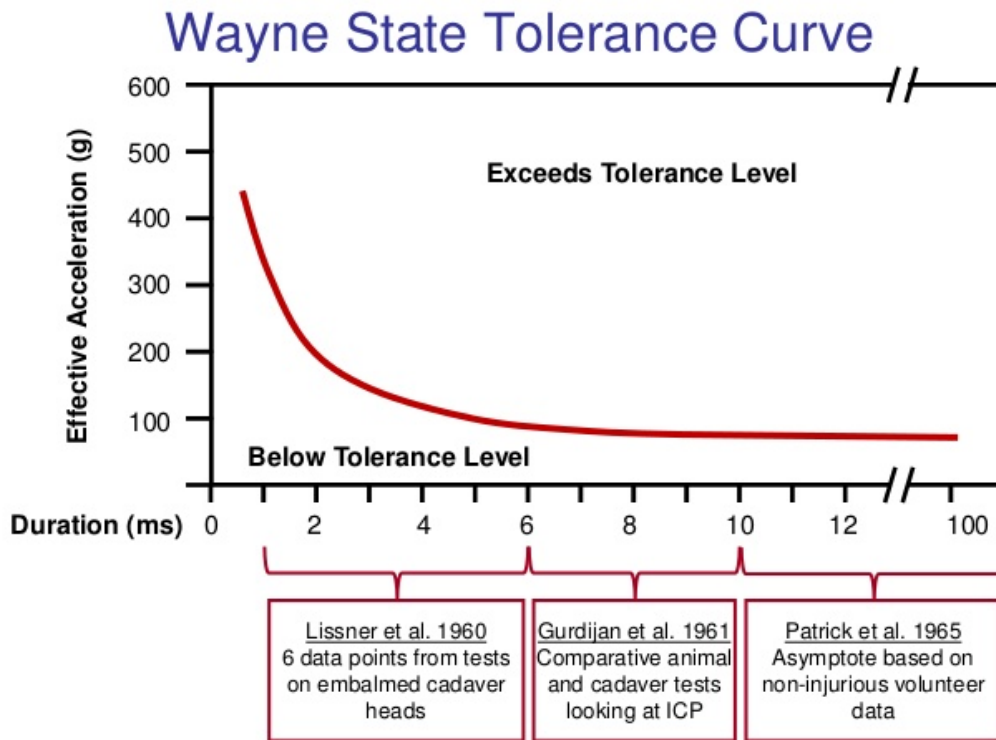


Figure 5: The Wayne state tolerance curve

[23,24,127-133]

## 2.8 HIC – HEAD INJURY CRITERION

The Gadd Severity Index is used and recommended as threshold criterion for frontal impacts; when the National Highway Traffic Safety Administration (NHTSA) adopts the GSI, the acceleration is redefined imposing it to be equal to the resulting acceleration, keeping the limit value. Changing the GSI formula leads to the definition of the Head Injury Criterion.

The free motion headform head injury criterion HIC is calculated in accordance with the following formula:

$$HIC = \max \left\{ (t_2 - t_1) \left[ \frac{1}{(t_2 - t_1)} \int_{t_1}^{t_2} a(t) dt \right]^{2,5} \right\} \quad (9)$$

*with  $(t_2 - t_1) \leq 36$  milliseconds*

Where:

- " $a(t)$ " is the resultant acceleration expressed as a multiple of the acceleration of gravity (g).
- " $t_2$ " and " $t_1$ " are any two points in time during the period of head impact which are separated by not more than a 36 millisecond time interval selected so as to maximize HIC.

It should be remarked that the head injury criterion is an empirical formulation founded upon experimental work. This criterion can be valid only if the following statements are verified:

- The experimental data upon which it is based is accurate.
- The experimental data should reflect human resistance to impact.
- The approximation to the experimental data incorporated in the regulation is accurate.
- The range of application of this formulation does not surpass that confirmed by experimental data.

Therefore, the head injury criterion can be effective only if human head injury phenomena are related to:

- The linear acceleration of the centre of gravity of the headform test device.
- Dependence of the time of the linear acceleration.

Old regulation revised by NHTSA related to the head injury criteria specify the threshold of the HIC index in function of the time window and the dummy type as can be seen in Table 4.

Dummy Type	Large sized Male	Mild-sized Male	Small sized female	6-Year-old Child	3-Year-old Child	1-Year-old infant
$HIC_{15}$ Threshold	700	700	700	700	570	390
$HIC_{36}$ Threshold	1000	1000	1000	1000	-	-

Table 4: Head Injury Criterion Threshold related to time window and dummy type

It is important to remark that, as has been pointed out by Chou and Nyquist, the  $HIC_{max}$  is independent of the skewness (and hence of rate of onset) for a pulse. The  $HIC_{max}$  is determined by evaluating the area bounded by the acceleration pulse during a specific time interval,  $\Delta T_{HIC_{max}}$ . Hence, all  $a(t)$  curves bounded by the same  $\Delta T_{HIC_{max}}$ , having the same area, will have the same  $HIC_{max}$ .  $HIC_{max}$  is determined by evaluating an area not a curve shape. The  $HIC_{max}$  is thus independent of curve shape and hence of rate of change of acceleration.

All the pulse shapes shown in Figure 6 have the same maximum acceleration, time averaged acceleration, the same severity index and the same total pulse duration. The results is that all these pulse shape have the same tolerable  $HIC_{max}$ .

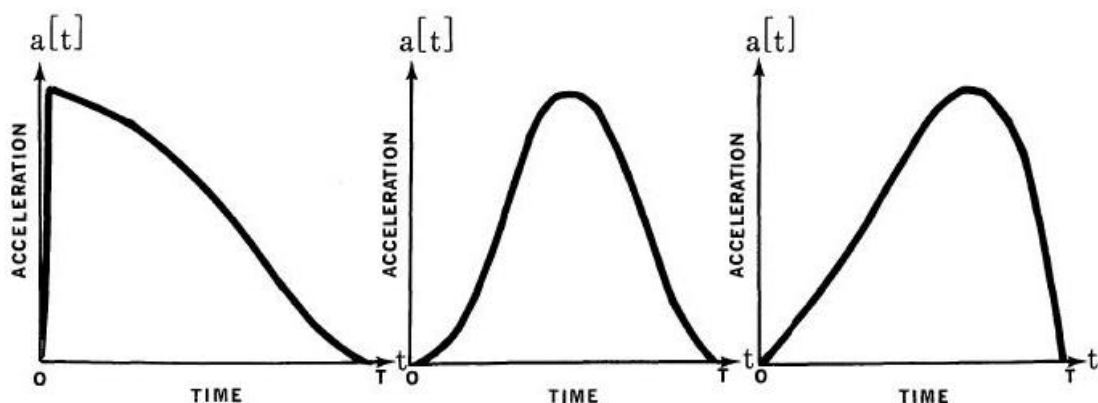


Figure 6: Distorted waveform each of which have the same HIC

[8,9,13-133]

## 2.9 CORRELATION BETWEEN HIC AND AIS

It is generally recognized that the concept of either a "safe" head impact or an "unsafe" impact is an inadequate scale of measurement. Investigators in this field have thus adopted the concept of a degree or level of head injury severity and attempted to correlate with kinematic parameters that were carried out. The usual severity scale is that of the so-called abbreviated injury scale (AIS).

One of the most extensive and detailed examinations of brain injury measurements and head motion parameters was undertaken by Mucciardi. Here an analysis of experimental head impact data was performed, to try to demonstrate that kinematic waveforms did contain information relating to head and brain injuries and that analysis techniques did exist that could properly exploit this information to create injury predictive functions.

Their experimental database consisted of 26 monkey head impacts, which had been performed by other investigators. Translational and rotational acceleration time histories of the head were available. Parameters computed from these kinematic waveforms were the input variables to an analysis technique. The output variable was the experimentalist's evaluation of the severity of the injuries.

Based on many post mortal experiments (experiments with dead bodies) a correlation between HIC and AIS has been developed. It should be noted that the following correlation is based on only head-on impact tests.

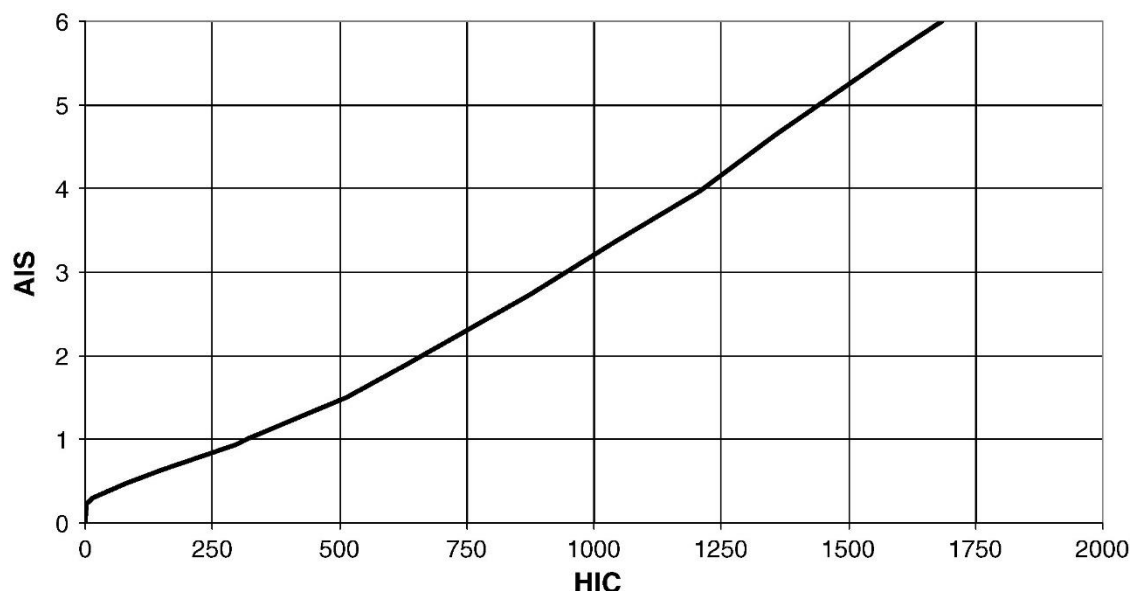


*Figure 7: Correlation between HIC and AIS*

[8, 13-30, 116-133]

## 2.10 CORRELATION BETWEEN ASI AND HIC

In published literature there are only three studies regarding the correlation between ASI and HIC:

- Shojaati works on the correlation between ASI, HIC and vehicle occupants injury risk;
- Sturt and Fell analysed the relationship between injury risk and impact severity in collisions with safety barriers;
- Klootwijk and Hoogvelt, used a multi-body simulation program to analyse the sensitivity of injuries to some parameters in car-guardrail collisions.

In the first study, nine side impact crash tests with a Hybrid III dummy were performed, measuring the ASI and then determining the corresponding head injury criterion (HIC).

The results suggest an exponential relationship between HIC and ASI. For ASI values lower than 1.0, the HIC value is below 100. For ASI values between 1.5 and 2.0 estimated values for HIC were between 350 and 1000. Due to the limited number of tests conducted, the correlation between ASI and HIC was only calculated on an approximate basis.

Sturt and Fell executed three crash tests with anthropometric test device equipped vehicles and ran 50 computer simulations. The results confirmed the existence of a correlation between the measured head and neck injury marks using anthropometric test device based injury criteria (in particular HIC) and the accident severity as estimated with the EN1317 vehicle-based injury criteria (ASI and THIV). According to this study, the neck and head are the body regions more vulnerable to harm in safety barrier impacts.

According to Sturt and Fell, the boundary as defined in EN 1317 for impact severity levels B (ASI greater than 1.0 and not more than 1.4) and C (ASI greater than 1.4 and not more than 1.9) does not match any significant increase in injury risk. Also according to the same authors, the threshold value established in EN1317 for THIV (below 33 km/h) is, by itself, reasonable: below this value, it is unlikely that significant injuries may be inflicted.

As in the study by Shojaati, the results obtained by Sturt and Fell suggest an exponential relationship between HIC and ASI. However, the values obtained by Shojaati are significantly greater than those estimated by Sturt and Fell for HIC (Figure 8).

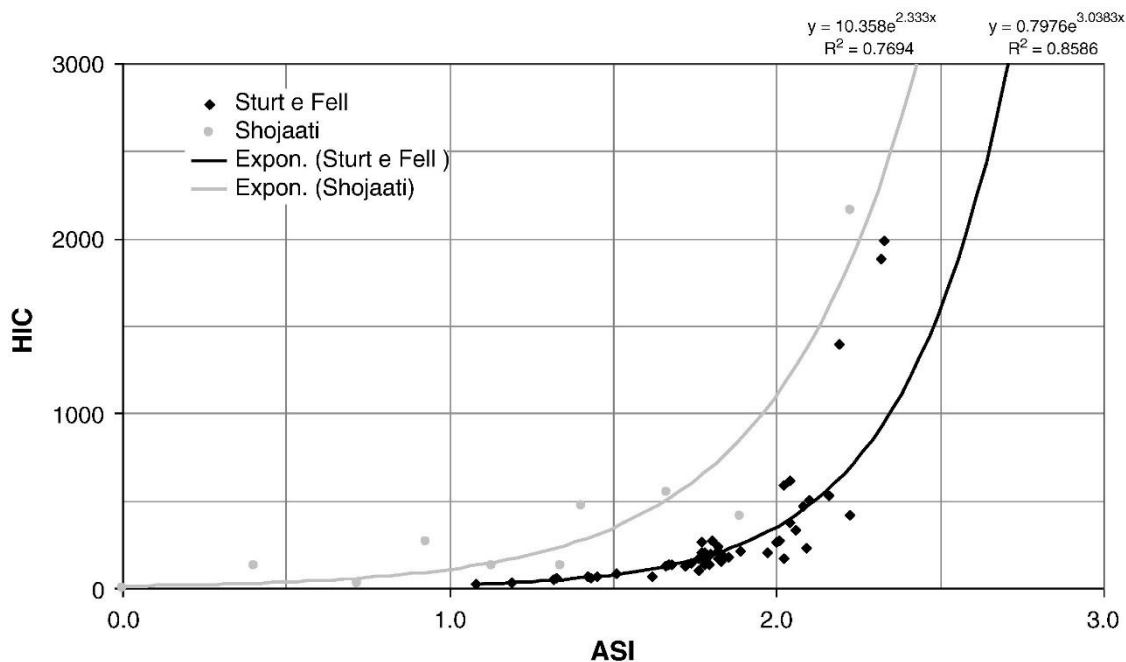


Figure 8: Relation between HIC and ASI index

[8,13-30, 116-133]

## 2.11 CLASSIFICATION BETWEEN THE PREVIOUS INDEXES

Through figure 9 the different injury indexes and their classifications can be seen.

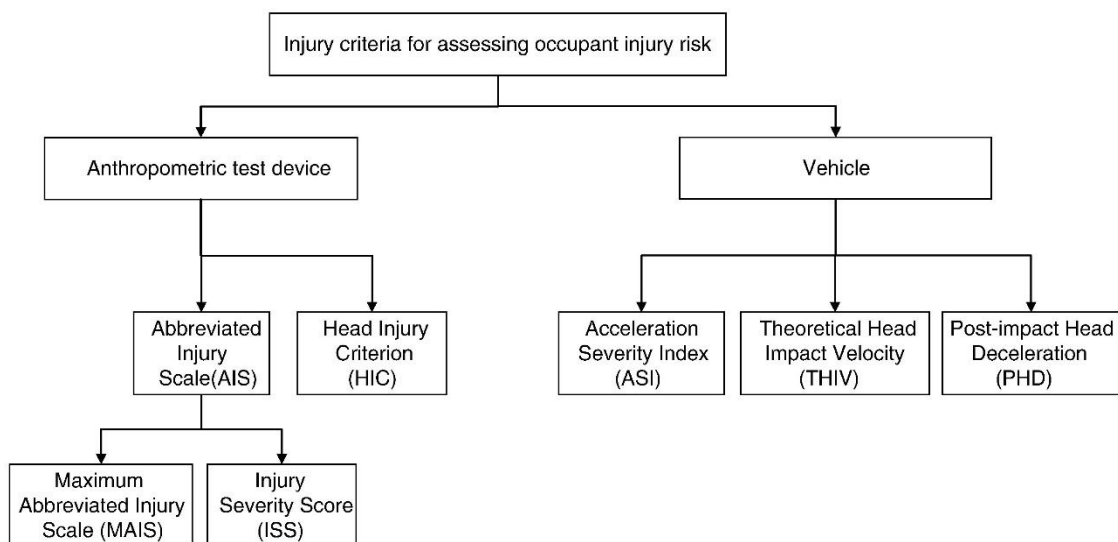


Figure 9: Injury criteria for assessing occupant injury risk for a motor vehicle crash test

An anthropometric testing device is based on the dummy used in a crash test to simulate the injury of a human being, designed to evaluate injury potential in a repeatable way. The instrumented device that simulate the human being collect data, like velocity, acceleration and displacement, with the aim of estimation of injury potential during the crash impact phase.

On the other hand, Vehicle-based injury criteria are based on theoretical indicators that define occupant injury potential established only on the response of the vehicle during the crash impact phase. These criteria are largely used for the evaluation of the risk assessment through non-dummy prepared vehicle crash tests like safety barriers.

[8,13-30, 116-133]

## 3 HEAD INJURY MECHANISM

---

### 3.1 BIOMECHANICAL PRINCIPLES

The biomechanical principles of the head injuries is the most important area of knowledge that contributes to the prevention of head injuries. Deceleration occurring during the crash can cause intracranial damage. The mechanisms of the injury are directly linked with linear and angular acceleration.

When dealing with head injuries from a biomechanical point of view, some particular parts of the anatomy of the head are worthy of attention:

One of the five layers of the scalp, the aponeurotic layer consists of compressed fibrous tissue and is liberally movable over the skull. This movability enables tangential blows to the head to slide off. On the other hand, the looseness of the sub-aponeurotic layer consent the formation of enormous hematomas after tears in the connecting blood vessels between scalp and skull.

The cranial vault is a rigid vessel composed of several bones, each with its own unique internal and external geometry. It encloses the brain, and avoids local deformation of the brain at the impact site. The skull in turn protects the scalp. It has been estimated that the scalp yields a forty-fold increase of the skull fracture tolerance level. The cerebrospinal fluid hold shock absorbing properties: a liquid produces uniform pressure without shearing stress to any surface it contacts. Therefore, the cerebrospinal fluid distributes any concentrated external pressure to a uniform stress, which is better tolerated by neural tissues.

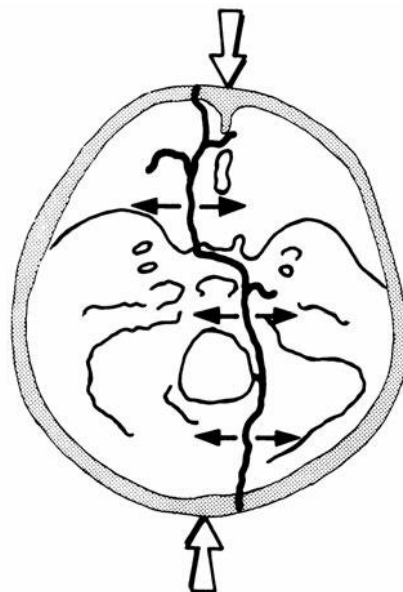


*Figure 10: Fracture mechanism of the base of the skull*

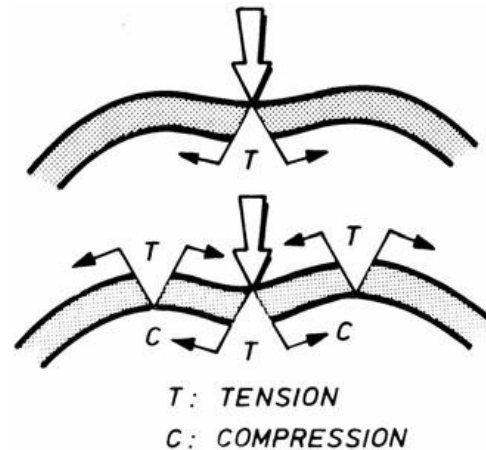


Figure 11: Fracture mechanism of an impression fracture of the skull

Head linear acceleration does not produce any noteworthy mass movement of the brain but yields negative pressure, which causes an excessive cohesive strength of the brain tissue, thereby causing cavitation of the cerebral parenchyma. Head impact commonly produces, not only linear acceleration but also angular acceleration that causes distortion of the brain tissue. Holbourn, that studied these phenomena, suggests that brain injury is produced by shear strains due to brain distortion following angular acceleration of the head. In a traumatic situation, the distortion of about one centimetre is sufficient to produce mechanical failure, thereby providing a traumatic mechanism.

In summary, the impact response of the head will be described in terms of its acceleration responses to prescribed impact conditions and/or the interaction forces that occur between the head and the contact surface for the prescribed impacts. Both of these impact response parameters are dependent on the head's mass, its mass distribution, the dynamic force-deformation characteristics of the skull and the soft flesh covering the skull, and on the location and direction of the impact force. Determination of the head's acceleration response is particularly important since most head injury criteria are based on measured head accelerations.

[12, 134-139]

### 3.2 INJURY MECHANISM

The primary cause of dysfunction and structural failure as a result of external forces acting on the human body is the relative displacement of adjacent body tissues and this in turn causes their deformation. In Figure 12 we can see that the relative displacement is illustrated by a series of fibres deformed by a force that has a proper direction and a specific point where it acts. The deformation can be defined by the total distances of the

displacement in three dimensions in function of time. The deformations are represented by the strains and the forces acting within a material are called stresses. The link between the external loading force and the resulting stresses and strains within a body is dependent upon the mechanical properties of the fibres as sketched in Figure 14.

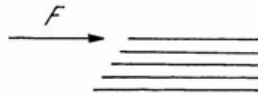


Figure 12: Applied force on the fibres

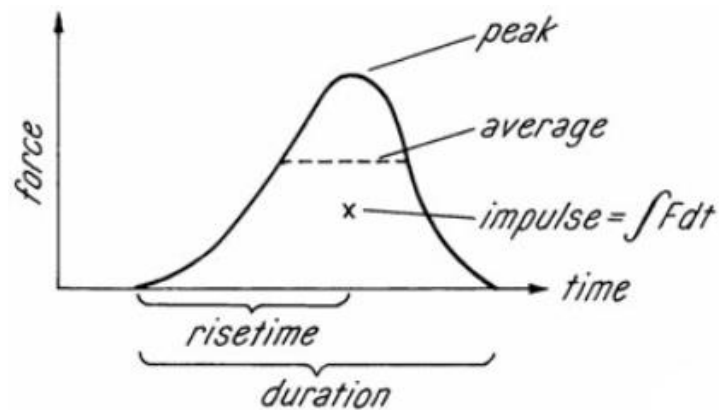


Figure 13: Applied force in function of time

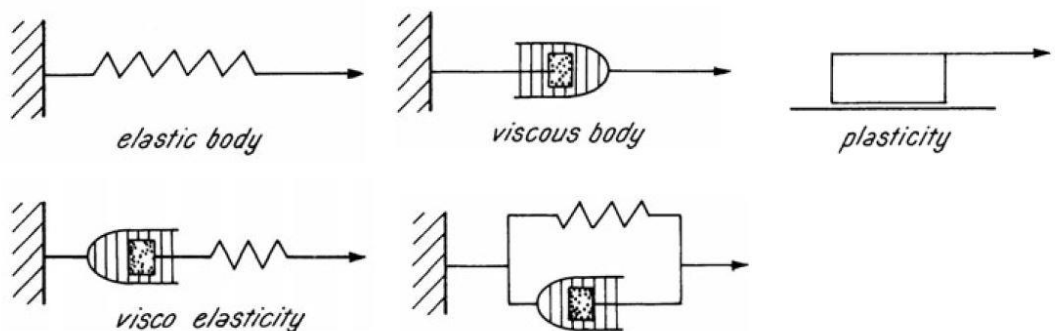


Figure 14: Illustration of mechanical properties: elasticity, viscosity, plasticity and visco-elasticity

The mechanical properties and the geometrical characteristics of a structure become critical for its lowest frequency when they reach their natural frequency. The duration of one oscillation is indicated with the “natural period”. The ratio between the duration of the loading and the natural period, represents the most important character for the magnitude of internal displacement and so, the degree of damage.

Different critical parameters can be distinguished depending on this ratio (as can be seen in Figure 15):

- If this ratio is lower than one: the same impulse will result in the same injury even if for instance the maximum force and acceleration will change over a wide range.
- if this ratio is higher than one: the same maximum force or acceleration will produce the same injury even if the impulse and duration will vary over a wide range.
- If this ratio is approximately one: neither the impulse nor the maximum force alone can characterize the sensitivity.

The complete force-time function must be considered. In real head injury crashes and in experimental impacts the duration of the loading is in the same range as the natural periods of the structures involved. For the brain of an animal or man, natural frequency is about 10-30 Hz and the natural period is about 30-100 milliseconds.

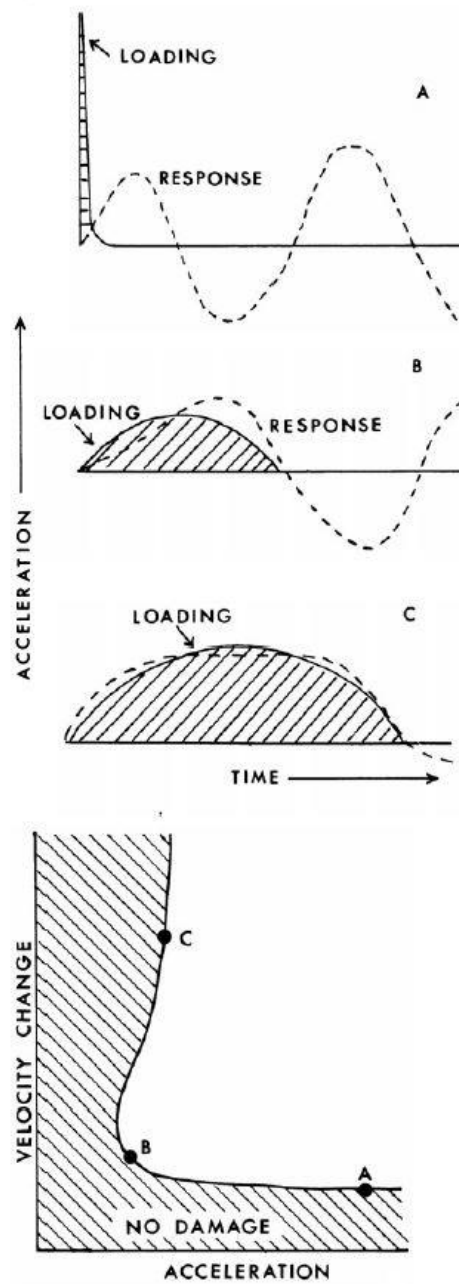


*Figure 15: Illustration of how the impact duration affects the peak acceleration necessary to induce a given amplitude level of response*

In Figure 16 and 17, we can see the so called Wayne State University Tolerance Curve and the tolerance curve obtained from NASA in 1959.

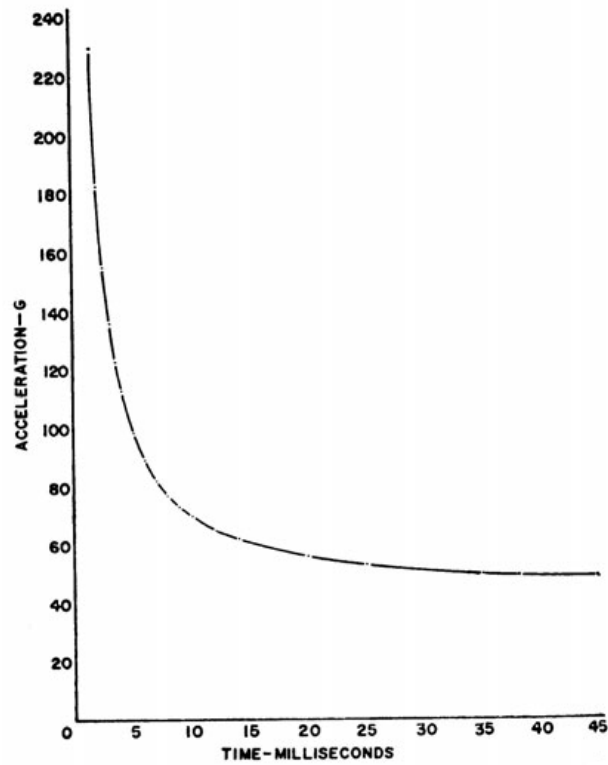


Figure 16: Wayne State Tolerance Curve

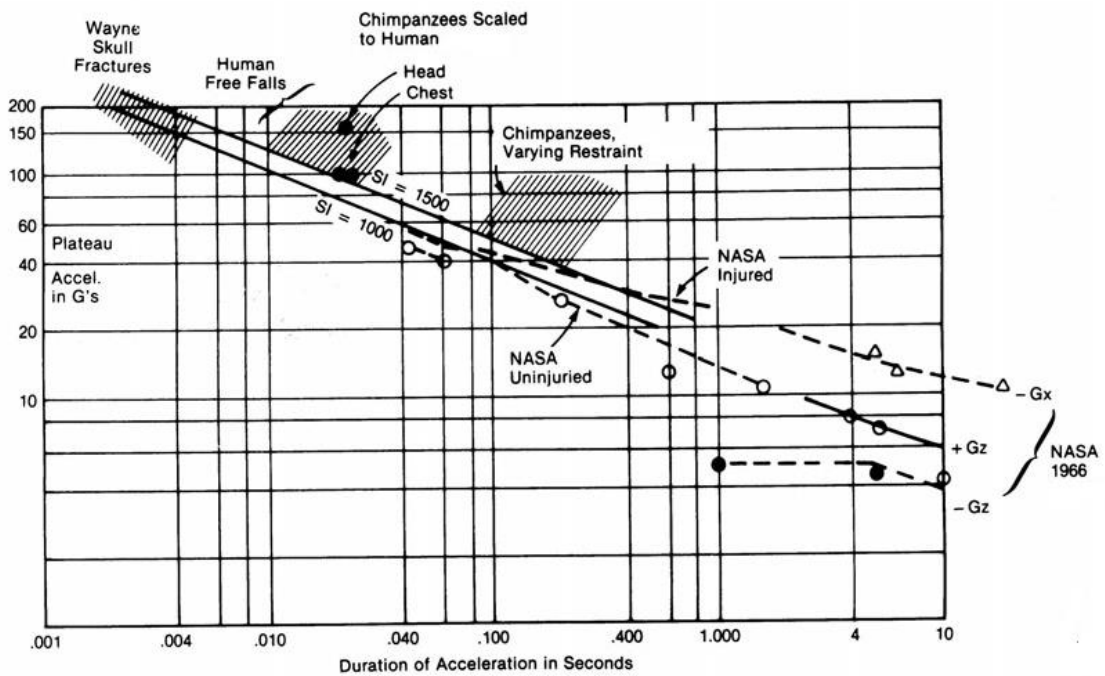


Figure 17: Tolerance curve constructed from NASA

More in detail, head injuries can be divided into three categories based on the type of load application and its time history as can be seen in Figure 18:

- **Impact load:** It is a collision of the head and a solid object at a high velocity. A "hard" impact will last about 1 - 3 milliseconds. A less hard impact will last about 5 - 15 milliseconds and a softer impact will last about 20-30 milliseconds.
- **Impulsive load:** The head is set in sudden motion without direct physical contact. Such a load may be in the range 50-200 milliseconds.
- **Compressive load:** A particular load has a duration higher than 200 milliseconds. Such a load may be denoted static or quasi static and consequences due to speed of load application may be totally neglected.

These three types of mechanical loading will engage diverse physical phenomena. It has to be remarked that these types of loading usually occur at the same time and their relative significance for production of injury is difficult to distinguish. In each case, to understand the physical processes that involve head injuries it is useful to consider these three main types of loading and their mechanical and biological effects separately. This is the approach taken into account by many investigators of head injury mechanisms.

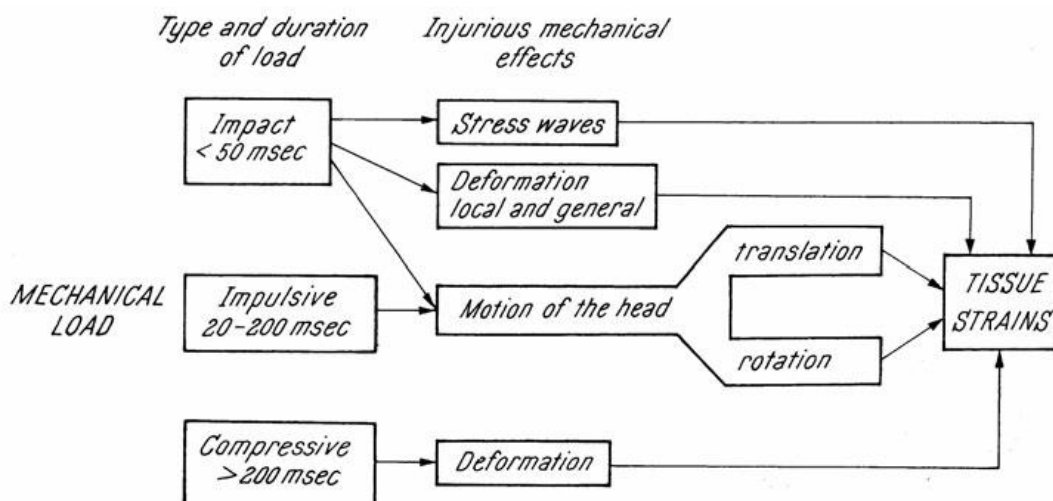


Figure 18: Mechanics of head injury

[12, 134-139]

### 3.3 ANALYSIS OF EXPERIMENTAL DATA ON BRAIN AND SKULL TRAUMA

The head injury criterion (HIC) is considered a good predictor of brain concussion that can be used for all types of impacts to the head, independent of a kind of crash or location. It is evaluated for flat object and also for blunt objects to assess diffuse brain injuries.

Due to the varying strength of the skull, the head injury criterion tolerance level can vary at different impact locations around the head, being potentially lower in the lateral direction to the frontal. But due to difficulties in assessing exactly the location and acceleration direction, it is proposed to use the same tolerance levels for any direction of impact.

An analysis of existing cadaver head crash data can be conducted taking into account some parameters used to quantify and predict the head damage. When revising all the literature, it can be noted that the major studies on human skull and brain damages are conducted by Got, Tarriere, Nahum, Smith and Hodson. These have all collected data on the impact test using human cadavers.

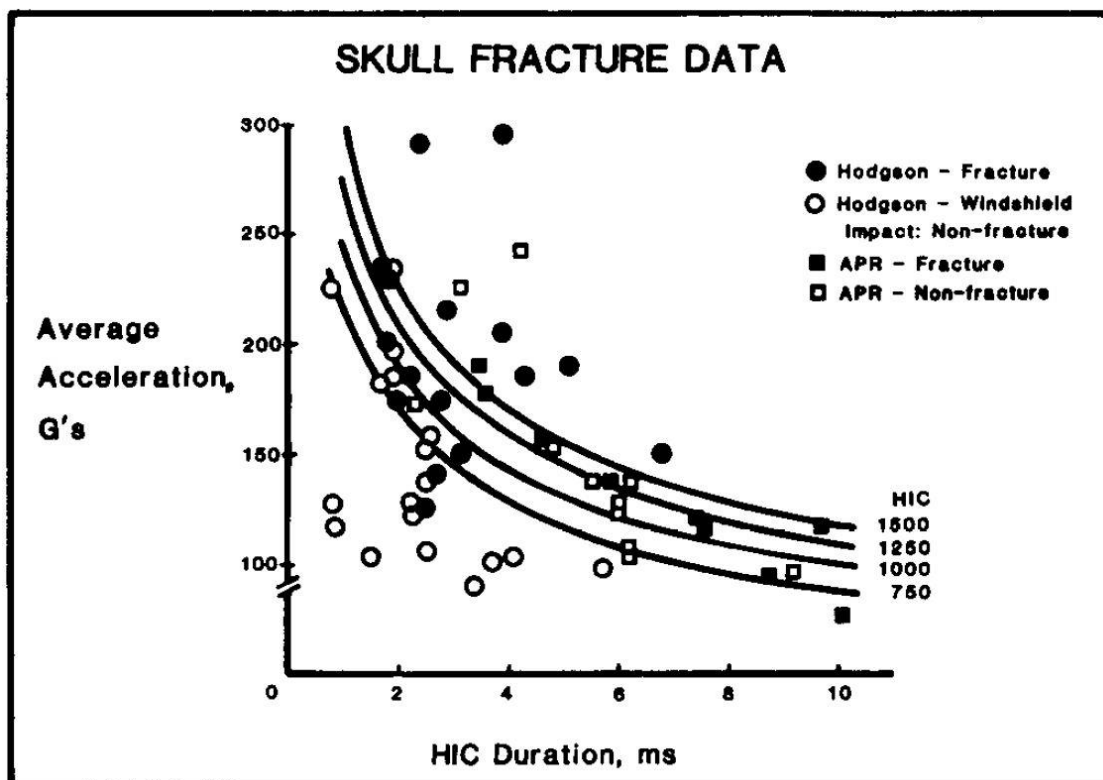


Figure 19: Skull fracture data

Despite there were many doubts with the relation and tolerance between human and cadaver test data, many studies use these data because they are considered the best available tests for making such inferences. The skull fracture collected data are based on the cadaver head drop tests on flat and rigid surfaces, cadaver sled tests against surfaces and helmeted cadaver drop tests. The data of these tests are the results of 54 cadaver head impact plotted in function of HIC duration (Figure 19).

The brain damage data is based on fresh cadaveric specimens whose average brain pressures were re-established through the re-pressurization with fluids in the arteries leading to the brain (Figure 20).

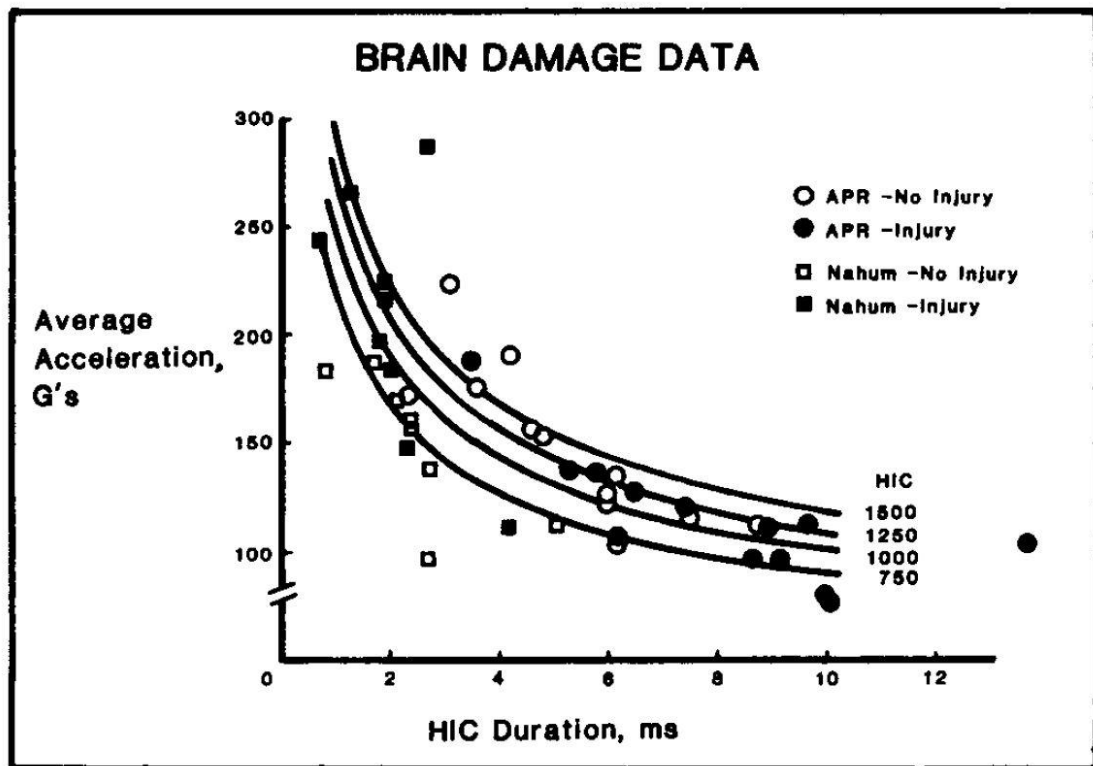


Figure 20: Brain damage data

Note that, as we wanted to prove, for both Figure 19 and 20, there is a trend of increasing frequency of skull and brain damage with the increase of HIC magnitude.

For HIC duration lower than 15 milliseconds, the trend of the results that follow the constant HIC curves in Figure 19 and 20 are consistent with the Wayne State Tolerance Curves. It can be seen that the average tolerable acceleration increases with the continuous decrease of HIC duration. On the contrary, the HIC relations is deficient for average acceleration with the HIC duration higher than 15 milliseconds. In effect, if we calculate an average deceleration of 1 g applied for 1000 seconds, the formulation of HIC gives a HIC index of 1000. For this reasons, to avoid errors, it was decided to limit

the calculation of HIC only in the portion of the resultant head deceleration – time history during the impact.

In Figure 21 and 22, we can be seen three different types of resulting cumulative distribution curve regarding skull fracture and brain damage.

A first approximation of the cumulative distribution curve of the limit of HIC values is evaluated assuming a linear relation. Of consequence, the curve is constructed by connecting the two extreme points, assuming one point equal to zero percent of the injured specimens and another point equal to one hundred percent of the highest measured response value of the non-injured specimens. For this reasons, this curve is called “linear method”.

Mertz and Weber outline other methods for the constructing of the cumulative distribution curve if one assumes that the threshold values are normally distributed.

Ran et el. proposed to use other methods taking into account the maximum likelihood technique in order to select appropriate 3-parameter Weibull distributions for skull and brain damage databases. The resulting cumulative distributions curves in Figure 21 and 22 show the inability of this technique in providing a good approximation of the actual threshold curve.

The U.S. Advisory Group decided to use the cumulative distribution curves constructed by Mertz and Weber as their best method to estimate the risk curves for skull fracture and brain damage.

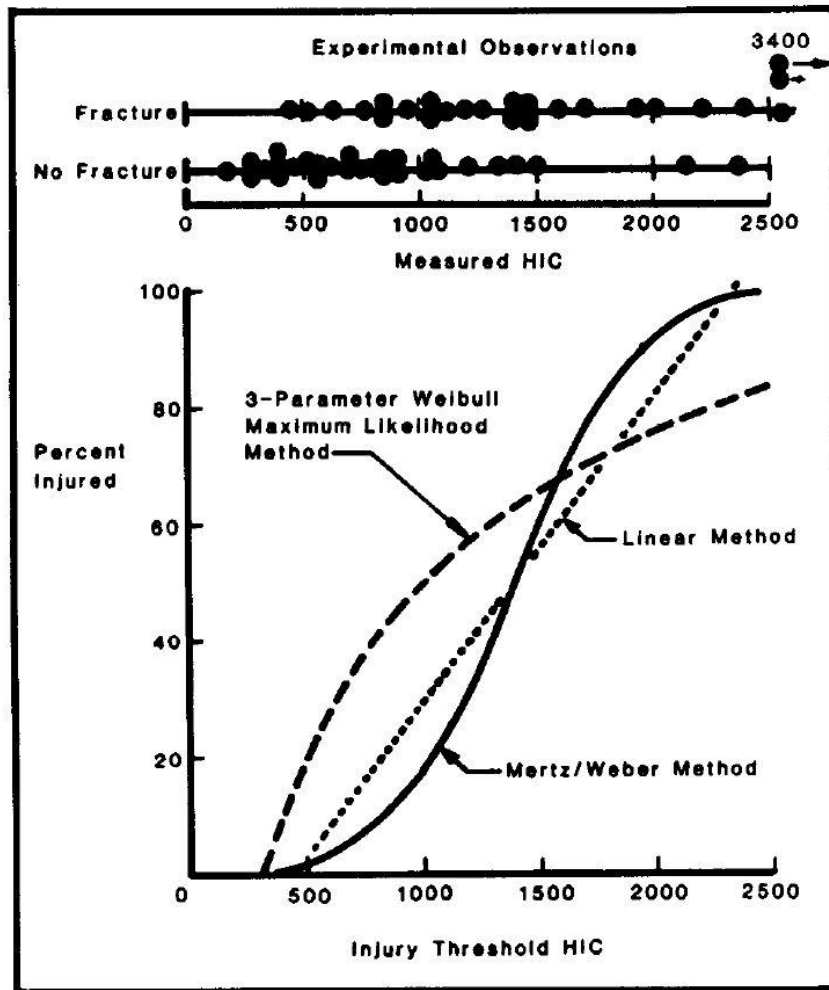


Figure 21: Predicted cumulative distribution curves of threshold HIC values for cadaver skull fracture

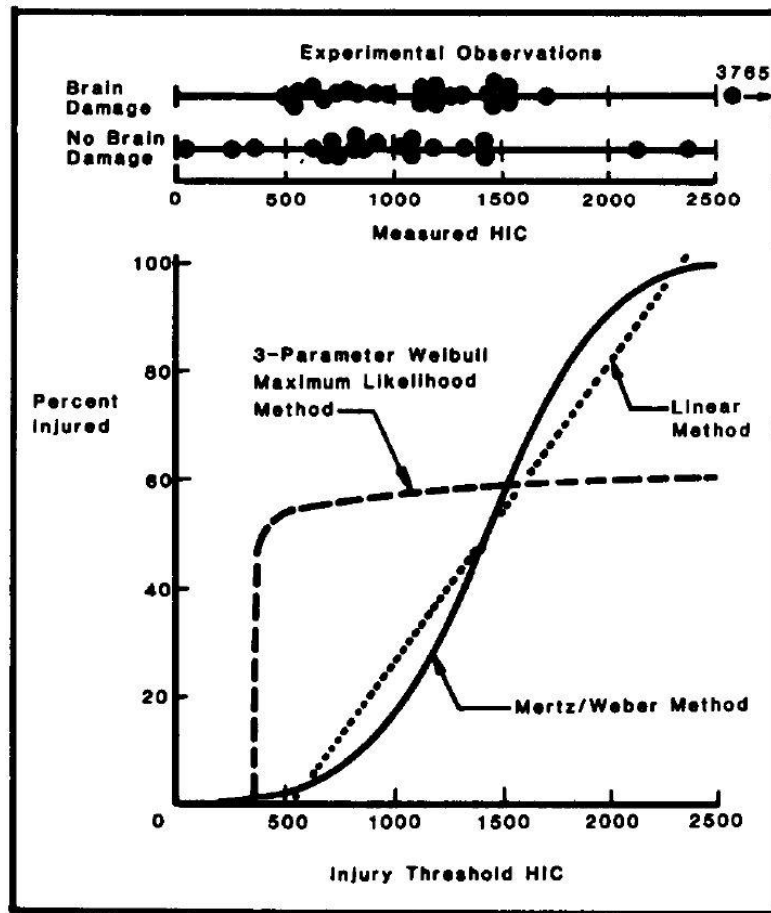


Figure 22: Predicted cumulative distribution curves of threshold HIC values for cadaver brain damage.

[12, 25, 134-139]

# 4 TESTS IN “CSI-SPA AUTOMOTIVE DIVISION” FACILITIES

## 4.1 GENERAL TEST CONDITIONS – ECE R043 REGULATIONS

### 4.1.1 Apparatus

In the case of headform tests with simultaneous determination of HIC-values the drop body is the phantom head as in Figure 23. The total mass of the phantom head should be  $10.0 + 0.2 / - 0.0$  kg.

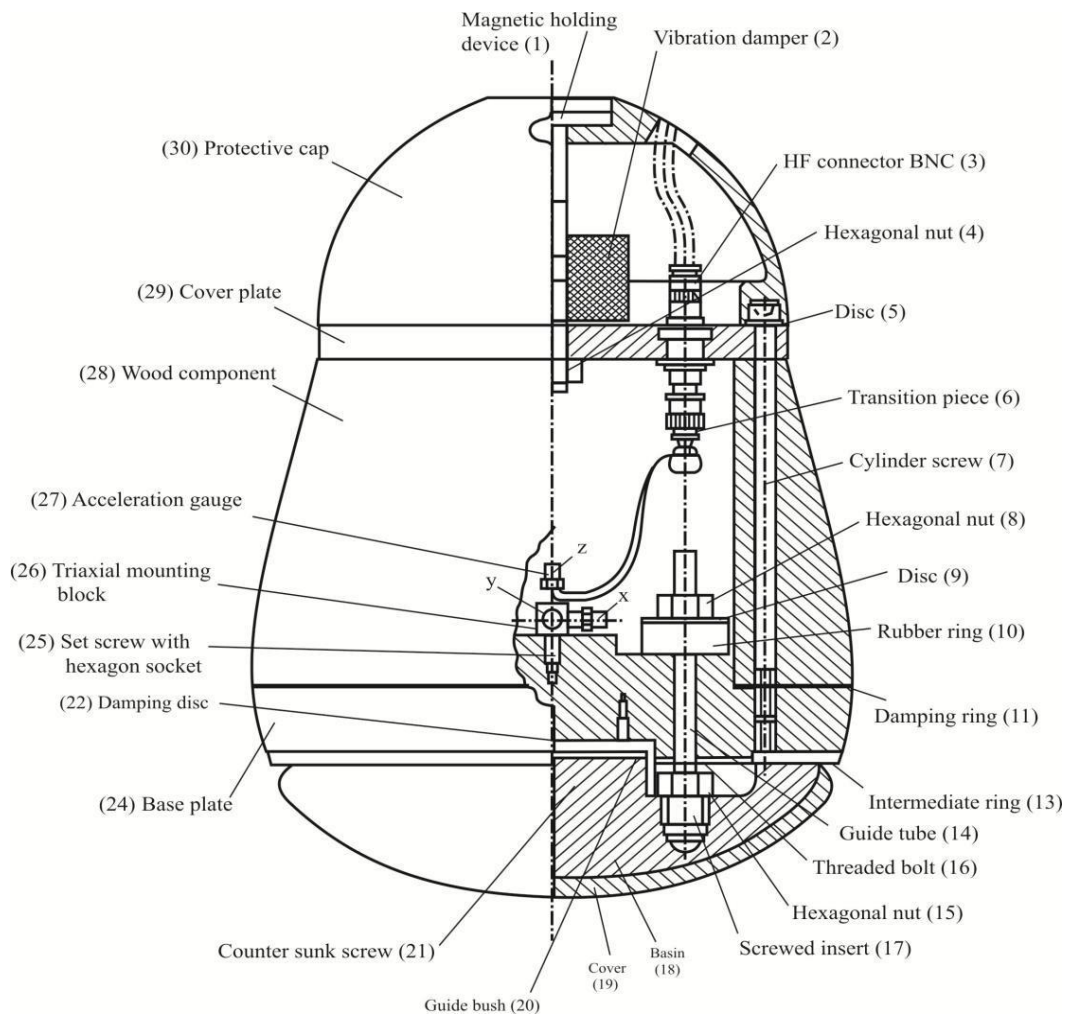


Figure 23: 10 kg headform

In the middle of the base plate (24) the triaxial mounting block (26) is mounted in the centre of gravity to receive the acceleration gauges (27). The acceleration gauges should be arranged vertically to each other.

The basin (18) and cover (19) situated under the base plate (24) share, to a great extent, the elastic properties of the human skull. The elastic properties of the phantom head on impact are determined by the hardness and the thickness of the intermediate ring (13) and the basin.

<b><i>Position No.</i></b>	<b><i>Number of pieces</i></b>	<b><i>Standard notation</i></b>	<b><i>Material</i></b>	<b><i>Remarks</i></b>
1	1	Magnetic holding device	Steel DIN 17100	-
2	1	Vibration damper	Rubber / Steel	Diameter: 50 mm Thickness: 30 mm Thread: M10
3	4	HF connector BNC	-	-
4	1	Hexagonal nut DIN 985	-	-
5	6	Disc DIN 125	-	-
6	3	Transition piece	-	-
7	6	Cylinder screw DIN 912	-	-
8	3	Hexagonal nut	-	-
9	3	Disc	Steel DIN 17100	Hole Diameter: 8 mm Outer Diameter: 35 mm Thickness: 1.5 mm
10	3	Rubber ring	Rubber, hardness 60 IRHD	Hole Diameter: 8 mm Outer Diameter: 30 mm Thickness: 10 mm
11	1	Damping ring	Packing with paper	Hole Diameter: 120 mm Outer Diameter: 199 mm Thickness: 0.5 mm
12	-	-	-	-
13	1	Intermediate ring	Butadien-rubber, hardness IRHD about 80	Hole Diameter: 129 mm Outer Diameter: 192 mm Thickness: 4 mm
14	3	Guide tube	Polytetra-fluorethen (PTFE)	Inner Diameter: 8 mm Outer Diameter: 10 mm Length: 40 mm
15	3	Hexagonal nut	-	-
16	3	Threaded bolt DIN 976	-	-
17	3	Screwed insert	Cast alloy DIN 1709-GD-CuZn 37Pb	-

18	1	Basin	Polyamid 12	-
19	1	Cover	Butadien-rubber	Thickness: 6 mm Rib on one side
20	1	Guide bush	Steel DIN 17100	-
21	4	Counter sunk screw	-	-
22	1	Damping disc	Packing with paper	Diameter: 65 mm Thickness: 0.5 mm
23	-	-	-	-
24	1	Base plate	Steel DIN 17100	-
25	1	Set screw with hexagonal socket	Class of strength 45H	-
26	1	Triaxial mounting block	-	-
27	3	Acceleration gauge	-	-
28	1	Wood component	Hornbeam, glued in layers	-
29	1	Cover plate	Alloy (AlMg5)	-
30	1	Protective cap	Polyamid 12	-

[128]

*Table 5: List of pieces for the 10kg headform*



*Figure 24 : 10,2 kg headform used in the tests*

#### 4.1.2 Test conditions

Temperature:  $20\text{ °C} \pm 5\text{ °C}$   
 Pressure: 860 to 1,060 mbar  
 Relative humidity:  $60 \pm 20$  per cent.  
 [128]

#### 4.1.3 Adjustment and calibration

To perform the headform test the phantom head is fixed to the cross arm of the guide system (Figure 25) and moved to the required drop height by means of a lifting device.

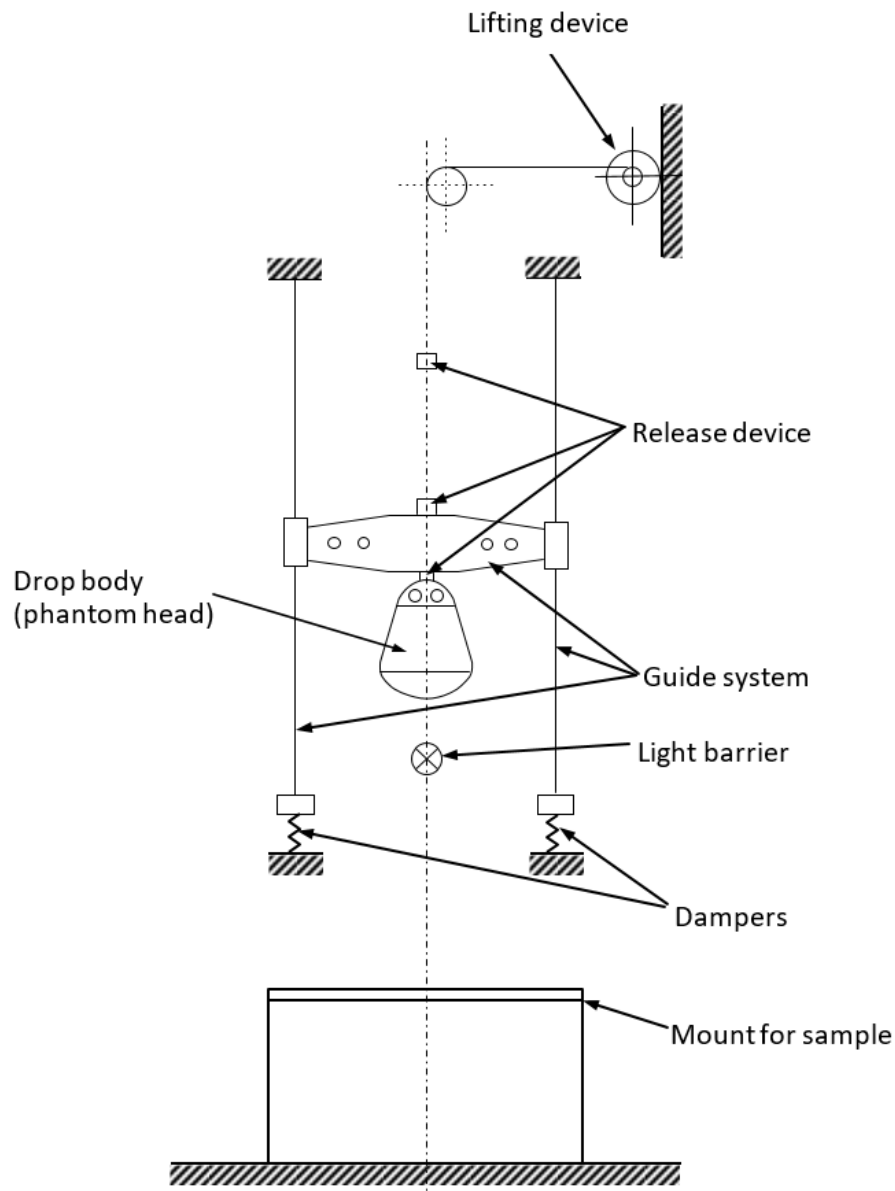
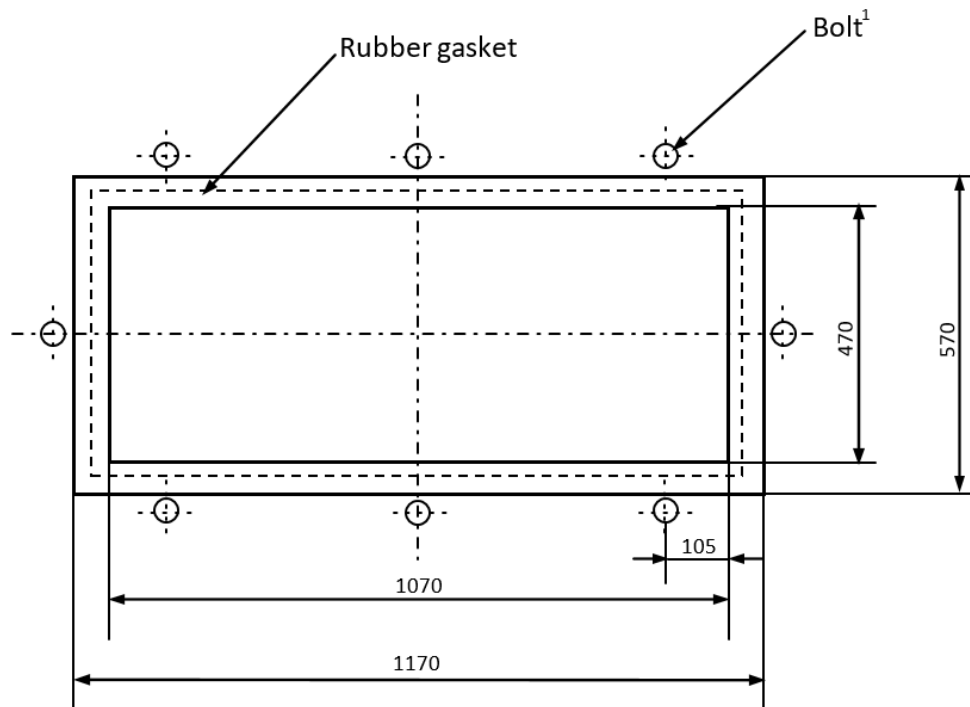


Figure 25: Test apparatus for the headform experiment with deceleration measurement

During the headform test the cross arm with the phantom head is released. After passing the height adjustable light barrier the phantom head is released from the cross arm, the cross arm's fall is dampened and the phantom head falls onto the sample.

No impulse may be given to the phantom head by the drop appliance or by the measuring cable, so that it is accelerated only by gravity and falls vertically.

Measuring device which allows determining HIC-values with the headform described under paragraph 4.1.1.



- Dimensions in millimetres
- The minimum recommended torque for M 20 is 30 Nm.

*Figure 26: Support for headform tests*

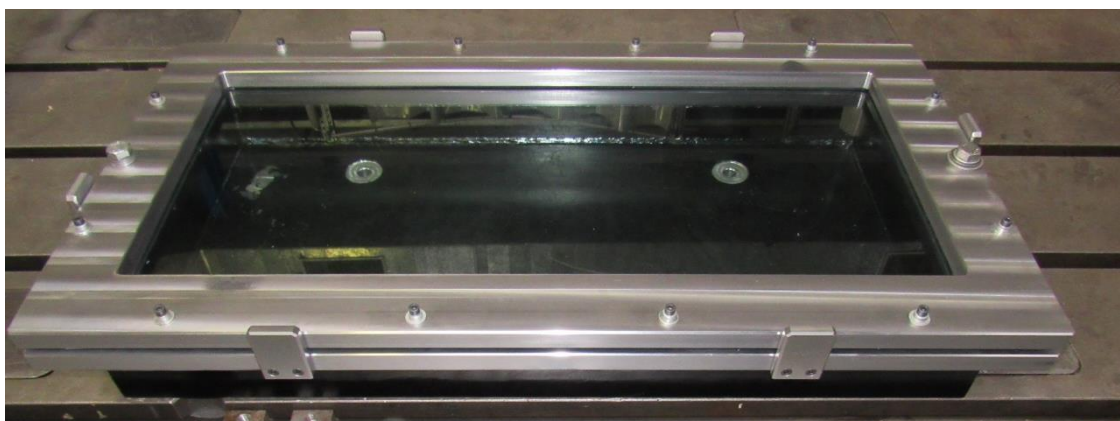


*Figure 27: Support for headform tests used*

#### 4.1.3.1 Equipment to calibrate the phantom head

The drop appliance shall allow drop heights between 50 mm and 254 mm to be adjusted exactly to within 1 mm. A guide system is not necessary for these small drop heights.

A steel impact plate which is made of steel is 600 mm x 600 mm in size and at least 50 mm thick. The impact surface shall be polished:

- surface roughness  $R_{max} = 1 \mu m$
- flatness tolerance  $t = 0.05 mm$ .

[128]

#### 4.1.3.2 Calibration and adjustment of the phantom head

Before each test series and no later than each 50 tests within a series, the phantom head shall be calibrated and adjusted if necessary.

The impact plate shall be clean and dry and during the test shall lie non-positively on a concrete base.

The phantom head is allowed to hit the impact plate vertically. The drop heights (measured from the lowest point of the phantom head to the surface of the impact plate) are 50, 100, 150 and 254 mm. The deceleration curves should be recorded.

The greatest deceleration  $a_z$  from the various drop heights on the z-axis shall lie within the limits given in the table 6:

<i>Drop height mm</i>	<i>Greatest deceleration <math>a_z</math> as a multiple of acceleration due to gravity g</i>
50	$64 \pm 5$
100	$107 \pm 5$
150	$150 \pm 7$
254	$222 \pm 12$

*Table 6: Greatest deceleration  $a_z$  as a multiple of acceleration due to gravity g in function of the drop height*

The deceleration curves should be based on a unimodal vibration. The deceleration curve of the drop height of 254 mm shall run at least 1.2 ms and at most 1.5 ms over 100 g.

If the requirements given in paragraph 3.1.3.2. are not met, the elastic properties of the phantom head shall be adjusted by varying the thickness of the intermediate ring (13) in the base plate (24). Corrections can be carried out by adjusting the three self-locking hexagonal nuts (8) on the threaded bolts (16) with which the basin (18) is fixed to the

base plate (24). The rubber rings (10) under the hexagon nuts (8) should not be brittle or cracked.

The cover (19) of the impact surface and the intermediate ring (13) should always be replaced immediately if damaged, especially when the phantom head can no longer be adjusted.

[128]

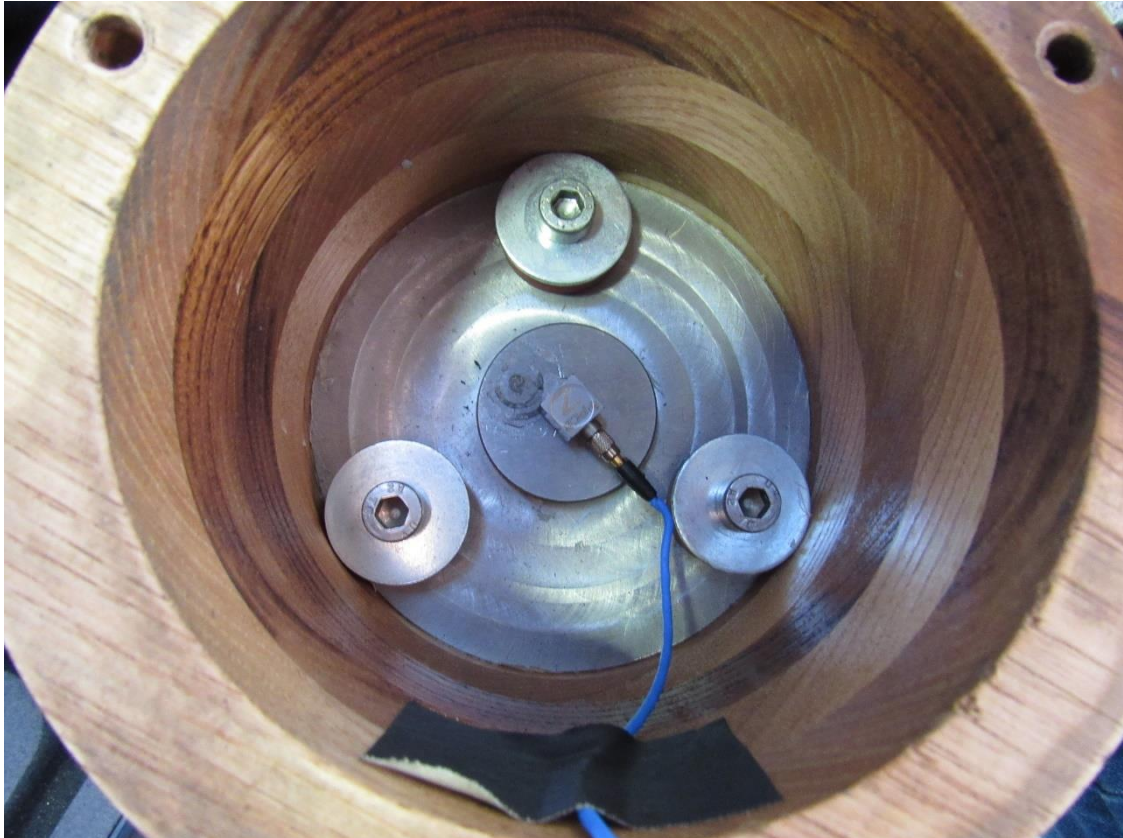


*Figure 28: PCB triaxial accelerometer used in the tests*

#### 4.1.4 Supporting fixture for testing flat test pieces.

Supporting fixture, as shown in Figure 26, for testing flat test pieces. The fixture is composed of two steel frames, with machined borders 50 mm wide, fitting one over the other and faced with rubber gaskets about 3 mm thick and  $15 \text{ mm} \pm 1 \text{ mm}$  wide and of hardness 70 IRHD. The upper frame is pressed down against the lower frame by at least eight bolts.

[128]

#### 4.1.5 Procedure

Tests on complete glazing (used for a drop height between 1.5 m and 3 m). Place the glazing freely on a support with an interposed strip of rubber of hardness 70 IRHD and thickness of about 3 mm.

The glazing shall be clamped to the supporting structure by means of appropriate devices. The surface of the glazing shall be substantially perpendicular to the incident direction of the headform weight. The headform weight shall strike the glazing at a point within 40 mm of its geometric centre on that face which represents the inward face of the plastic glazing when the latter is mounted on the vehicle, and shall be allowed to make only one impact.

Starting from a selected initial drop height, the drop heights should be raised by 0.5 m respectively in each further experiment. The deceleration curves occurring on impact on the sample for  $a_x$ ,  $a_y$  and  $a_z$  should be recorded according to time  $t$ .

After the headform test, it is necessary to check whether a glazing edge has moved more than 2 mm in the mount and whether the requirement for the point of impact was met. The acceleration components  $a_x$  and  $a_y$  should be smaller than 0.1  $a_z$  for vertical impact.

[128]

#### 4.1.6 Evaluation

The deceleration curves should be evaluated as follows:

The resulting deceleration  $a_{res}(t)$  in the centre of gravity according to the following equation from the measured deceleration curves  $a_x(t)$ ,  $a_y(t)$  and  $a_z(t)$  is to be compounded as multiples of the acceleration due to gravity.

$$a_{res}(t) = \sqrt{[a_x^2(t) + a_y^2(t) + a_z^2(t)]} \quad (10)$$

The time for which a deceleration of 80 g with  $a_{res}$  is continually exceeded and the greatest deceleration of  $a_{res}$  should be determined. The HIC-value should be calculated as a measurement of the danger of blunt skull-brain injuries using the following equation:

$$HIC = \max \left\{ (t_2 - t_1) \left[ \frac{1}{(t_2 - t_1)} \int_{t_1}^{t_2} a(t) dt \right]^{2,5} \right\} \quad (11)$$

The integral limits  $t_1$  and  $t_2$  should be selected in such a way that the integral takes a maximal value.

[128]

## 4.2 RESULTS OF HEADFORM CALIBRATION

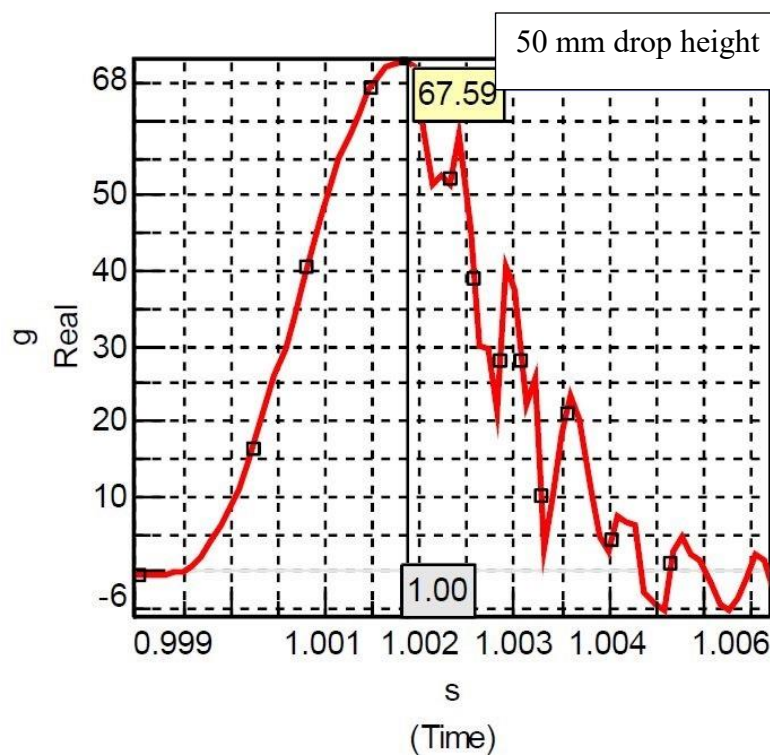


Figure 29: Results of 50mm drop height

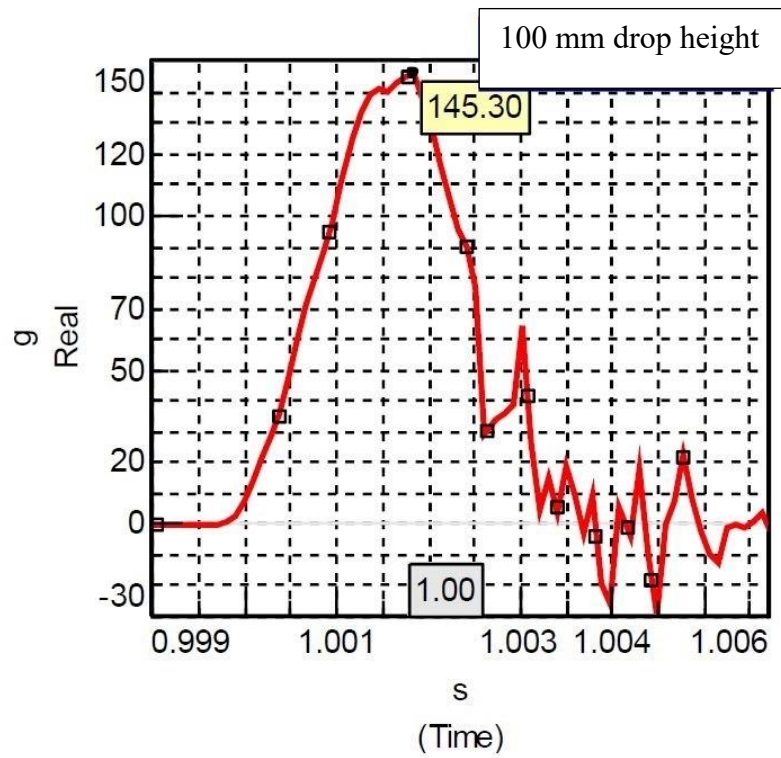


Figure 31: Results of 100mm drop height

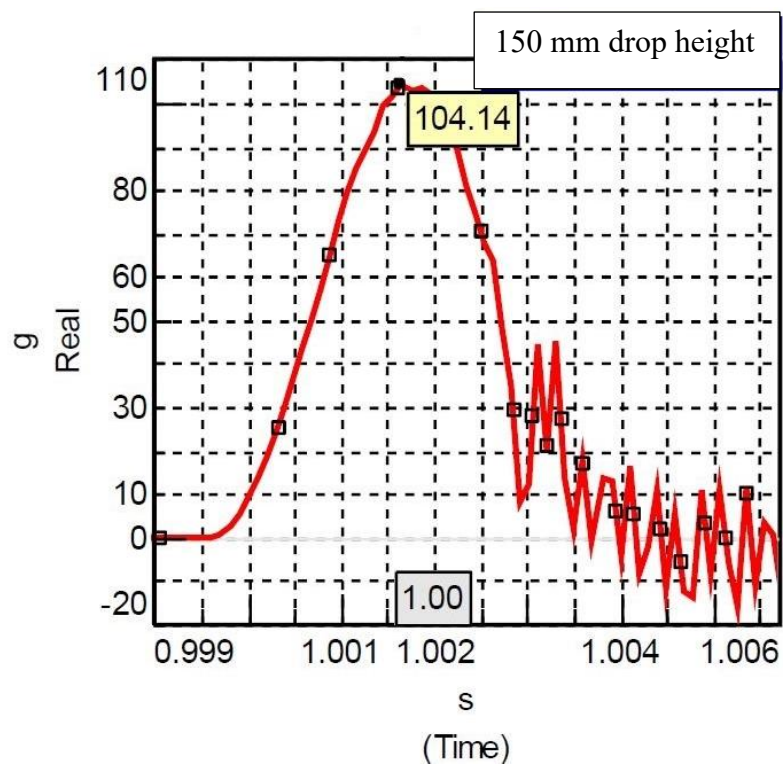


Figure 30: Results of 150mm drop height

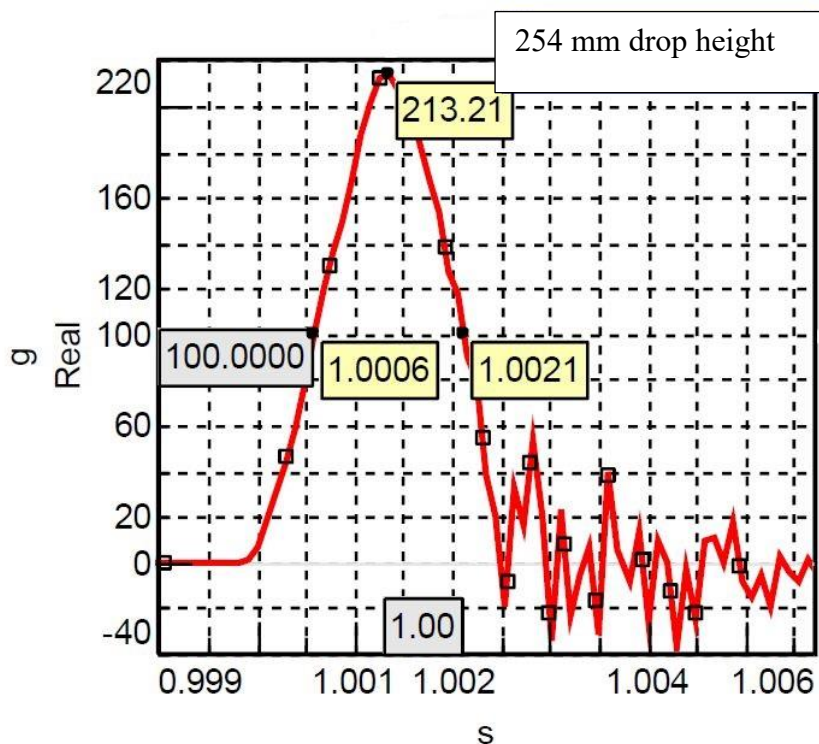


Figure 32: Results of 254mm drop height

	RESULT	TARGET	ENDING
<b>Drop height 50 mm</b>	$a_z = 67,59$	$a_z = 64 \pm 5$	POSITIVE
<b>Drop height 100 mm</b>	$a_z = 104,14$	$a_z = 107 \pm 5$	POSITIVE
<b>Drop height 150 mm</b>	$a_z = 145,30$	$a_z = 150 \pm 7$	POSITIVE
<b>Drop height 254 mm</b>	$a_z = 213,21$ $\Delta T_{over\ 100g} = 1,5\ ms$	$a_z = 222 \pm 12$ $1,2\ ms \leq \Delta T_{over\ 100g} \leq 1,5\ ms$	POSITIVE

Table 7: Numerical results of headform calibration

## 4.3 EXECUTION OF HEADFORM IMPACT TEST

### 4.3.1 Explanation of HIC calculation through dedicated MATLAB program\code

It is important to remark, that the PCB accelerometer used in the tests has an analogue output data. So this means that, in the output, it gives the acceleration in function of time. In our case, it collects data every 0,1 milliseconds and saves it on an excel datasheet.

First of all, it uses the command “xlsread” to import the data from the datasheet to the Matlab sheet.

Matlab Code:

```
%DATA READ FROM EXCEL
t=xlsread('sample_1',1,'A4:A364');
a_z_t=xlsread('sample_1',1,'B4:B364');
a_y_t=xlsread('sample_1',1,'C4:C364');
a_x_t=xlsread('sample_1',1,'D4:D364');
```

Then, a vector is calculated that contains, each 0.1 milliseconds, the resultant deceleration, starting from the acceleration along x axis, y axis and z axis. It is evaluated with the following equation:

$$Acceleration_{resultant} = \sqrt{a_x^2 + a_y^2 + a_z^2} \quad (12)$$

Matlab Code:

```
%RESULTING DECELERATION
a_tot=sqrt((a_x_t).^2+(a_y_t).^2+(a_z_t).^2);
```

Knowing that the acceleration of gravity is equal to  $9,81 \text{ m/s}^2$ , the drop height is equal to 1,5 m and neglecting the air resistance, the theoretical impact velocity is calculated in this way:

$$Impact_{velocity} = \sqrt{2gh} \quad (13)$$

Matlab Code:

```
%THEORETICAL IMPACT_VELOCITY CALCULATION  
THEOR_IMP_VEL=sqrt(2*g*h); %m/s
```

Multiplying the headform mass (scalar data) and the vector that contains the resultant deceleration each 0,1 milliseconds, one can obtain the head impact force during the crash.

Matlab code:

```
%HEAD IMPACT FORCE  
F = m*a_tot;
```

Since  $a(t)$  is a real-world physical acceleration profile, it may be assumed as continuous and integrable in the time domain  $0 < t < T$  where  $T$  is the total duration of the acceleration pulse.

Now, one can calculate the HIC index:

$$HIC = \max \left\{ (t_2 - t_1) \left[ \frac{1}{(t_2 - t_1)} \int_{t_1}^{t_2} a(t) dt \right]^{2,5} \right\} \quad (14)$$

The limits of integration  $t_1$  and  $t_2$  are defined to be within this time domain, and therefore HIC is a function of these limits. One can write:

$$HIC = f(t_1, t_2) \quad (15)$$

where  $f(t_1, t_2)$  is a differentiable function.

Through the following Matlab code, given a discrete acceleration array, the computation of the HIC, involves all possible iterative combinations to satisfy the maximization requirements for the HIC function.

In order to calculate the field of HIC during all period of time during the crash, this following code is used:

Matlab code:

```
% HIC COMPUTATION
for i = 1:length(t)
    for j = 1:length(t)
        HIC(i,j)=((((trapz(a_tot(i:j)))/((j-i+1)))^2.5).*(((j-i+1)*s_f))));
    end
end
[HIC_max,I]=max(HIC(:));
[T_1,T_2]=(ind2sub(size(HIC),I));
dt_HIC_max=(T2-T1); %milliseconds
```

In order to have a comparison between the HIC value and the threshold one, it is important to calculate the value of the HIC with  $(t_2 - t_1)$  equal to 15 or 36 milliseconds.

Matlab code:

```
%CALCULATION OF THE HIC 15
for i = 1:length(t)
    for j = 1:length(t)
        if (j-i+1)==150
            HIC_15(i,j)=HIC(i,j);
        end
    end
end
HIC_max_15=max(HIC_15);
[HIC_max_15,I]=max(HIC_15(:));
[T1__15,T2__15]=ind2sub(size(HIC_15),I);
```

Then, it is necessary to verify that the acceleration components  $a_x$  and  $a_y$  are smaller for vertical impact than  $0.1 a_z$ .

Matlab code:

```
%CONSTRAIN AND CONDITIONS
%a_x_t constrain
for i=1:length(t)
    if ((a_x_t(i))/10)<a_z_t(i)
        disp(['The acceleration components along X axis respect the constrain']);
    else
        disp(['The acceleration components along X axis DO NOT respect the constrain']);
    end
end
```

```
%a_y_t constrain
for i=1:length(t)
    if ((a_y_t(i))/10)<a_z_t(i)
        disp(['The acceleration components along Y axis respect the constrain']);
    else
        disp(['The acceleration components along Y axis DO NOT respect the
constrain']);
    end
end
```

## 4.4 RESULTS

### 4.4.1 Results of the tests on the first type of plastic compound glass

#### 4.4.1.1 First sample (type one):

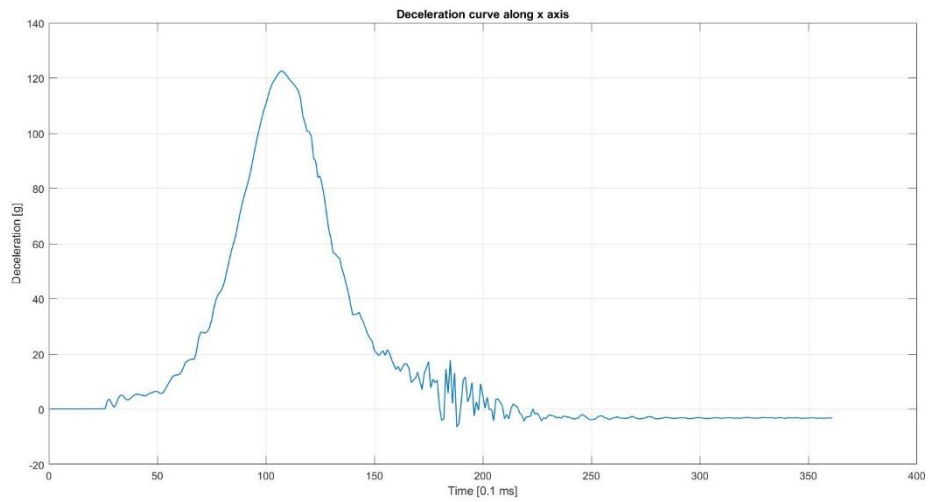


Figure 33: Deceleration curve along x axis

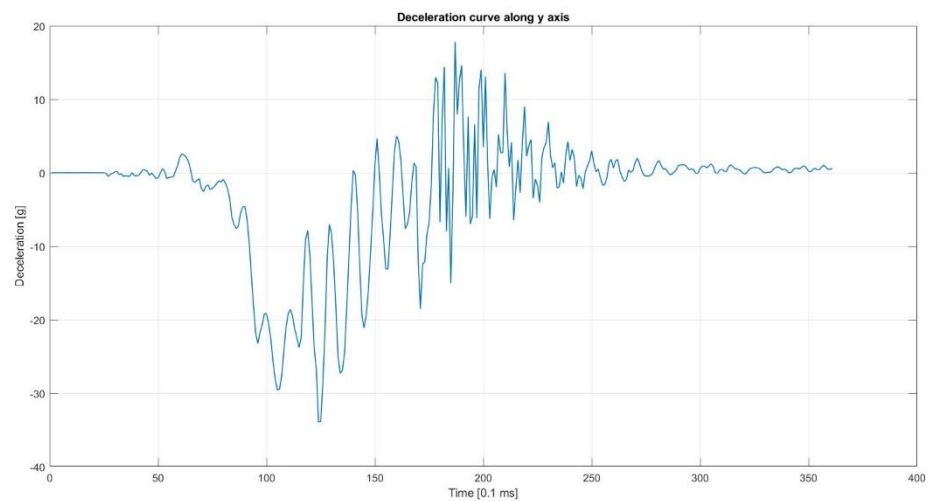


Figure 34: Deceleration curve along y axis

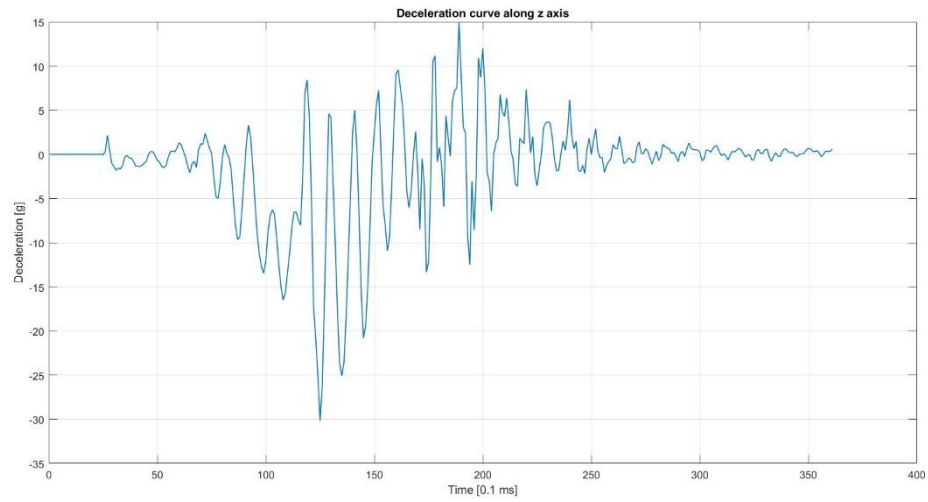


Figure 35: Deceleration curve along z axis

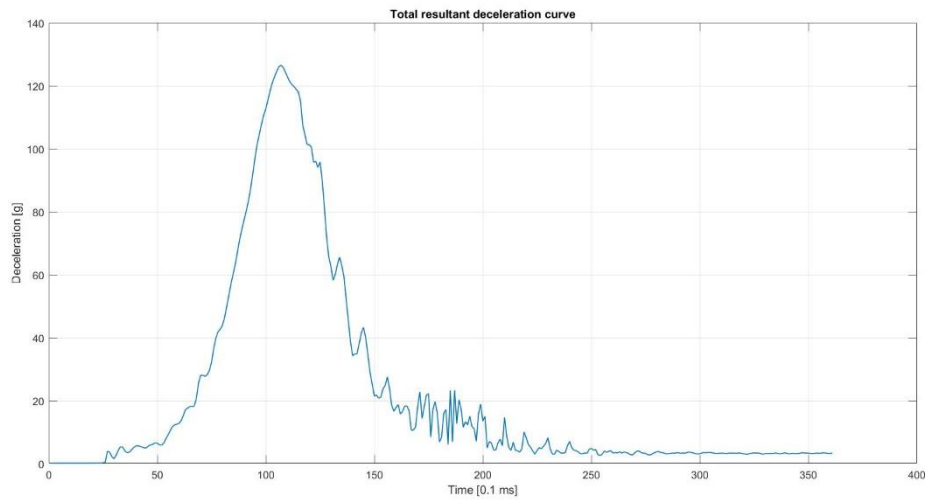


Figure 36: Total resultant deceleration curve

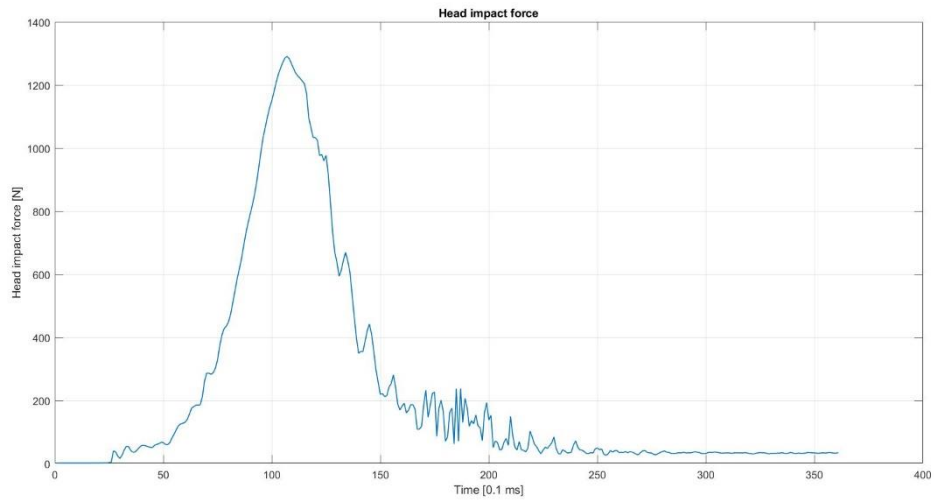


Figure 37: Head impact force

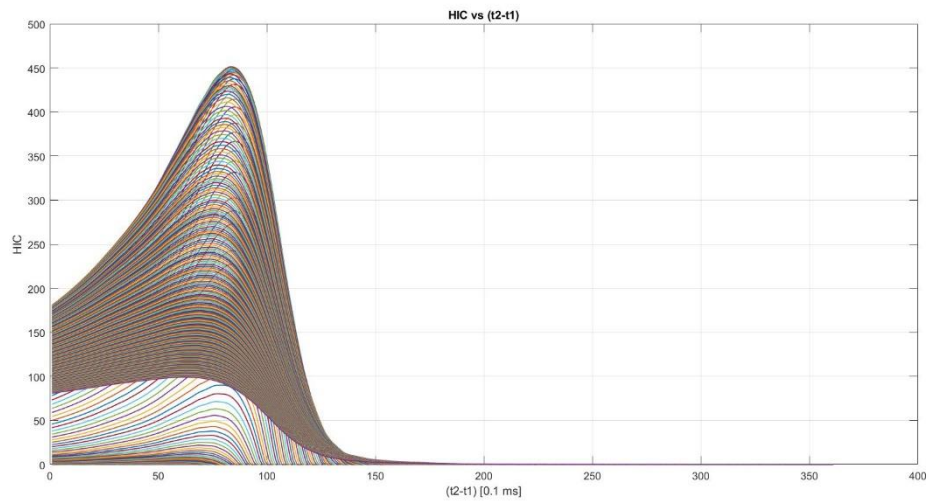


Figure 38: HIC vs  $(t_2-t_1)$

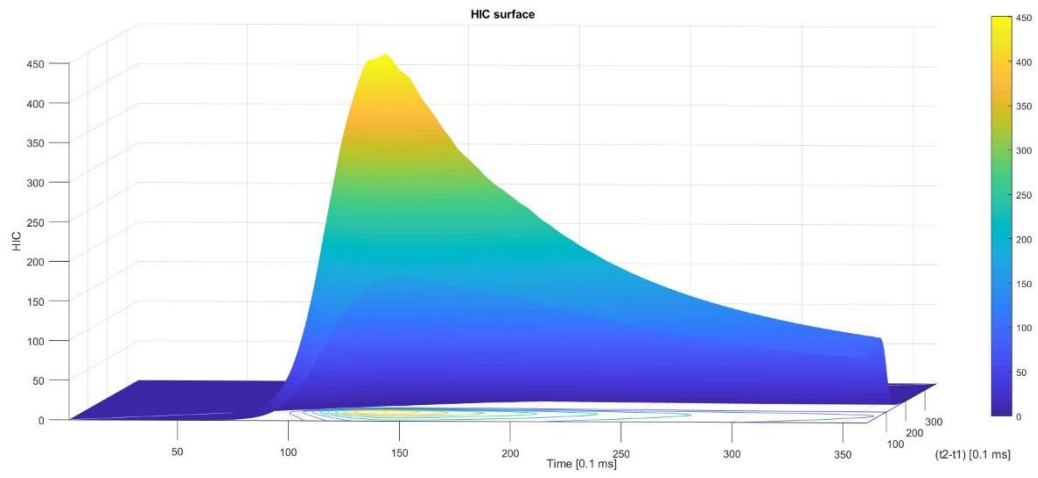


Figure 39: HIC surface

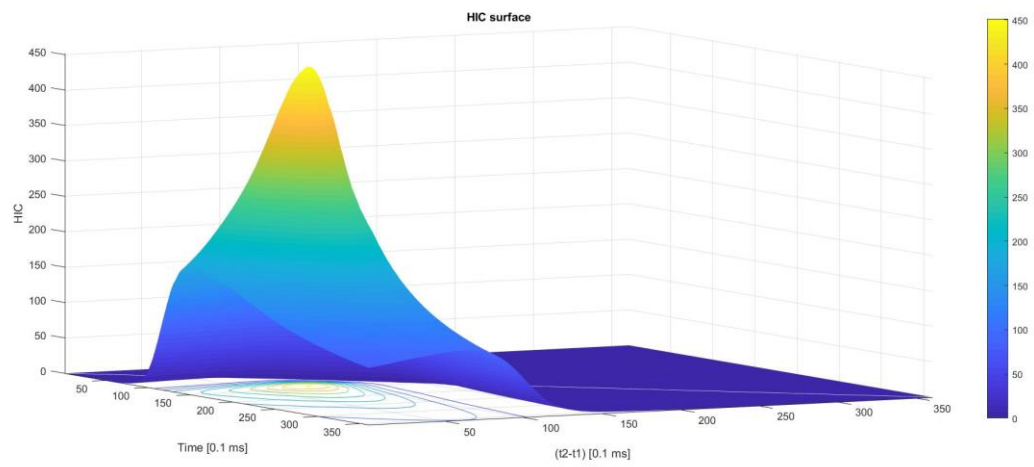


Figure 40: HIC surface

#### 4.4.1.2 Second sample (type one):

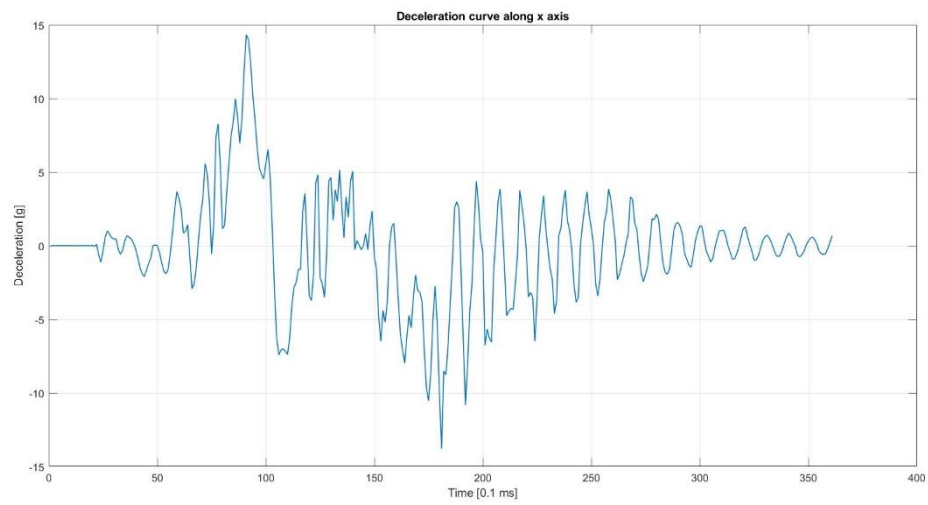


Figure 41: Deceleration curve along x axis

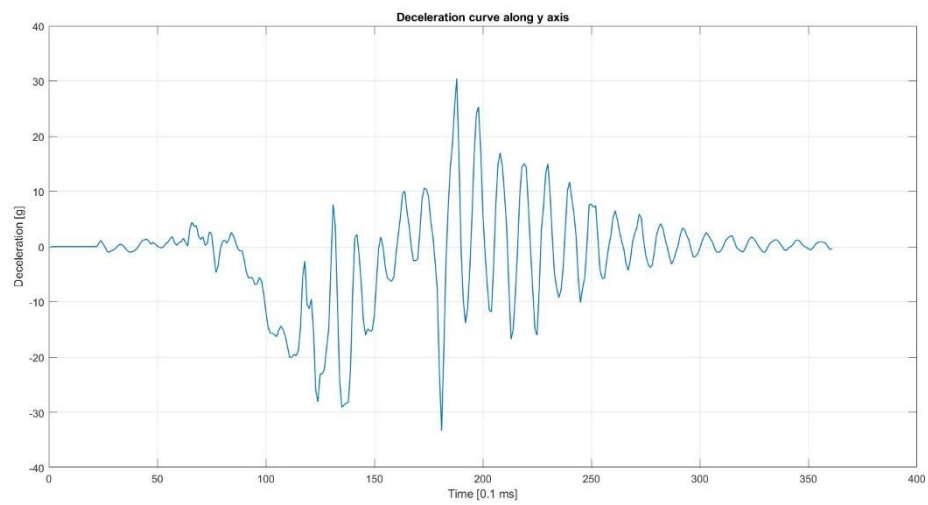


Figure 42: Deceleration curve along y axis

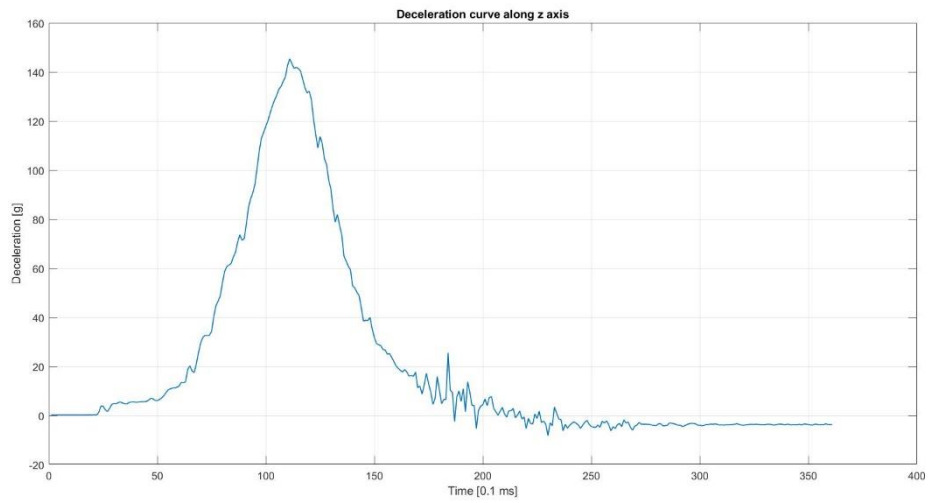


Figure 43: Deceleration curve along z axis

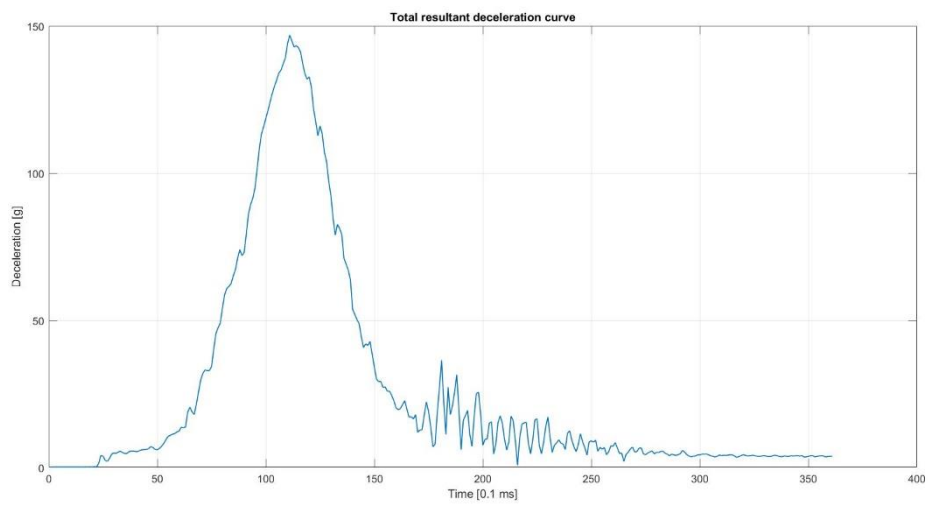


Figure 44: Total resultant deceleration curve

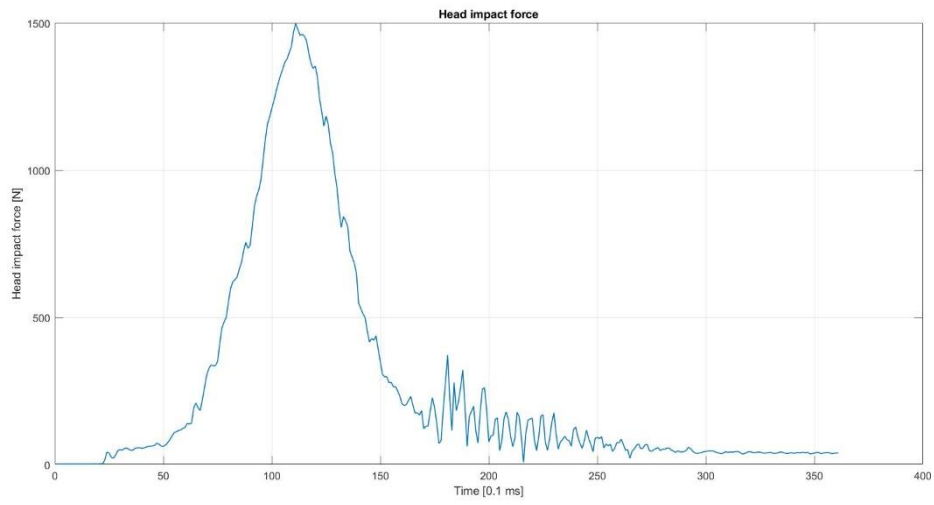


Figure 45: Head impact force

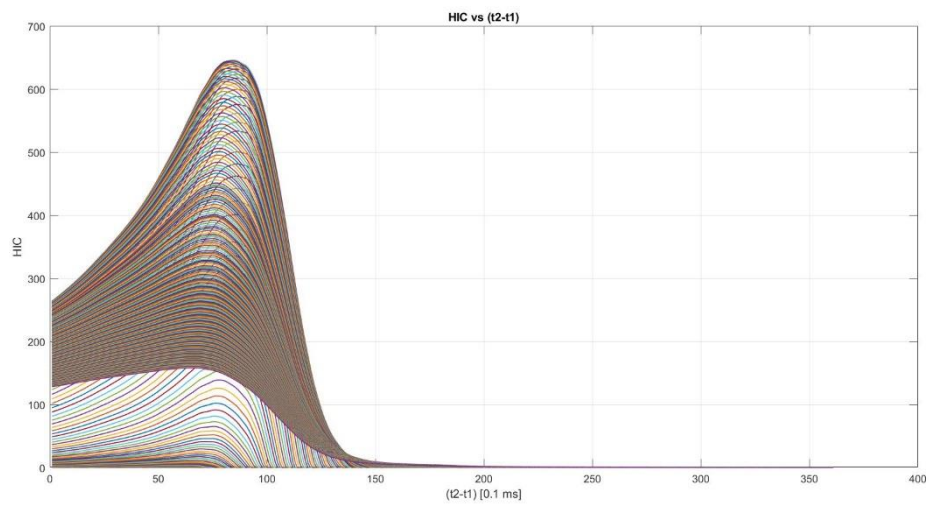


Figure 46: HIC vs  $(t_2-t_1)$

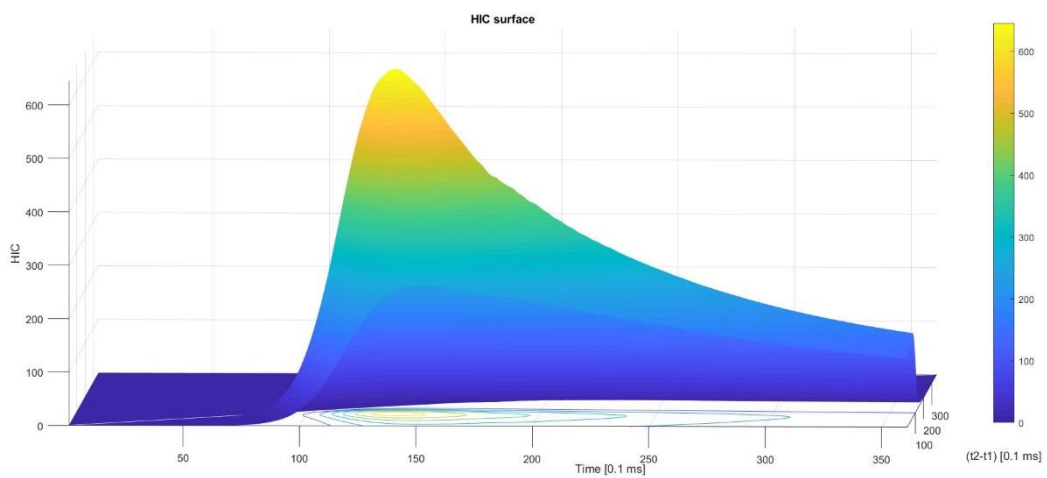


Figure 47: HIC surface

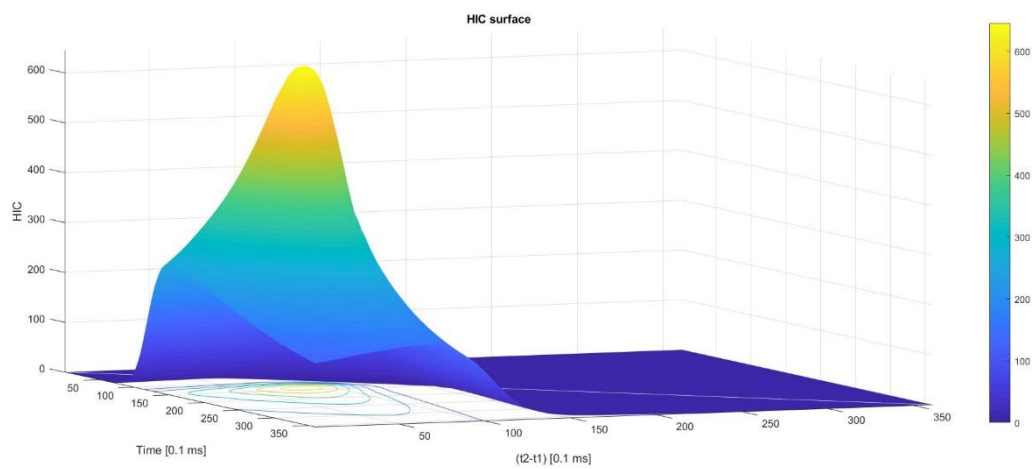


Figure 48: HIC surface

#### 4.4.1.3 Third sample (type one):

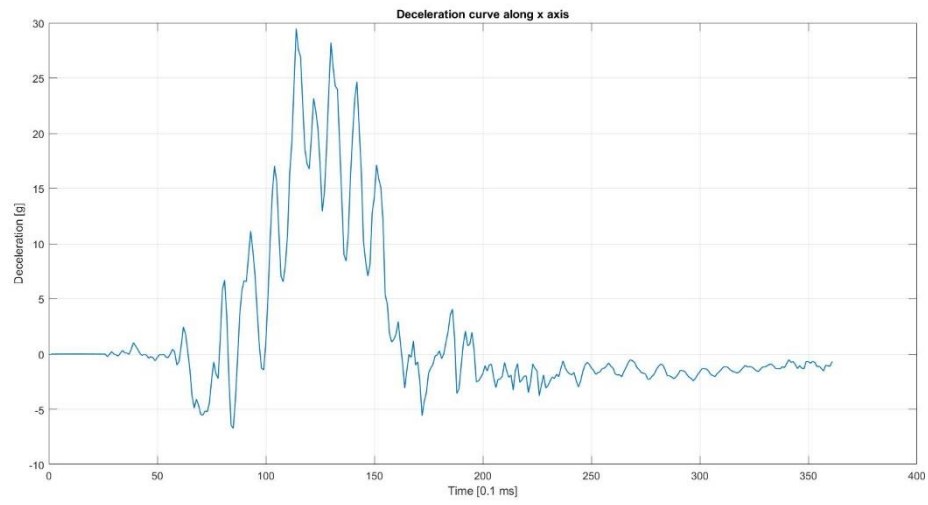


Figure 49: Deceleration curve along x axis

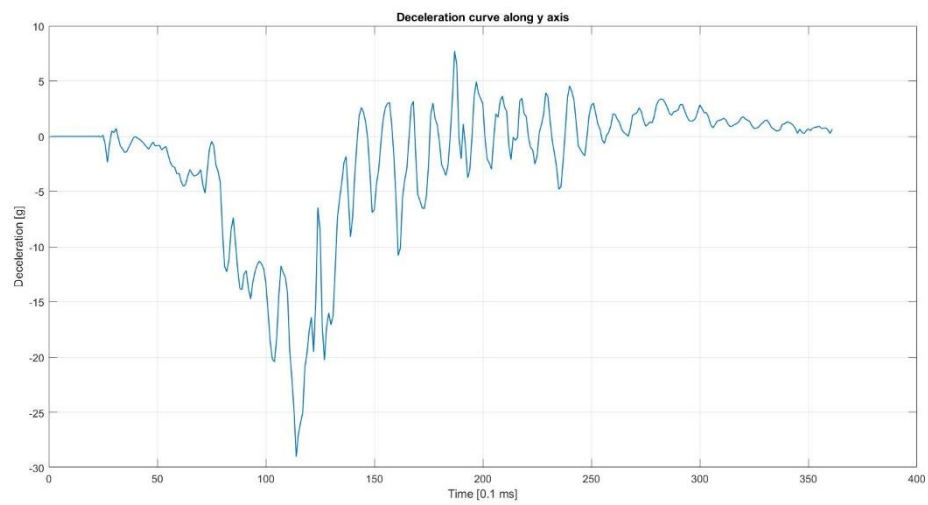


Figure 50: Deceleration curve along y axis

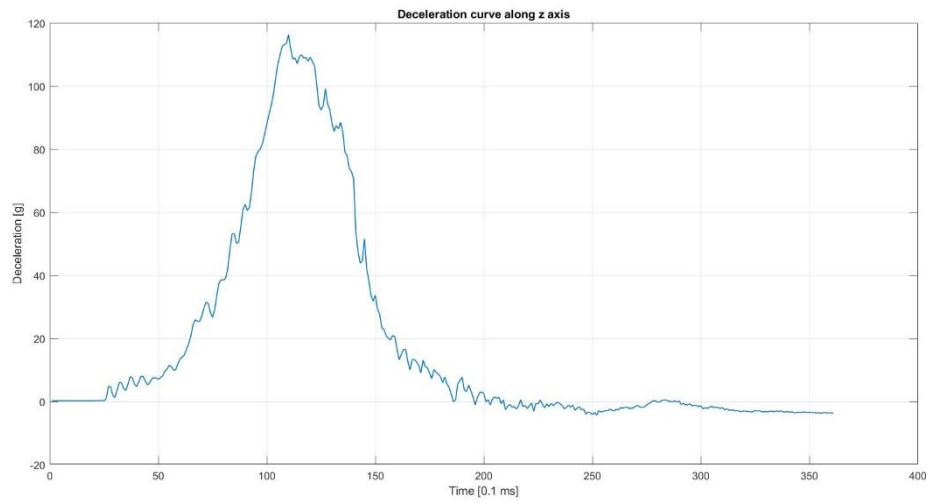


Figure 51: Deceleration curve along z axis

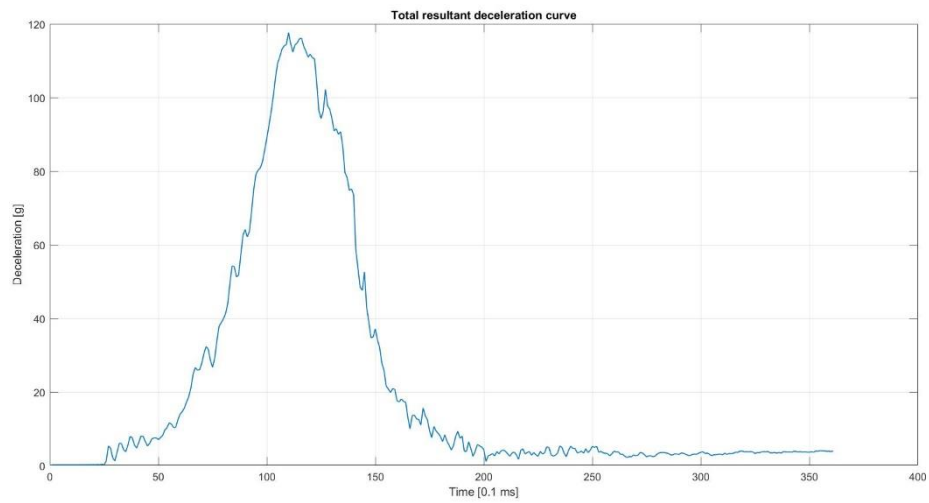


Figure 52: Total resultant deceleration curve

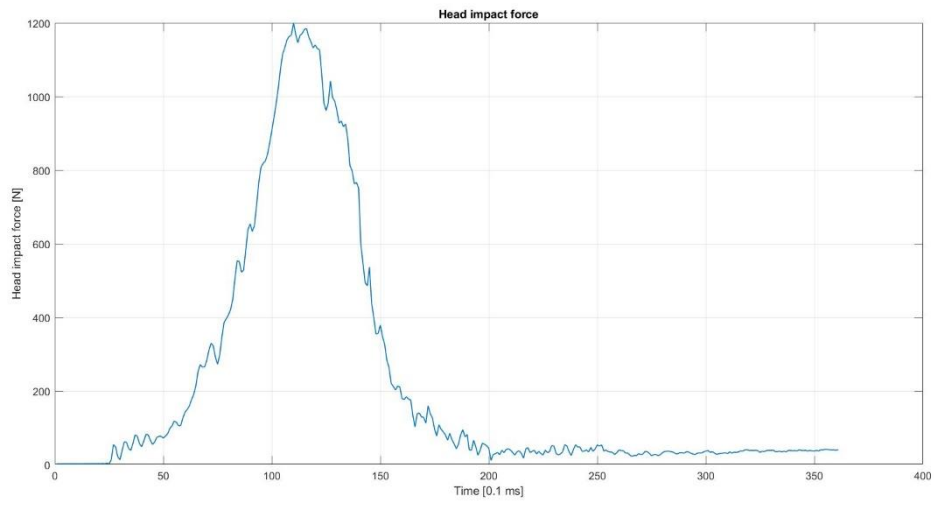


Figure 53: Head impact force

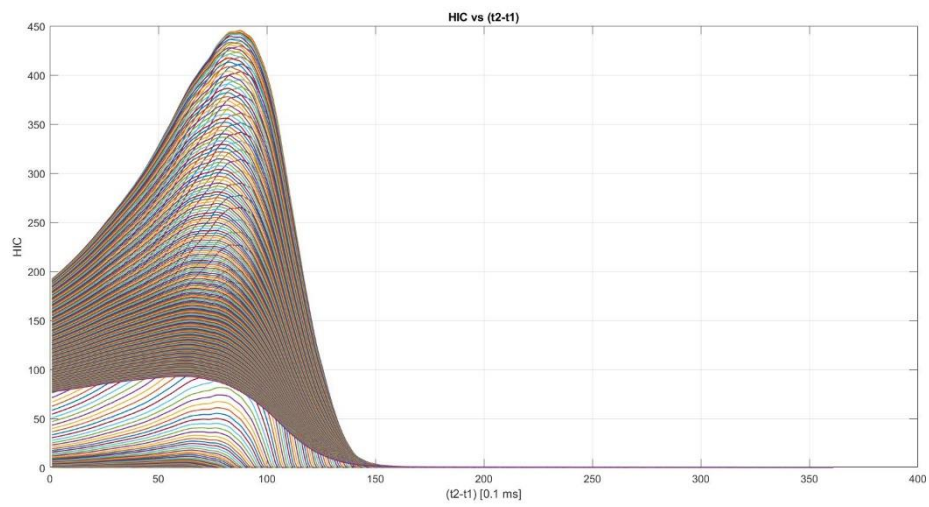


Figure 54: HIC vs  $(t_2-t_1)$

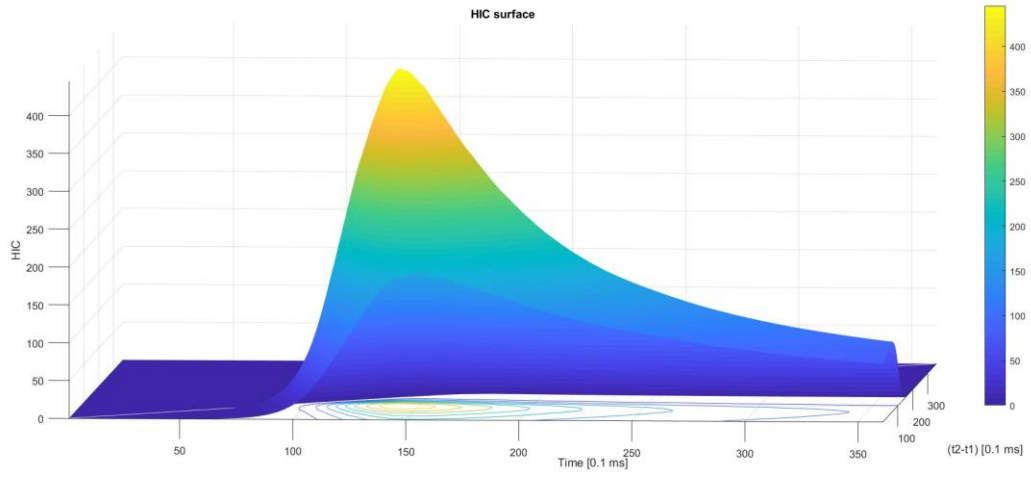


Figure 55: HIC surface

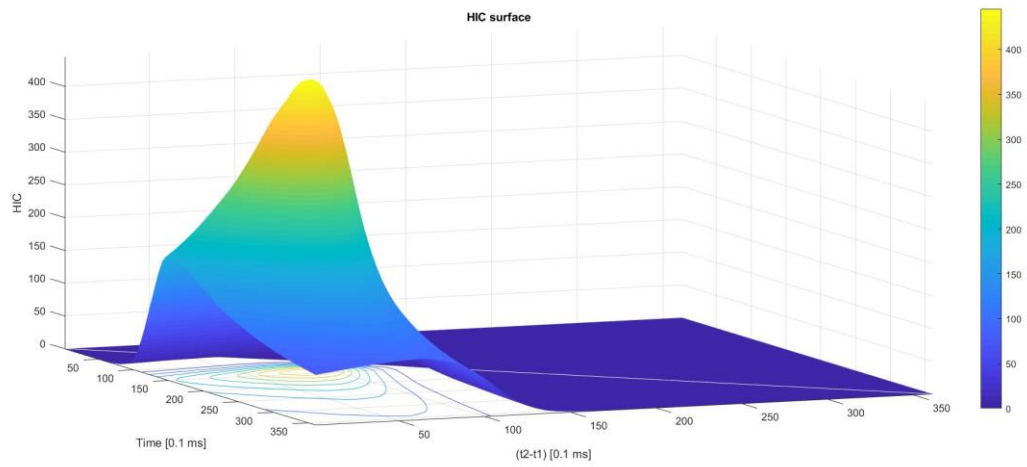


Figure 56: HIC surface

#### 4.4.1.4 Numerical results :

	Sample 1	Sample 2	Sample 3
<b><math>HIC_{15}</math></b>	235.5541	347.0165	228.6473
<b><math>T1_{15}</math></b>	5.3 ms	6 ms	4.1 ms
<b><math>T2_{15}</math></b>	20.2 ms	20.9 ms	19 ms
<b><math>HIC_{max}</math></b>	451.2636	645.5623	445.1867
<b><math>T1_{HIC_{max}}</math></b>	8.4 ms	8.4 ms	8.8 ms
<b><math>T2_{HIC_{max}}</math></b>	13.6 ms	13.9 ms	14.2 ms
<b><math>\Delta T_{HIC_{max}}</math></b>	5.2 ms	5.5 ms	5.4 ms
<b>Max g</b>	126.5301 g	146.8439 g	117.6418 g
<b>Impact velocity</b>	5.4249 m/s	5.4249 m/s	5.4249 m/s

Table 8: Numerical results of the three sample - type one

## 4.4.2 Results of the tests on the second type of plastic compound glass

### 4.4.2.1 First sample (type two):

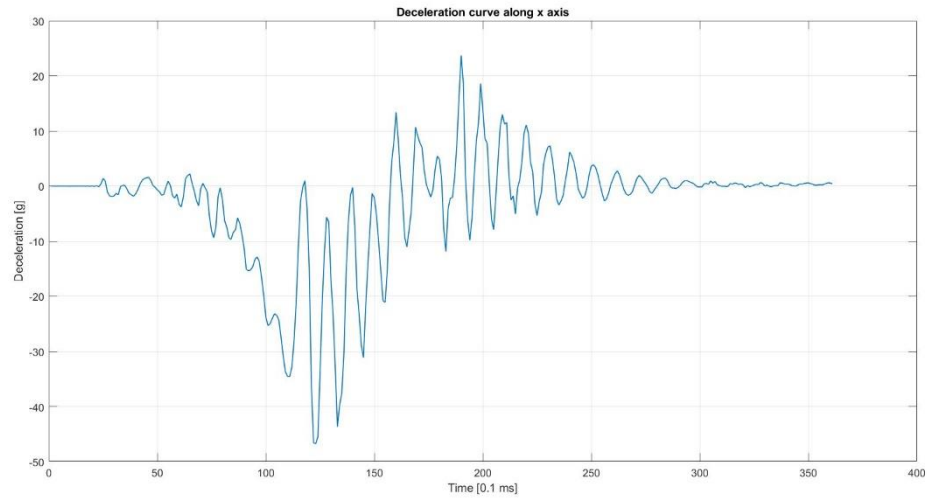


Figure 57: Deceleration curve along x axis

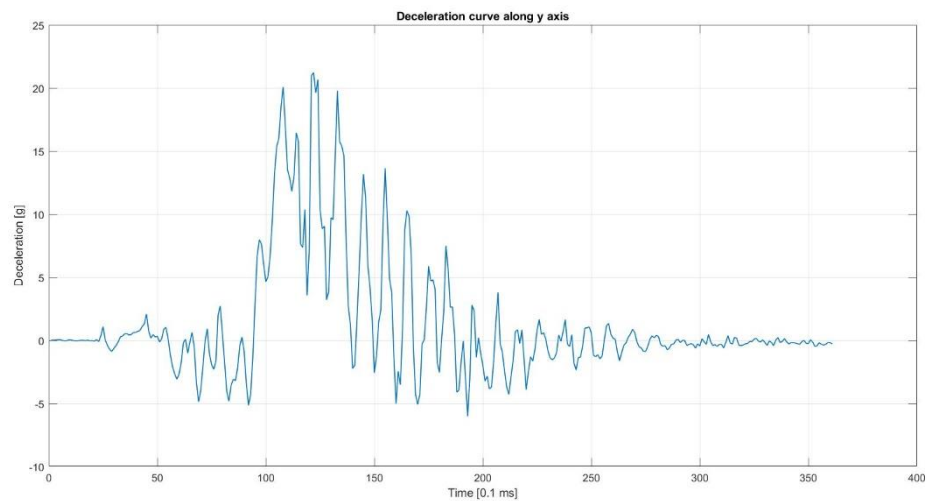


Figure 58: Deceleration curve along y axis

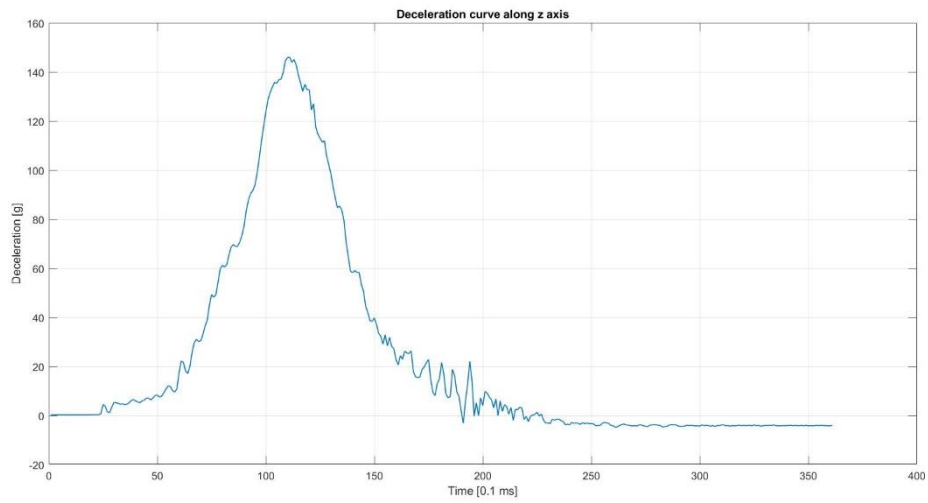


Figure 59: Deceleration curve along z axis

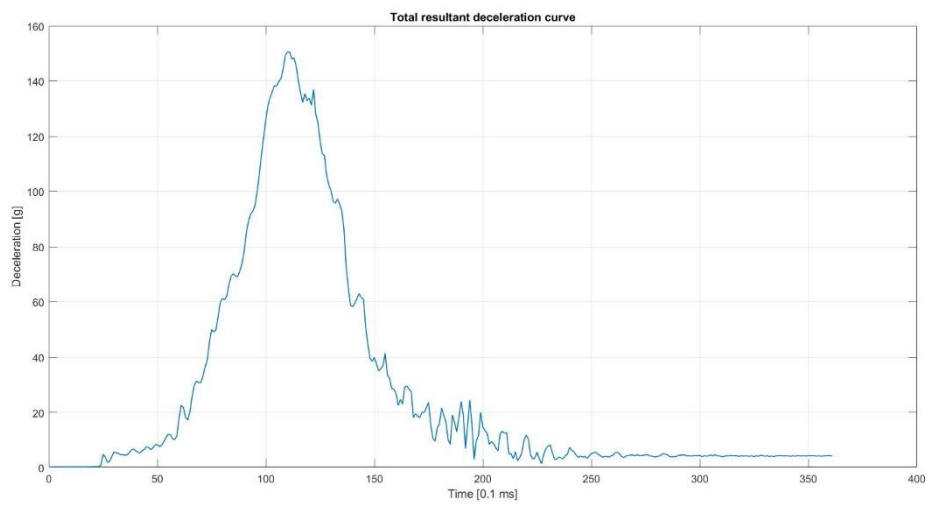


Figure 60: Total resultant deceleration curve

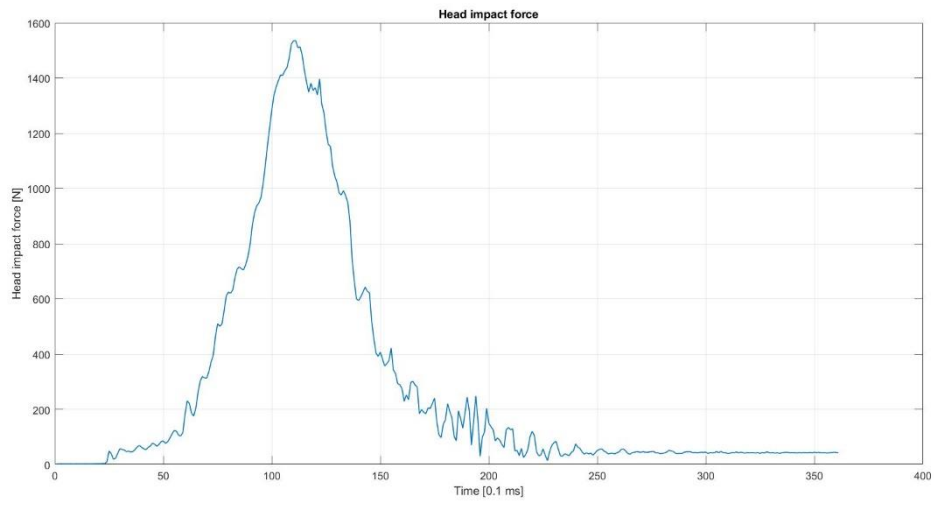


Figure 61: Head impact force

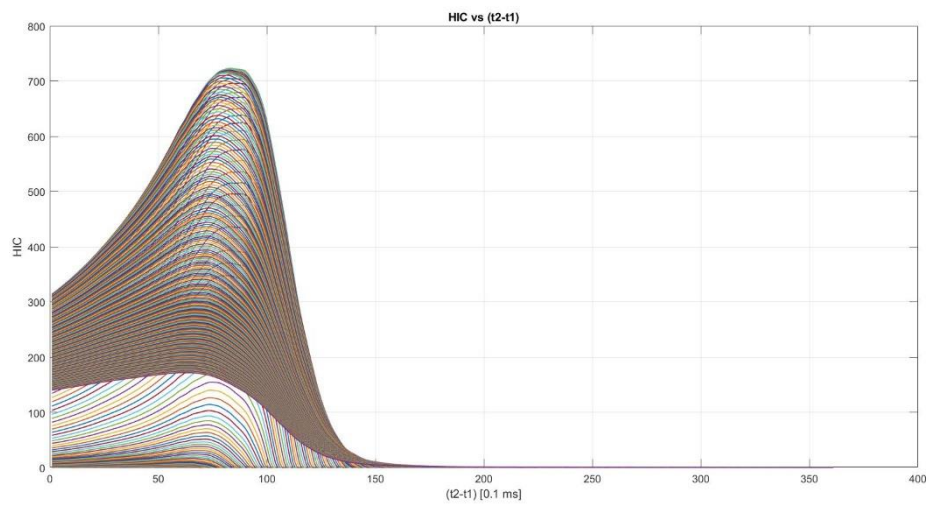


Figure 62: HIC vs (t2-t1)

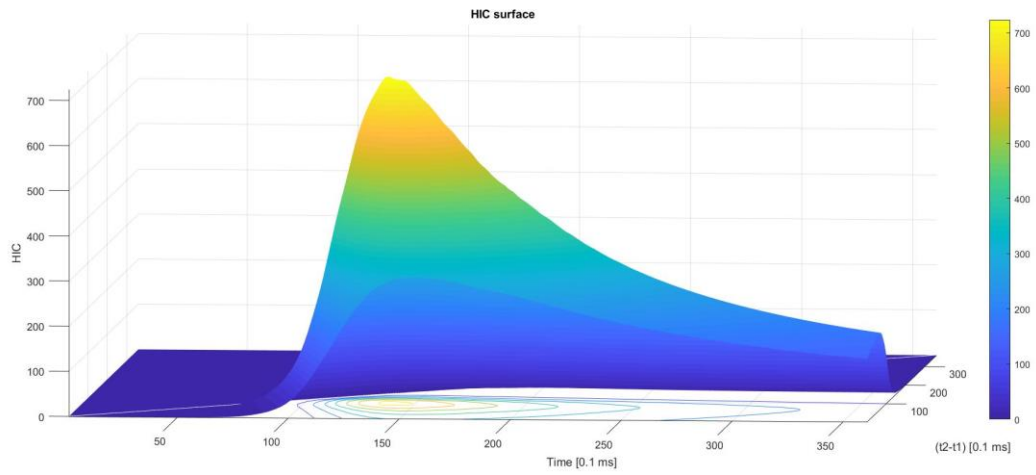


Figure 63: HIC surface

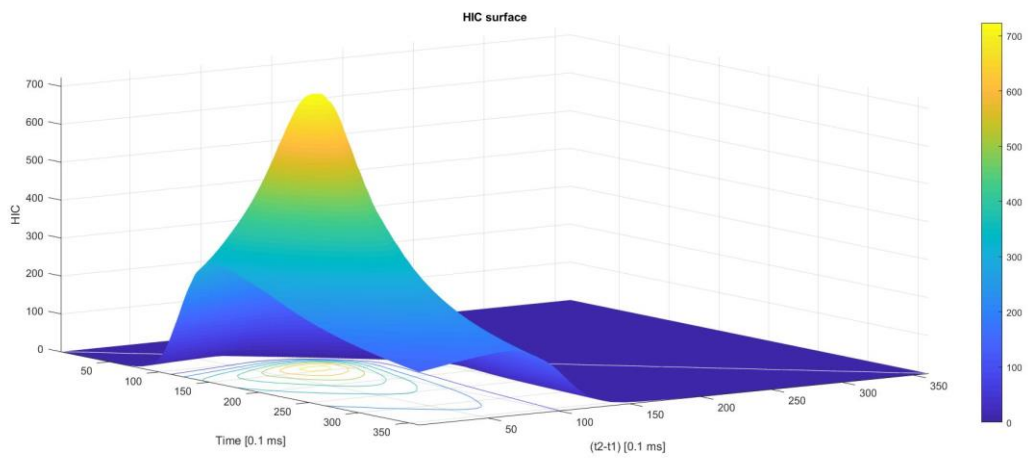


Figure 64: HIC surface

#### 4.4.2.2 Second sample (Type two):

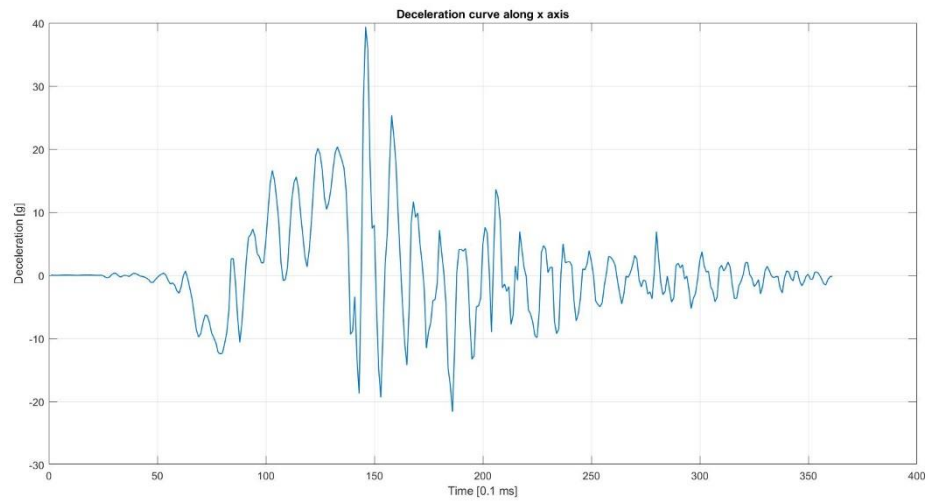


Figure 65: Deceleration curve along x axis

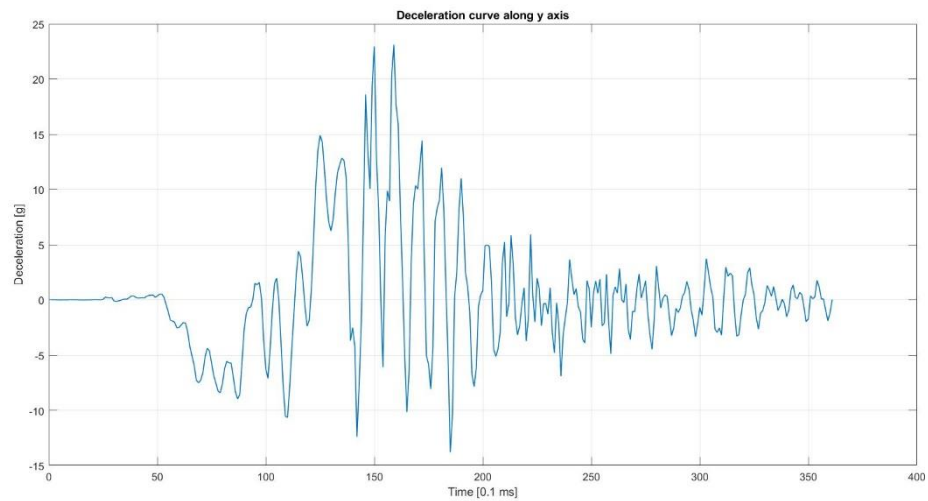


Figure 66: Deceleration curve along y axis

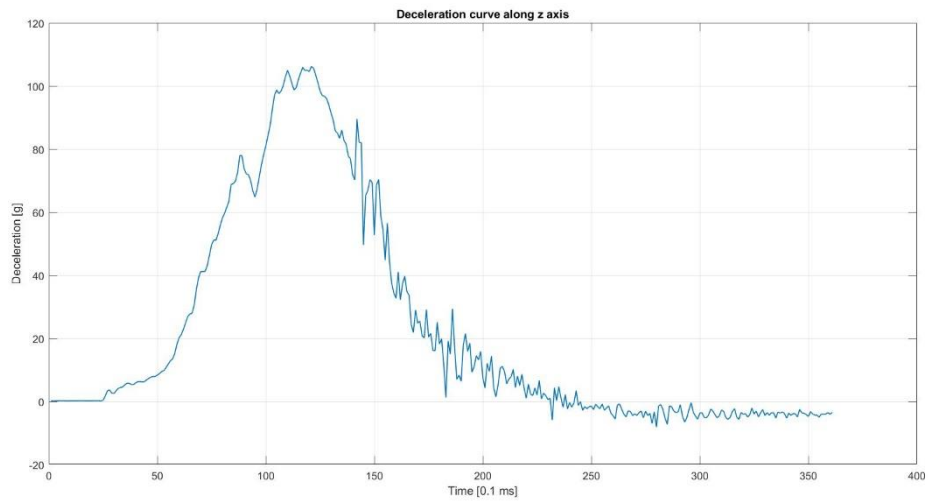


Figure 67: Deceleration curve along z axis

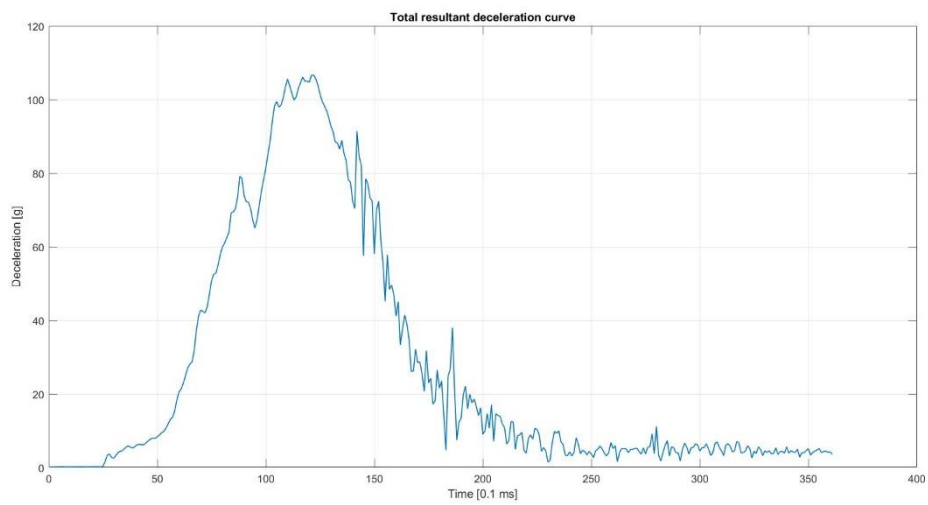


Figure 68: Total resultant deceleration curve

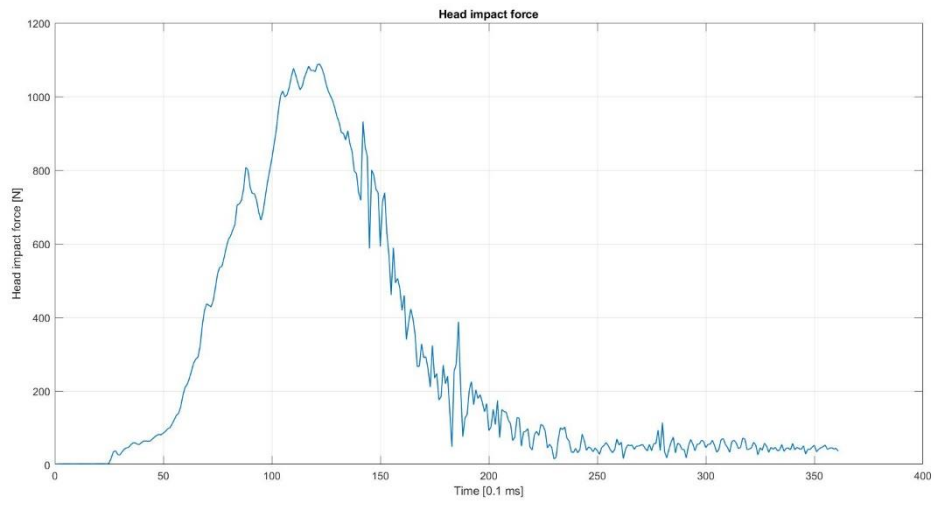


Figure 69: Head impact force

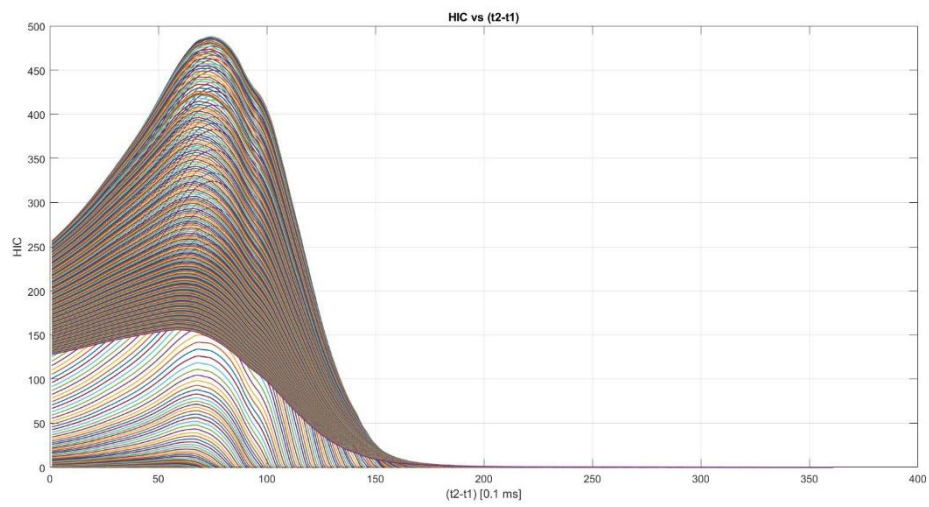


Figure 70: HIC vs  $(t_2-t_1)$

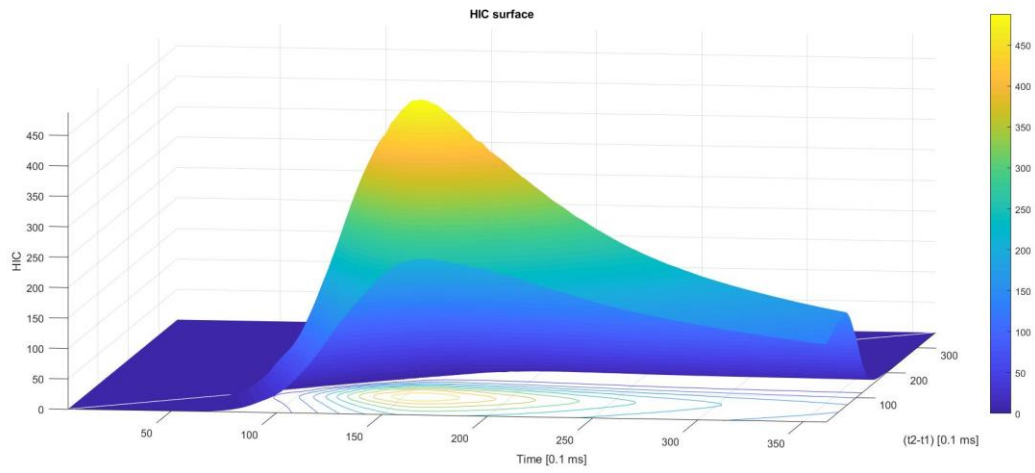


Figure 71: HIC surface

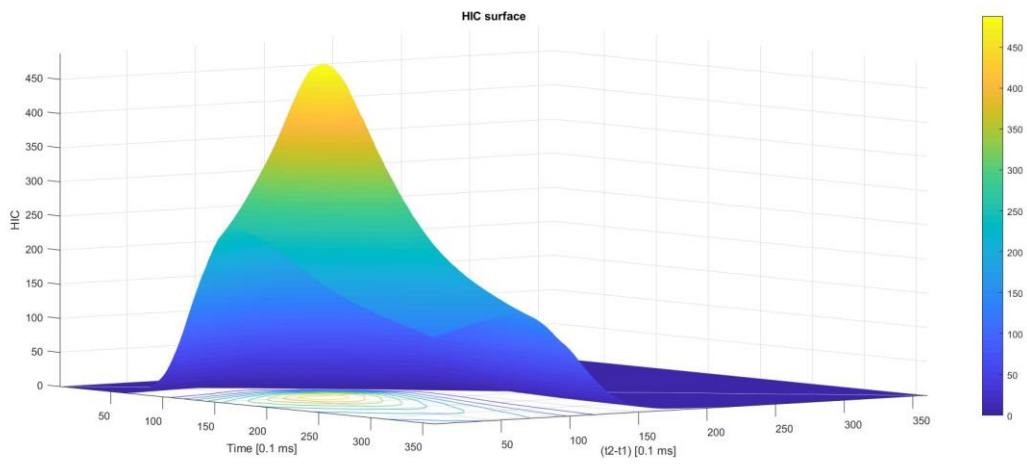


Figure 72: HIC surface

#### 4.4.2.3 Third sample (Type two):

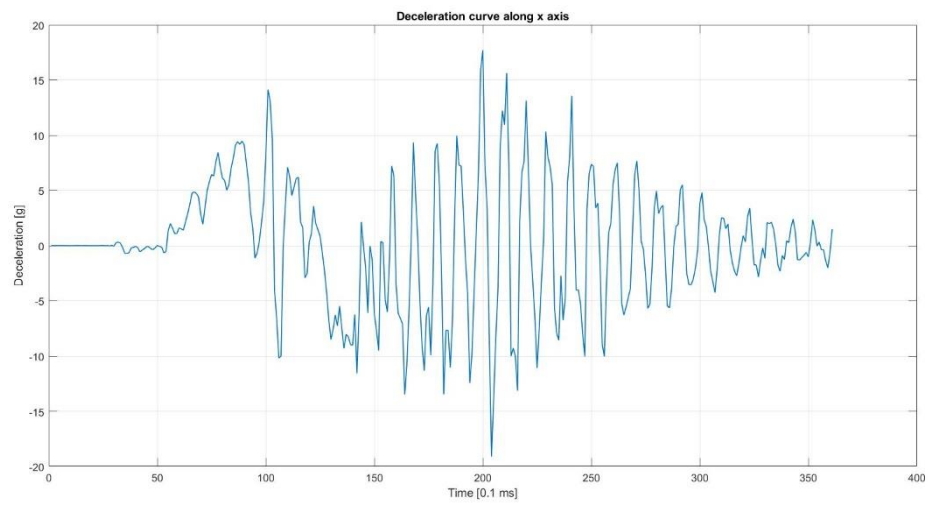


Figure 73: Deceleration curve along x axis

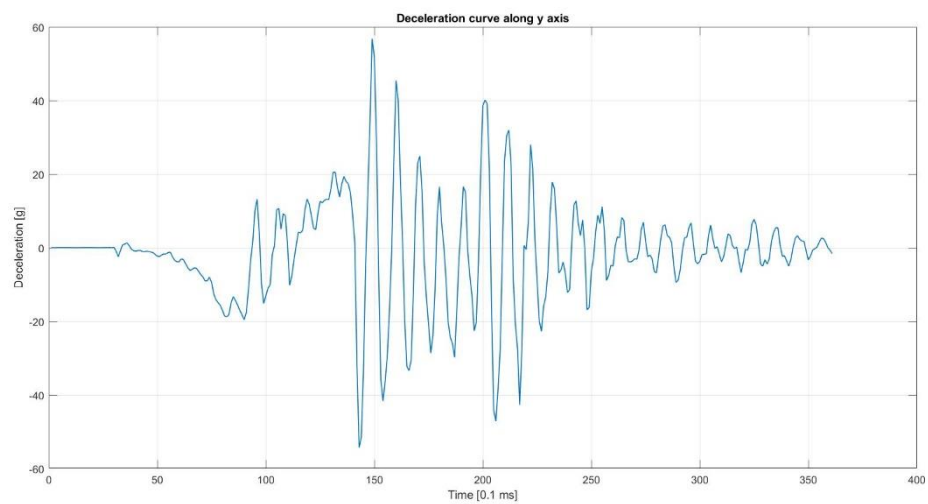


Figure 74: Deceleration curve along y axis

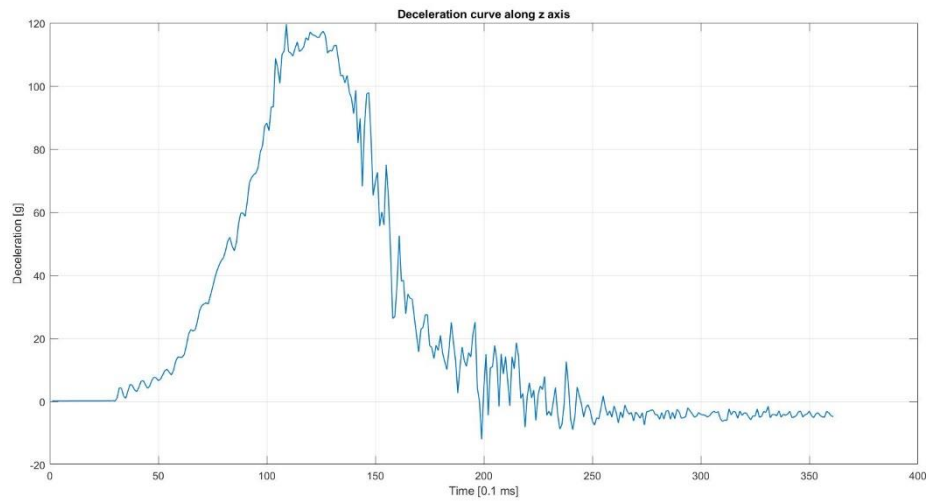


Figure 75: Deceleration curve along z axis

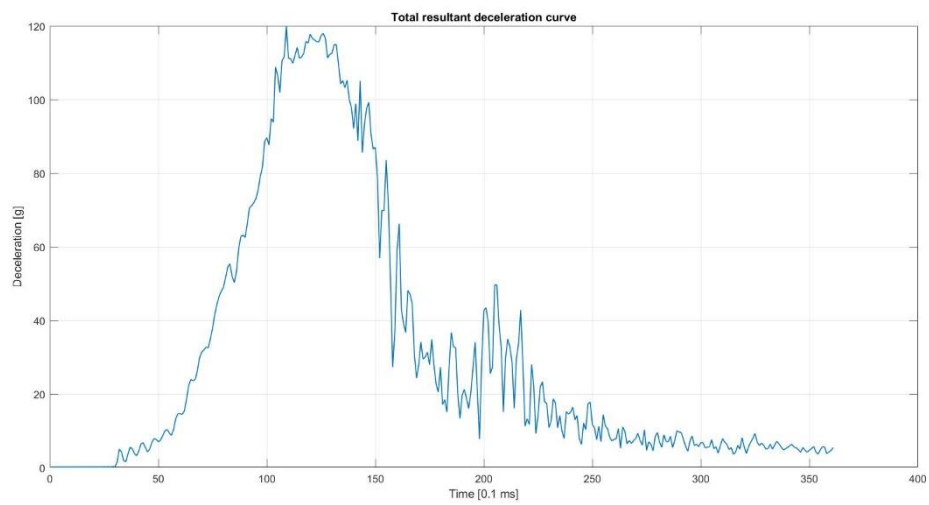


Figure 76: Total resultant deceleration curve

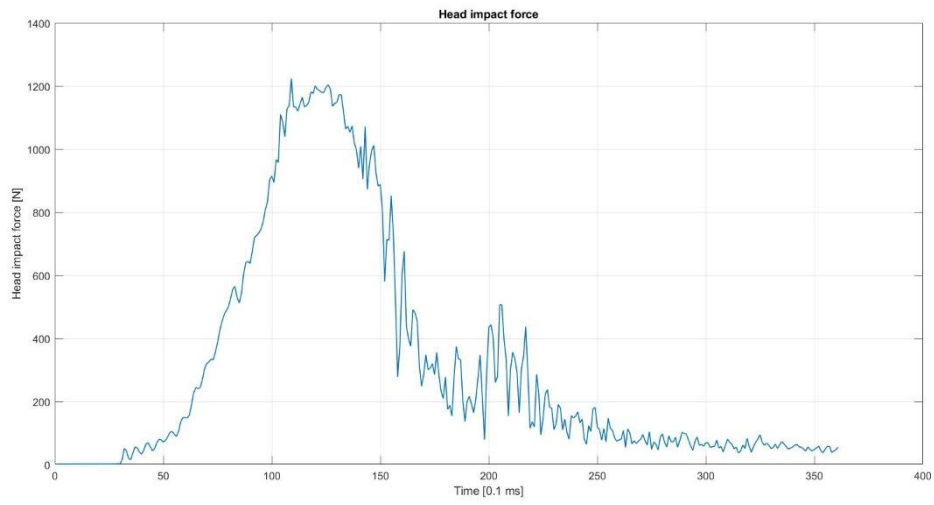


Figure 77: Head impact force

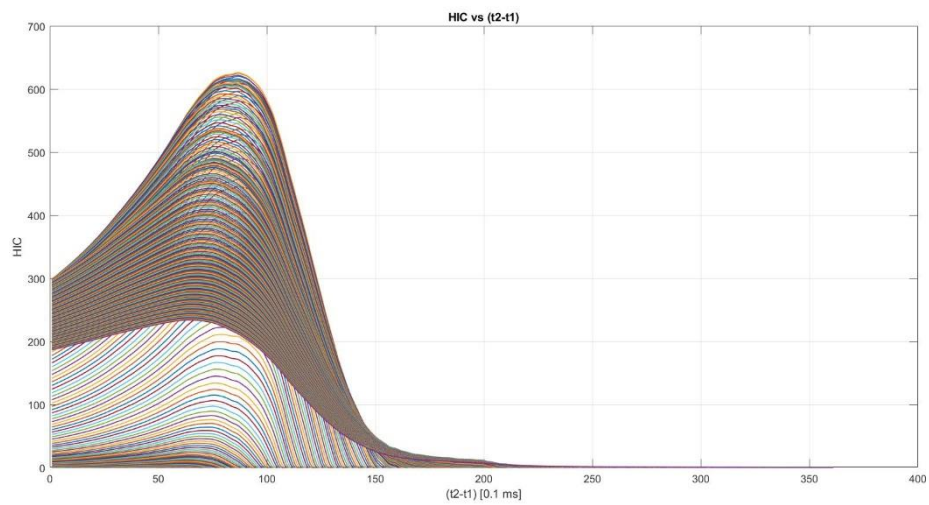


Figure 78: HIC vs  $(t_2-t_1)$

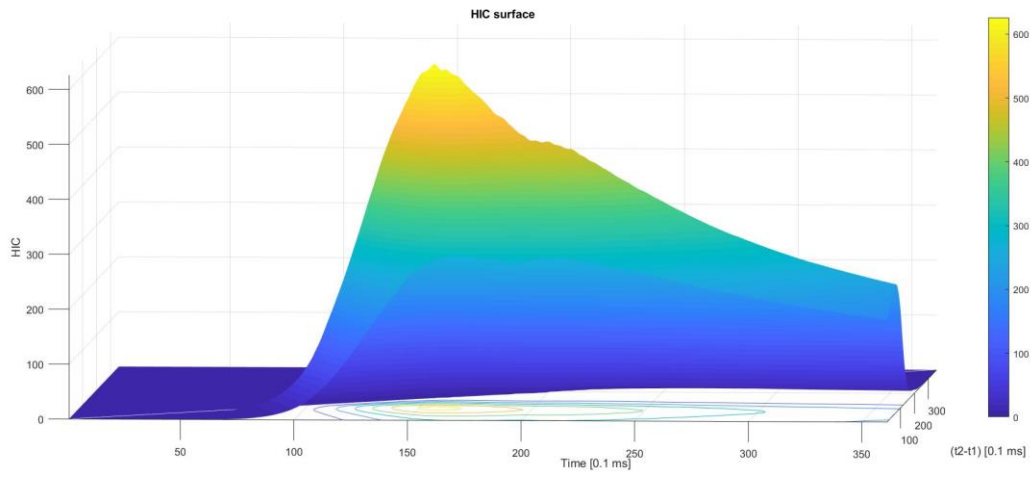


Figure 79: HIC surface

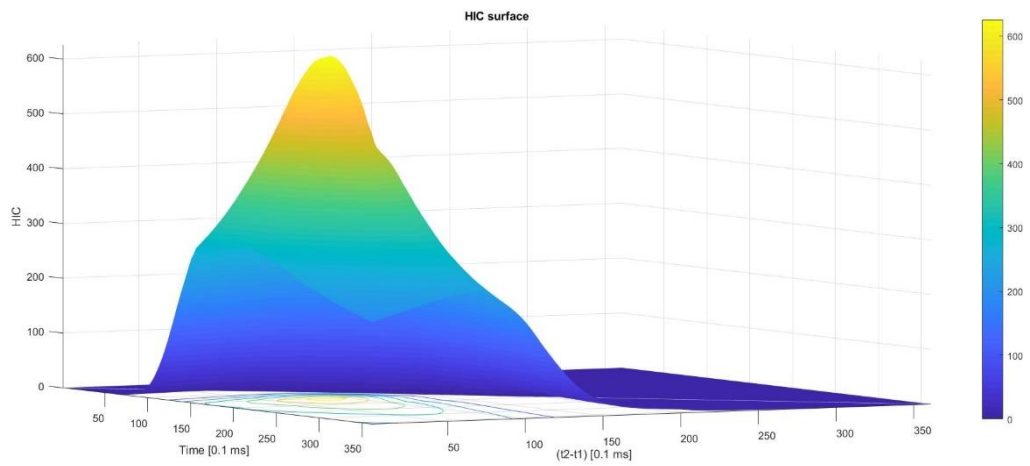


Figure 80: HIC surface

#### 4.4.2.4 Numerical results:

	<b>Sample 4</b>	<b>Sample 5</b>	<b>Sample 6</b>
<b><math>HIC_{15}</math></b>	408.3833	356.6472	470.8924
<b><math>T1_{15}</math></b>	5.4 ms	5.5 ms	6.9 ms
<b><math>T2_{15}</math></b>	20.3 ms	20.4 ms	21.8 ms
<b><math>HIC_{max}</math></b>	723.4477	487.9021	625.8713
<b><math>T1_{HIC_{max}}</math></b>	8.3 ms	7.4 ms	8.7 ms
<b><math>T2_{HIC_{max}}</math></b>	13.8 ms	15.9 ms	15.7 ms
<b><math>\Delta T_{HIC_{max}}</math></b>	5.5 ms	8.5 ms	7 ms
<b><math>Max g</math></b>	150.5624 g	106.6665 g	119.9638 g
<b><math>Impact\ velocity</math></b>	5.4249 m/s	5.4249 m/s	5.4249 m/s

Table 9: Numerical results of the three sample - type two

## 4.5 DISCUSSION OF RESULTS

First of all, the headform impact test is developed on six samples. Three samples are made of the same type of plastic compound material (type one) and the other three on the other type of material (type two).

It can be seen that both types of plastic compound glass have  $HIC_{15}$  lower than the threshold of 700. So, according to this, both types of glass have passed the HIC test, taking into account that the first type of plastic compound shows an  $HIC_{15}$  lower than the second type.

An important observation is that  $HIC_{15}$  is used and not  $HIC_{36}$  due to the fact that the impact duration of this particular type of material is very short, so the  $HIC_{15}$  is surely better suited to capture the characteristics of the impact. In fact, analysing the graphs of HIC or accelerations, the total duration of impact is included in 36,5 milliseconds. So the calculation of  $HIC_{36}$  on the 36,5 milliseconds impact range would be senseless. For this reason, the  $HIC_{max}$  is calculated on the overall impact duration to see if the  $HIC_{15}$  can be a reliable and representative index of this test.

As we wanted to prove, the  $HIC_{max}$  based on the three samples of the first compound type presents a  $\Delta T_{HIC_{max}}$  above one third of the range of  $HIC_{15}$ , so around one third of 15 milliseconds. This shows the critical issue of the use of HIC for impact tests that have a short duration like our tests. So, in our case it can be seen that  $HIC_{15}$  underestimates real-world skull fracture rates, and so for these reasons, not only the  $HIC_{15}$  is used to analyse the impact but also the Wayne Tolerance Curve that is almost reliable for very short impact duration. The relationship known as the Wayne State Tolerance Curve (WSTC) represents a connection between the acceleration magnitude and the duration of the impulse with respect to head injury. Other verifications are made by the use of the AIS and HIC correlation and ASI and HIC relations. In the following figure, the comparison of the results of the headform impact tests in the ASI and HIC correlations diagram and in the AIS and HIC relation picture can be seen.

#### 4.5.1 Analysis of first sample – type one

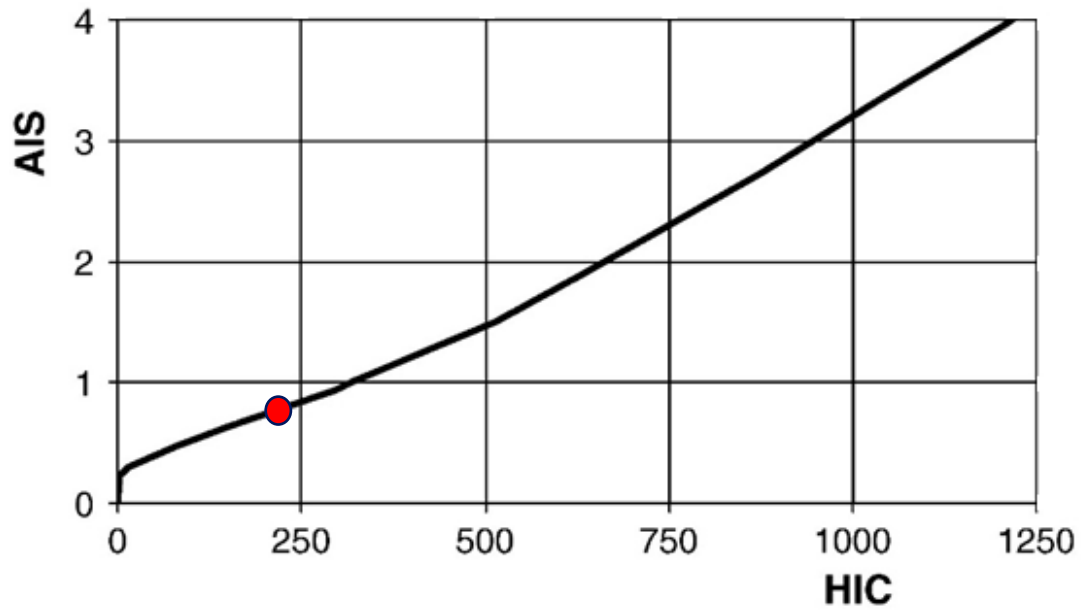


Figure 81: AIS and HIC correlation of the first sample - type one

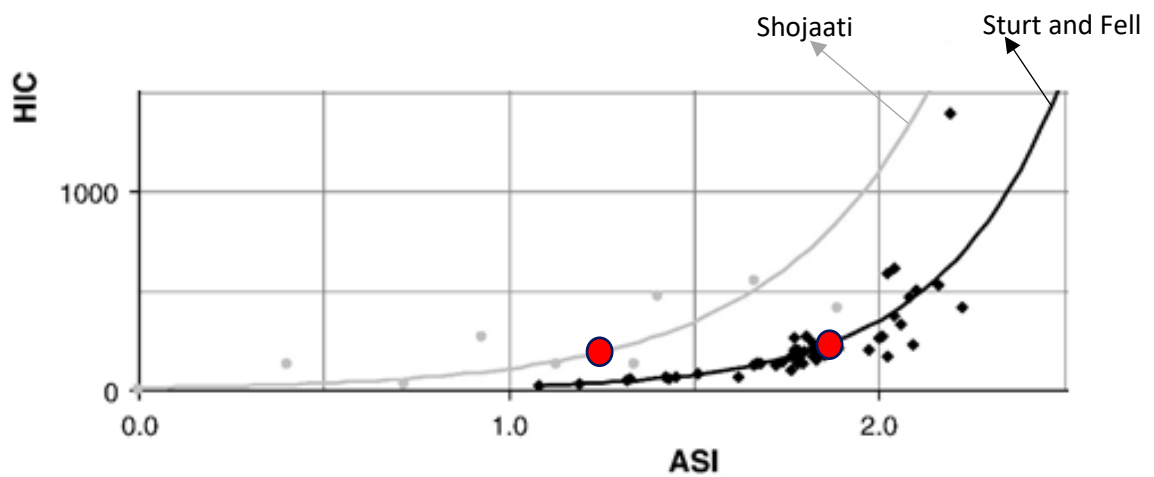


Figure 82: ASI and HIC relation of the first sample - type one

#### 4.5.2 Analysis of second sample – type one

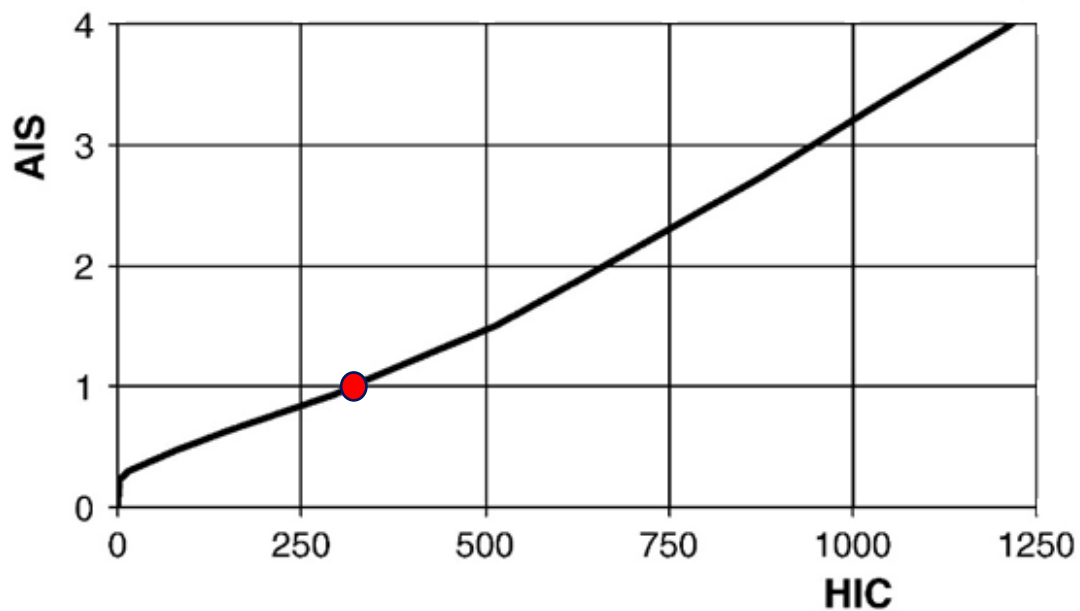


Figure 83: AIS and HIC correlation of the second sample - type one

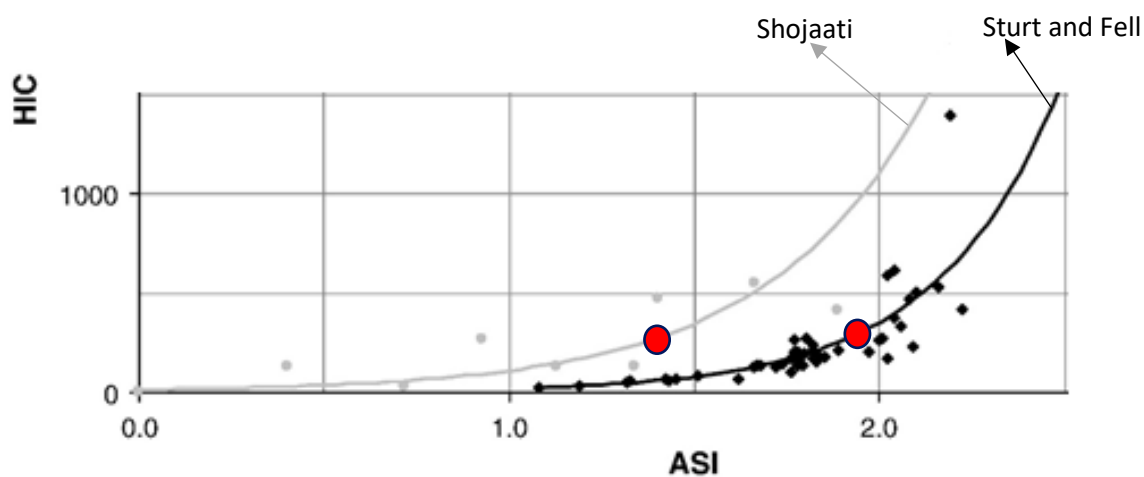


Figure 84: ASI and HIC relation of the second sample - type one

### 4.5.3 Analysis of third sample – type one

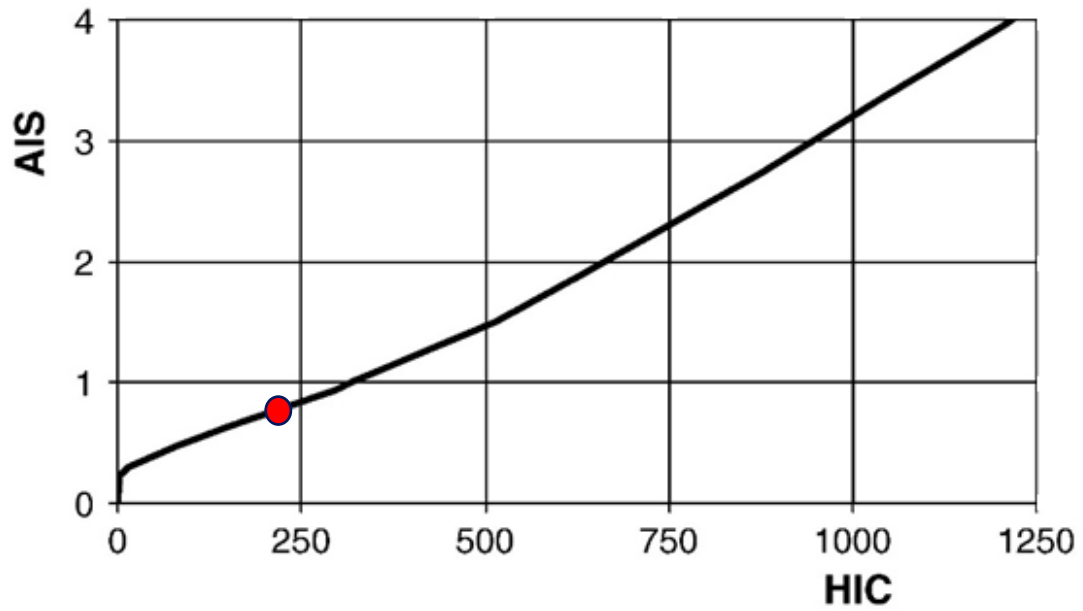


Figure 85: AIS and HIC correlation of the third sample - type one

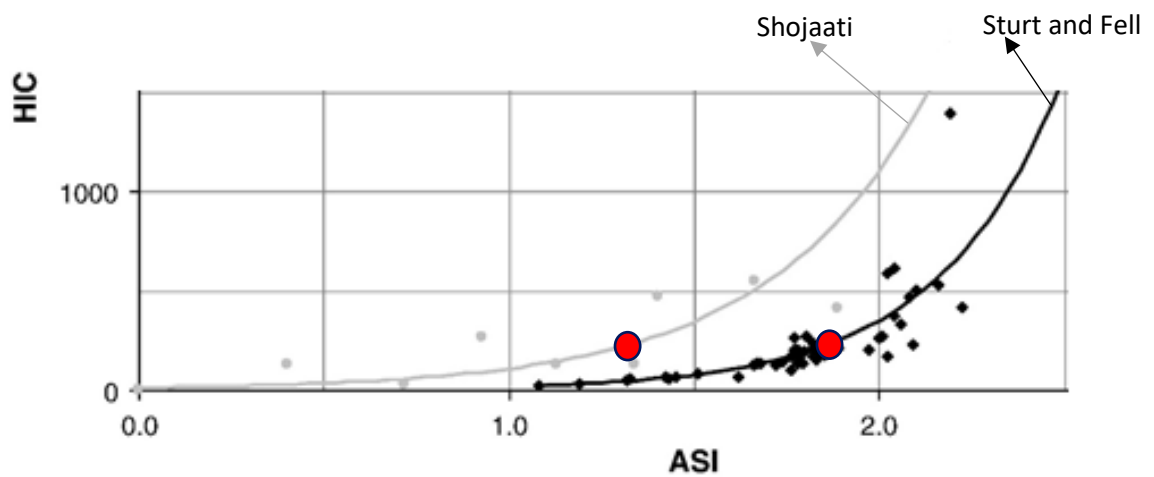


Figure 86: ASI and HIC relation of the third sample - type one

#### 4.5.4 Analysis of first sample – type two

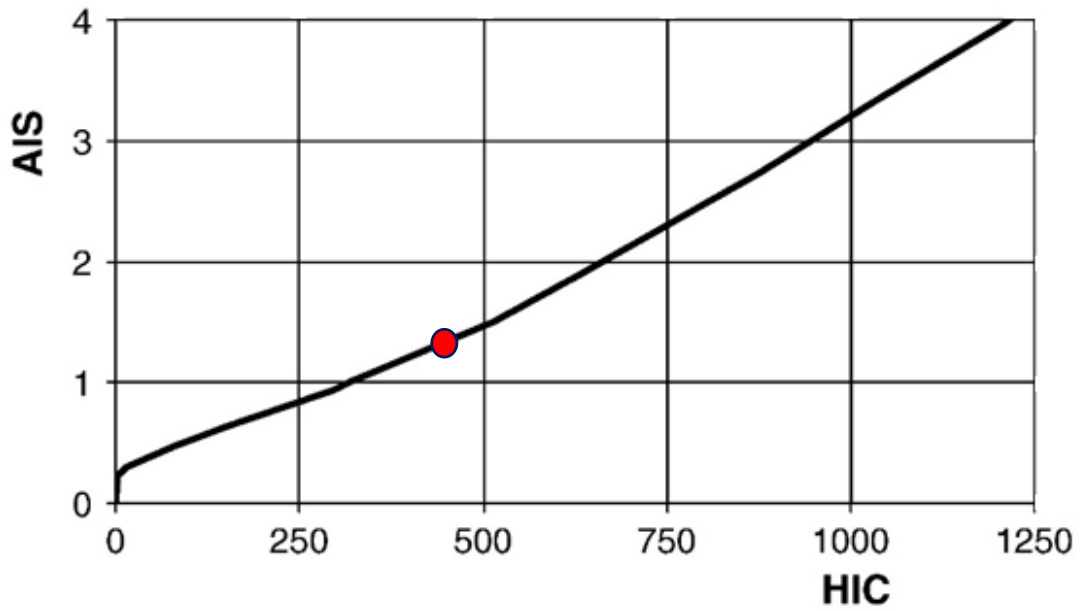


Figure 87: AIS and HIC correlation of the first sample - type two

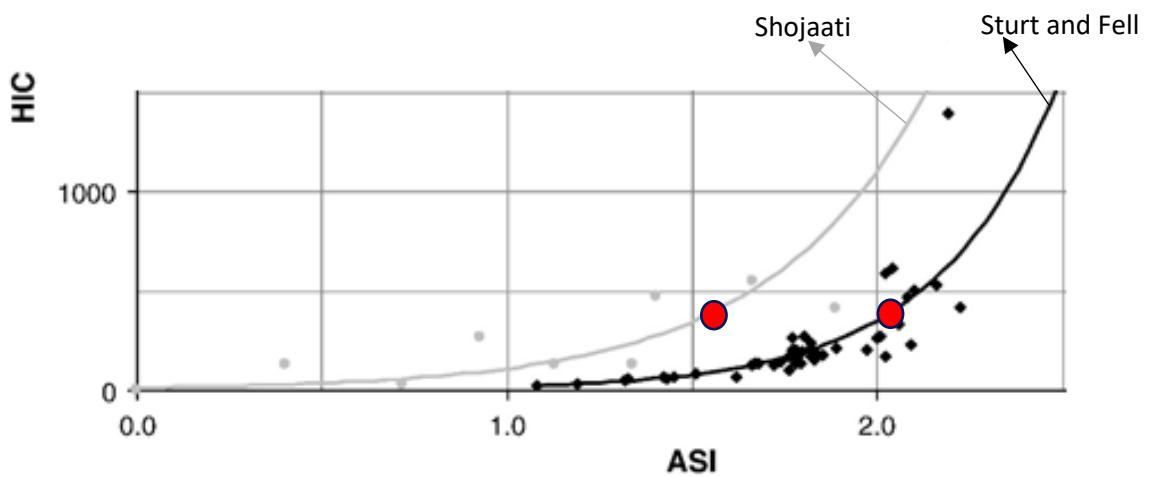


Figure 88: ASI and HIC relation of the first sample - type two

#### 4.5.5 Analysis of second sample – type two

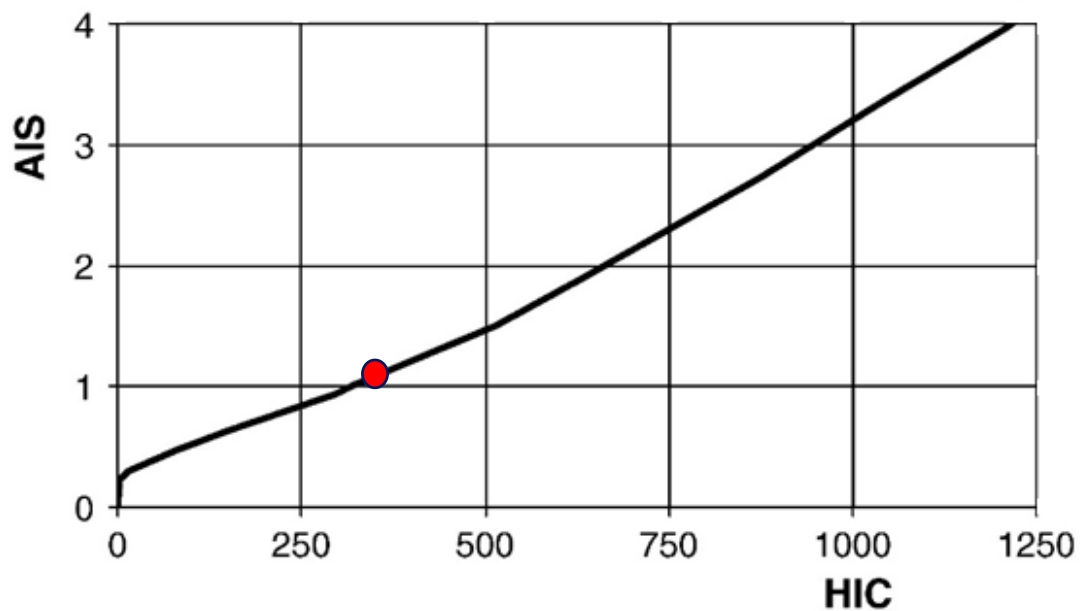


Figure 89: AIS and HIC correlation of the second sample - type two

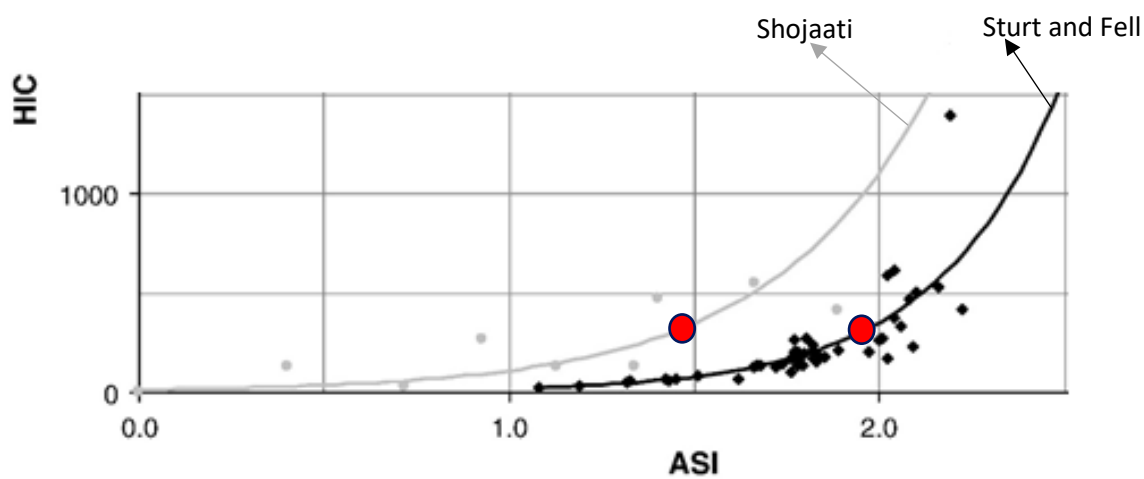


Figure 90: ASI and HIC relation of the second sample - type two

#### 4.5.6 Analysis of third sample – type two

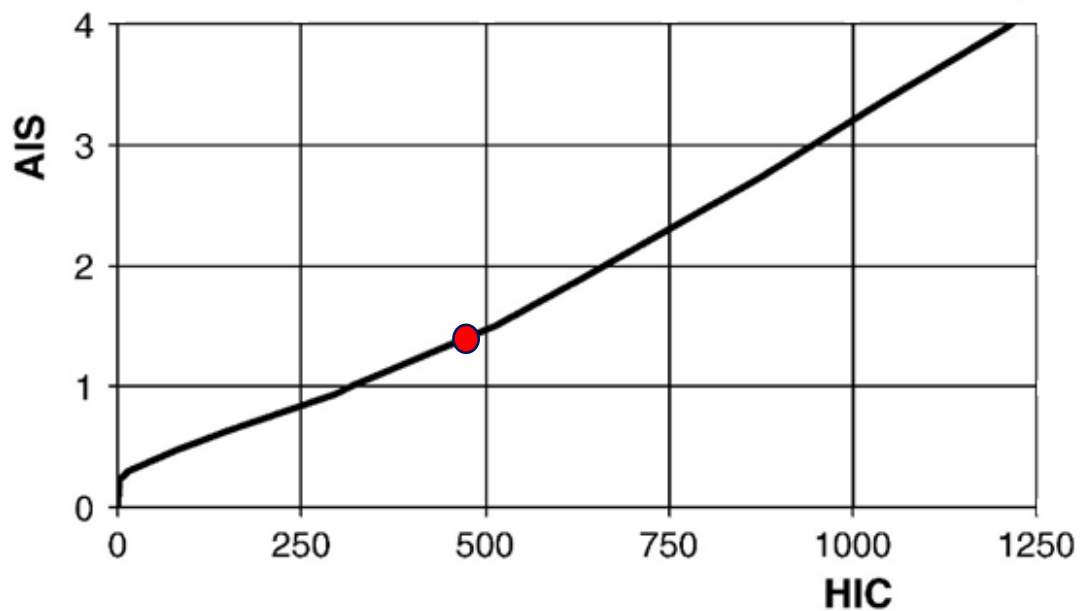


Figure 91: AIS and HIC correlation of the third sample - type two

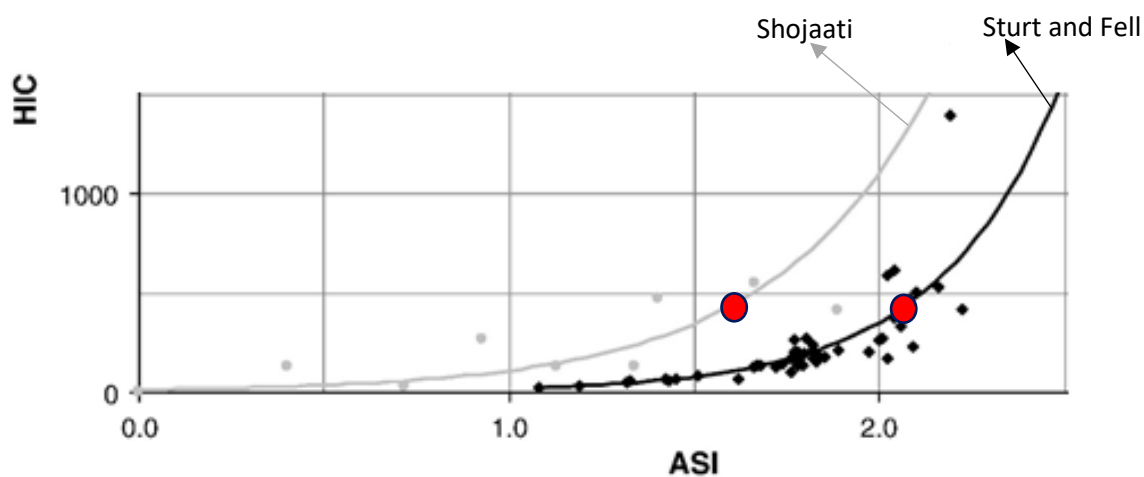


Figure 92: ASI and HIC relation of the third sample - type two

## 5 CONCLUSIONS

---

As previously exposed, the first efforts to quantify human head injury tolerance, in order to decrease losses in human lives and therefore increase research into the biomechanics of the human head crash, were based on the head kinematics from cadaver experiments. These tests constitute a portion of the Wayne State Tolerance Curve (WSTC), which links human tolerance to linear head acceleration to the impact duration. The curve was later protracted for longer durations using a combination of animal and cadaver experimental data, and non-injurious human volunteer data. This curve was interpreted and a weighted injury criterion was developed. This criterion was later converted into the Head Injury Criterion (HIC) and used in many legislations regarding homologation, certification and thus improve the crashworthiness of cars.

Despite the fact that the Head injury criterion has been very effective at reducing serious injuries and fatalities, and it still is the most established method to assess head injury in automotive impact conditions, it is heavily criticized.

One criticism that is highlighted directly through the performed headform impact tests, is the inability of the HIC based on 36 milliseconds to capture the characteristics of the impact because it under-estimates the injury a lot, as discussed in paragraph 4.5.

In fact, we have to remark that all pulses with equal average acceleration and time duration by definition have the same HIC. Due to this reason, the HIC is therefore fundamentally incapable of distinguishing between different pulses.

This is pointed out using the HIC equation,

$$HIC = \max \left\{ (t_2 - t_1) \left[ \frac{1}{(t_2 - t_1)} \int_{t_1}^{t_2} a(t) dt \right]^{2,5} \right\} \quad (9)$$

because it is a continuous mathematical function whose limits of integration may be chosen arbitrarily.

As “J. Versace” has said in “A review of Severity Index”, “it is possible that in an extremely irregular pulse, some portion of HIC could actually have a higher value than the pulse as a whole”. The fact is that for virtually any pulse, the HIC will be different when evaluated at different time intervals and at one such interval will be maximized. So, in this case, the criticism of the formulation of HIC is highly discussed. As said James A Newman, in “On the use of the head injury criterion (HIC) in protective headgear evaluation”, “this being the case, the question is which, if any, is the number that is most meaningful in terms of representing the seriousness of a particular acceleration pulse? There appears to be only two logical choices; that of the entire pulse

or that which is the maximum value attained during the pulse. These in general will not be the same.”

So, summarizing, the maximum HIC is obtained by calculating the area bounded by the acceleration pulse during a determined time interval. Hence, all acceleration curves bounded by the same time interval, having the same area, will have also the same maximum HIC. So, the maximum HIC is determined by evaluating an area not a curve shape and it is independent of curve shape and hence of rate of change of acceleration.

In conclusion, it is pointed out that the use of the HIC approach leads to apparently different tolerance levels for different head responses even when peak and average accelerations and time durations are the same and yet it does not differentiate between pulses of known differing severity.

In a similar way, it can be seen that pulses with lower average acceleration but with the same peak acceleration and time duration can have the same maximum HIC (figure 93 and figure 94).

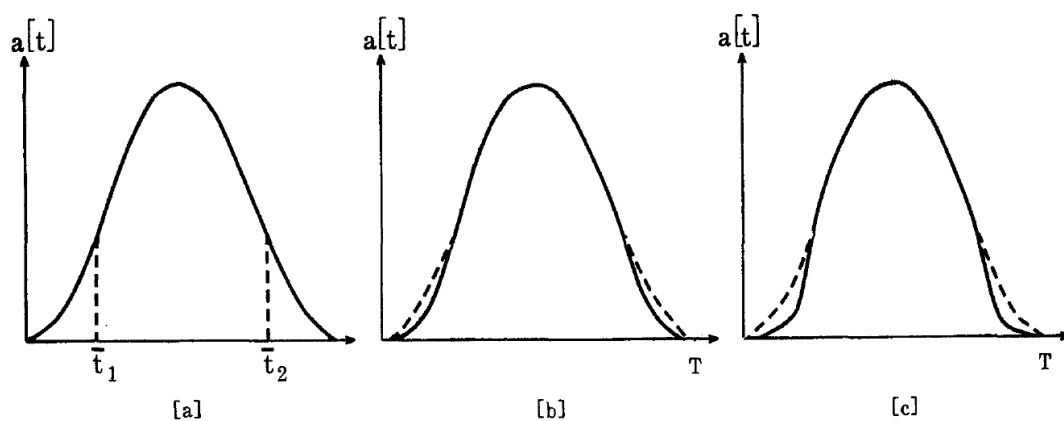


Figure 93: Distorted waveforms each of which have the same maximum HIC

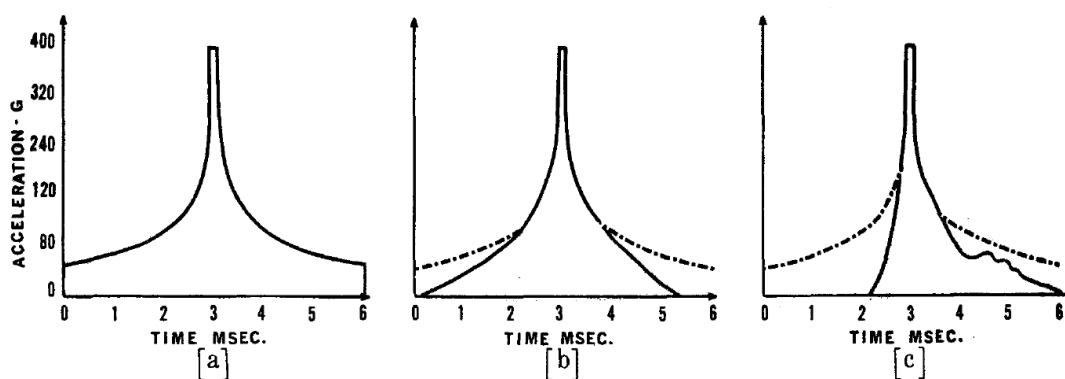


Figure 94: Distorted waveforms each of which have the same maximum HIC

We have to remark, that in all this elaboration, what is not taken into account is the rotational head kinematics because the head injury criterion are based only on linear acceleration. This represents other criticism about this injury criteria used in automotive standard tests.

The importance of rotational kinematics in brain injury is the key point of the critics of the head injury criterion. Numerous tests made with animal models were performed to clarify human tolerances to rotational acceleration. These experiments exposed that both linear and rotational motion were critical factors in order to determine brain injury severity.

In animals subject to purely translational motion, only focal lesions were seen, while diffuse injuries could be reproduced with a combination of translational and rotational motion.

This is due to the fact that the brain is mostly sensitive to rotational motion in respect to linear motion. The bulk modulus of brain tissue is approximately five orders of magnitude bigger than the shear modulus so that for a given impact it tends to deform predominantly in shear. This contributes to have a large sensitivity of the strain in the brain under rotational loading and a small sensitivity under a linear kinematics.

In order to show the difference between radial and oblique impacts, perpendicular impacts through the centre of gravity of the head and 45° oblique impacts were simulated (Figure 95). It is clearly illustrated that the radial impact lead to higher stresses in the skull with a higher risk of skull fractures, and traumatic brain injuries secondary to those.

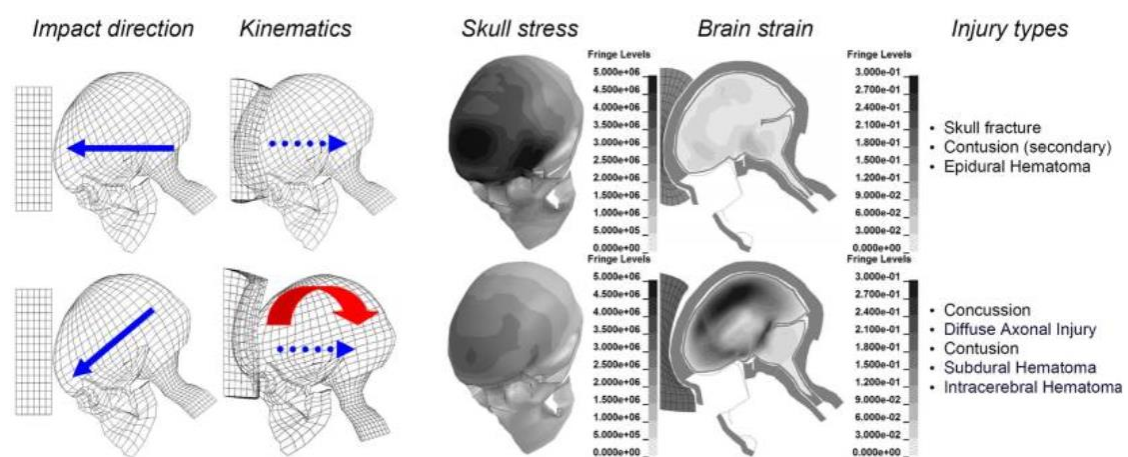


Figure 95: Illustration of the biomechanics of an oblique impact (lower), compared to a corresponding perpendicular one (upper), when impacted against the same padding using an identical initial velocity of 6.7 m/s.

So, a rotational injury criterion is proposed in order to supplement the current automotive standards based only on linear acceleration alone.

Concluding, the Head injury criterion, in some cases can be unreliable and unsatisfactory tools for evaluating the head injury. So, it is important to verify and analyse the compatibility to the regulation not only with the conventional HIC index but also with others techniques and also with the use of comparative results and curves formulated before and after the headform impact criterion, in order to obtain more reliable results.

[23,24,63,140,141]

## 6 REFERENCES

---

1. Paul Du Bois, Clifford C. Chou, Bahig B. Fileta, Tawfik B. Khalil, Albert I. King, Hikmat F. Mahmood, Harold J. Mertz, Jac Wismans, Editors: Priya Prasad and Jamel E. Belwafa, "Vehicle crashworthiness and occupant protection", sponsored by Automotive Applications Committee American Iron and Steel Institute Southfield, Michigan, 2004.
2. Shopping for Safety: Providing Consumer Automotive Safety Information, Edizione 248, National Academy Press Whashington, D.C. 1996.
3. Crash Tests and the Head Injury Criterion, HANS-WOLFGANG HENN, Submitted January 1998, accepted February 1998.
4. Teaching Mathematics and its applications, Volume 17, No. 4, 1998
5. Adnan A. Hydera, Colleen A. Wunderlich, Prasanthi Puvanachandra, G. Gururaj and Olive C. Kobusingye, "The impact of traumatic brain injuries: A global perspective", *Neuro-Rehabilitation* 22 (2007).
6. Chih-FenHu, Hueng-ChuenFan, Cheng-FuChang, Shyi-Jou, *Pediatrics & Neonatology*, Volume 54, Issue 2, April 2013.
7. R Schram, F J W Leneman, C D van der Zweep, J S H M Wismans and W J Witteman, "Assessment criteria for assessing energy absorbing Front Underrun Protection on Trucks", *ICrash* 2006.
8. Richard Sturt\* and Christina Fell, "The influence of ASI on injury risk in impacts with roadside safety barriers".
9. Manual for Assessing Safety Hardware, American Association of State Highway and Transportation Officials, 2009 .
10. C Kammel, Safety barrier performance predicted by multi-body dynamics simulation, Pages 115-125 | Published online: 24 Aug 2007.
11. Rolf Eppinger, Emily Sun, Faris Bandak, Mark Haffner, Nopporn Khaewpong, Matt Maltese, Shashi Kuppa, Thuvan Nguyen, Erik Takhounts, Rabih Tannous, Anna Zhang, Roger Saul, "Development of Improved Injury Criteria for the Assessment of Advanced Automotive Restraint Systems – II", November 1999.
12. Koji Mizuno, Hideki Yonezawa, Janusz Kajzer, "Pedestrian headform impact tests for various vehicle locations".
13. Arun Chickmenahalli, "Analysis of Different Countermeasures in Response to FMVSS 201 Upper Interior Head Impact Protection and a Comparison Study on the Injury Parameters and Energy Absorption", SAE technical paper series No. 2001-01-3058, International Body Engineering Conference and Exhibition Detroit, Michigan October 16-18, 2001.
14. Hans-wolfgang Henn, "Crash tests and the Head Injury Criterion", February 1998.
15. A. Deb, C. C. Chou, "Headform Impact Safety Design Through Simulation and Testing", SAE technical paper series No. 2003-01-1386, 2003 SAE World Congress Detroit, Michigan, March 3-6, 2003.
16. Peter J. Schuster, "Current Trends in Bumper Design for Pedestrian Impact", SAE technical paper series No. 2006-01-0464.

17. Jianping Wu and Brian Beaudet, "Optimization of Head Impact Waveform to Minimize HIC", SAE technical paper series No. 2007-01-0759, 2007 World Congress Detroit, Michigan, April 16-19, 2007.
18. Vishal P Jain and Zia A Mujawar, "Development of a Free Motion Headform Impactor", SAE technical paper series No. 2011-26-0105, 19th-21st January 2011 SIAT, India.
19. Clifford C. Chou, Gerald W . Nyquist, "Analytical Studies of the Head Injury Criterion (HIC)", SAE technical paper series No. 740082
20. C. W . Gadd, "Use of a Weighted-Impulse Criterion for Estimating Injury Hazard." Paper 660793, Proceedings of Tenth Stapp Car Crash Conference, P-12. New York: Society of Automotive Engineers, Inc., 1966.
21. L. M . Patrick, H . R . Lissner, and E . S. Gurdjian, "Survival by Design—Head Protection." Proceedings of Seventh Stapp Car Crash Conference. Springfield, III: Charles C Thomas, 1963.
22. Department of Transportation NHTSA Docket Number 69-7, Notice 19, Occupant Crash Protection-Head Injury Criteria, S6.2 of MVSS No.208.
23. James A. Newman, "On the Use of the Head Injury Criterion (HIC) in Protective Headgear Evaluation", SAE technical paper series No.751162.
24. James A. Newman, "Head Injury Criteria in Automotive Crash Testing", SAE technical paper series No. 801317.
25. Priya Prasad and Harold J. Mertz, "The Position of the United States Delegation to the ISO Working Group 6 on the Use of HIC in the Automotive Environment", SAE technical paper series No. 851246, Government/ industry Meeting & Exposition Washington, D.C., May 20 – 23 , 1985 .
26. C. C. Chou and R. J. Howell, B. Y. Chang, "A Review and Evaluation of Various HIC Algorithms", SAE technical paper series No. 8806556, International Congress and Exposition, Detroit, Michigan, February 29-March 4, 1988.
27. X. Trosseille, F. Chamouard, and C. Tarriere, "Reconsideration of the HIC, Taking into Account the Skull Bone Condition Factor (SBCF) - Limit of Head Tolerance in Side Impacts, SAE technical paper series No. 881710.
28. N.N. Ramanujam and Roger P. Daniel, Robert W. Hultman, "Preliminary Free-Motion Headform Testing of Vehicle Upper Interior Surfaces", SAE technical paper series No.911216, Government/Industry Meeting and Exposition Washington, DC May 15-17,1991.
29. Jack J. Reilly, P. Michael Miller II, "Headform Impact Testing of Plastic Glazing Materials", SAE technical paper series No. 930741, International Congress and Exposition, Detroit, Michigan, March 1-5,1993.
30. Thomas F. MacLaughlin and John F. Wiechel, Dennis A. Guenther, "Head Impact Reconstruction – HIC Validation and Pedestrian Injury Risk", SAE technical paper series No. 930895, International Congress and Exposition, Detroit, Michigan, March 1-5,1993.
31. Lorraine C. Yu and Edward L. Kowalski, Brian K. Elchison, "Material Comparisons Using Free Motion Head (FMH) Impact and Alternative Test Method", SAE technical paper series No.970165, International Congress & Exposition, Detroit, Michigan, February 24-27,1997.

32. Authority Of The United State Of America, SAE J211-1 (1995): Instrumentation for Impact Test, Part 1, Electronic Instrumentation, CFR Section(s): 72 FR 25514, May 4, 2007.
33. EEVC, "Improved Test Methods to Evaluate Pedestrian Protection Afforded by Passenger Cars", EEVC Working Group 17 Report, 1998.
34. EEVC, "Proposal for Methods to Evaluate Pedestrian Protection for Passenger Cars", EEVC Working Group 10 Report, 1994.
35. NHTSA, "Pedestrian Injury Reduction Research", Report to the Congress, 1993.
36. Igarashi, N., Yoshida, S., "Development of a Vehicle Structure with Protective Features for Pedestrians", SAE Paper 1999-01-0075.
37. K. Langwieder, "Passenger Injuries in Collisions and Their Relation to General Speed Scale", SAE Paper No. 730963, Proceedings of the Seventeenth Stapp Car Crash Conference, November 1973.
38. J.C. Marsh, R. Scott., and J.W. Melvin, "Injury Patterns by Restraint Usage in 1973 and 1974 Passenger Cars", SAE Paper No. 751143, Proceedings of the Nineteenth Stapp Car Crash Conference, November 1975.
39. J.R. Cromack, and H.H. Ziperman, "Three-Point Belt Induced Injuries: A Comparison Between Laboratory Surrogates and Real World Accident Victims", SAE Paper No. 751141, Proceedings of the Nineteenth Stapp Car Crash Conference, November 1975.
40. D.F. Huelke, T.E. Lawson, R. Scott, and J.C. Marsh, "The Effectiveness of Seat Belts in Reducing Injuries to Car Occupants", Proceedings of the Sixth IAATM International Conference, Melbourne, Australia, 1977.
41. G. Grime, "A Review of Research on the Protection Afforded to Occupants of Cars by Seat Belts Which Provide Upper Torso Restraint", Accident Analysis and Prevention, Vol. II, No. 4, December 1979, pp 293-306.
42. J.M. Henderson, and J.M. Wyllie, "Seat Belts-Limits of Protection: A Study of Fatal Injuries Among Belt Wearers", SAE Paper No. 730964, Proceedings of the Seventeenth Stapp Car Crash Conference, November 1973.
43. D. Cesari, R. Quincy, and Y. Derrien, "Effectiveness of Safety Belts Under Various Directions of Crashes", SAE Paper No. 720973, Proceedings of the Sixteenth Stapp Car Crash Conference, November 1972.
44. H. Mellander, and M. Koch, "Restraint System Evaluation - A Comparison Between Barrier Crash Tests, Sled Tests and Computer Simulations", SAE Paper No. 780605, Passenger Car Meeting, June 5-9, 1978.
45. M.J. Walsh, and D.J. Romeo, "Results of Cadaver and Anthropomorphic Dummy Tests in Identical Crash Situations", SAE Paper No. 760803, Proceedings of the Twentieth Stapp Car Crash Conference, October 1976.
46. D.H. Robbins, R.G. Snyder, J.H. McElhaney, and V.L. Roberts, "A Comparison Between Human Kinematics and the Predictions of Mathematical Crash Victim Simulators", SAE Paper No. 710849, Proceedings of the Fifteenth Stapp Car Crash Conference, November 1971.
47. C.L. Ewing, and D.J. Thomas, "Torque Versus Angular Displacement Response of Human Head to GK Impact Acceleration", SAE Paper No. 730976, Proceedings of the Seventeenth Stapp Car Crash Conference, November 1973.

48. J.P. Stapp, "Voluntary Human Tolerance Levels", Impact Injury and Crash Protection, Edited by E.S. Gurdjian, W. Lange., L.M. Patrick, and L.M. Thomas, Springfield, 111, Charles C. Thomas Publisher, 1970, p 308.
49. Department of Transportation, Motor Vehicle Safety Act, Schedule 1083, The Canada Gazette, Part 1, November 10, 1979.
50. W. Goldsmith., "The Physical Processes Producing Head Injuries", Head Injury, Edited by W.F. Caveness, and A.E. Walker, J.B. Lippincott Co., 1966, pp 350-382.
51. W. Goldsmith., "Some Aspects of Head and Neck Injury and Protection", Progress in Biomechanics, Sijthoff and Noordhoff, 1979.
52. L.M. Patrick, H.R. Lissner, and E.S. Gurdjian, "Survival by Design - Head Protection", Proceedings of the Seventh Stapp Car Crash Conference, 1963.
53. L.M. Patrick, and T.B. Sato, "Methods of Establishing Human Tolerance Levels: Cadaver and Animal Research and Clinical Observations", Impact Injury and Crash Protection, Edited by E.S. Gurdjian, W. Lange., L.M. Patrick, and L.M. Thomas.
54. V.R. Hodgson, "Physical Factors Related to Experimental Concussion", Impact Injury and Crash Protection, Edited by E.S. Gurdjian, W. Lange, L.M. Patrick, and L.M. Thomas, Charles C. Thomas Publisher, 1970, pp 275-302.
55. L.M. Thomas, "Mechanisms of Head Injury", Impact Injury and Crash Protection, Edited by E.S. Gurdjian, W. Lange., L.M. Patrick, and L.M. Thomas, Charles C. Thomas Publisher, 1970, pp 27-42.
56. E.S. Gurdjian, H.R. Lissner, F.R. Latimer, B.F. Haddad, and J.E. Webster, "Quantitative Determination of Acceleration and Intercranial Pressure in Experimental Head Injury", Neurology, Vol. 3., June 1953, pp 417-423.
57. E.S. Gurdjian, V.L. Roberts, and L.M. Thomas, "Tolerance Curves of Acceleration and Intercranial Pressure and Protective Index in Experimental Head Injury", Journal of Trauma, Pg, 600, 1964.
58. E.S. Gurdjian, V.R. Hodgson, W.G. Hardy, L.M. Patrick, and H.R. Lissner, "Evaluation of the Protective Characteristics of Helmets in Sports", Journal of Trauma, Vol. 4, 1964.
59. V.R. Hodgson, L.M. Thomas, and P. Prasad, "Testing the Validity and Limitations of the Severity Index", SAE Paper No. 700901, Proceedings of the Fourteenth Stapp Car Crash Conference, November 1970.
60. C.W. Gadd, "Use of a Weighted-Impulse Criterion for Estimating Injury Hazard", SAE Paper No. 660793, Proceedings of the Tenth Stapp Car Crash Conference, November 1966.
61. Department of Transportation NHTSA Notice 19, 36 F.R. 4600, "Occupant Crash Protection - Head Injury Criterion", S6.2 of MVSS 208, March, 1971.
62. Department of Transportation NHTSA Docket Number 69-7, Notice 19, "Occupant Crash Protection - Head Injury Criterion", S6.2 of MVSS 208.
63. J. Versace, "A Review of the Severity Index", SAE Paper No. 710881, Proceedings of the Fifteenth Stapp Car Crash Conference, November 1971.
64. J.A. Newman, "On the Use of the Head Injury Criterion (HIC) in Protective Headgear Evaluation", SAE Paper No. 751162, Proceedings of the Nineteenth Stapp Car Crash Conference, November 1975.
65. A.H.S. Holbourne, "Mechanics of the Head Injury", Lancet, Vol. 2, No. 438, October 1943.

66. F.J. Unterharnscheidt, "Translational Versus Rotational Acceleration - Animal Experiments with Measured Input", Proceedings of the Fifteenth Stapp Car Crash Conference, SAE Paper No. 710880, November 1971.
67. J.M. Abel, T.A. Gennarelli, and H. Segawa, "Incidence and Severity of Cerebral Concussion in the Rhesus Monkey Following Sagittal Plane Angular Acceleration". SAE Paper No. 780886, Proceedings of the Twenty-Second Stapp Car Crash Conference, October 1978.
68. T.A. Gennarelli, A.K. Ommaya, L.E. Thibault, "Comparison of Translational and Rotational Head Motions in Experimental Cerebral Concussion", Proceedings of the Fifteenth Stapp Car Crash Conference, November 1971.
69. T.A. Gennarelli, L.E. Thibault, and A.K. Ommaya, "Pathophysiologic Responses to Rotational and Translational Accelerations of the Head", SAE Paper No. 720970, Proceedings of the Sixteenth Stapp Car Crash Conference, November 1972.
70. A.E. Hirsch, and A.K. Ommaya, "Protection from Brain Injury% The Relative Significance of Translational and Rotational Motions of the Head After Impact", SAE Paper No. 700899, Proceedings of the Fourteenth Stapp Car Crash Conference, November 1970.
71. T.D. Clarke, CD. Gragg, J.F. Sprouffske, E.M. Trout, R.M. Zimmerman, and W.H. Muzzy, "Human Head Linear and Angular Acceleration During Impact", SAE Paper No. 710857, Proceedings of the Fifteenth Stapp Car Crash Conference, November 1971.
72. H.D. Portnoy, D. Benjamin, M. Brian, L.E. McCoy, B. Pince, R. Edgerton, and J. Young, "Intracranial Pressure and Head Acceleration During Whiplash", SAE Paper No. 700900, Proceedings of the Fourteenth Stapp Car Crash Conference, November 1970.
73. J.w. Melvin, J.H. McElhaney, and V.L. Roberts, "Evaluation of Dummy Neck Performance", Human Impact Response, Edited by W.F. King, and H.J. Mertz, Plenum Press, 1973, pp 247-262.
74. J.W. Melvin, J.H. McElhaney, and V.L. Roberts, "Improved Neck Simulation for Anthropometric Dummies", SAE Paper No. 720958, Proceedings of the Sixteenth Stapp Car Crash Conference, November 1972.
75. H.J. Mertz, R.F. Neathery, and C.C. Culver, "Performance Requirement and Characteristics of Mechanical Necks", Human Impact Response, Edited by W.F. King, and H.J. Mertz, Plenum Press, 1973, pp 17-34.
76. M.P. Haffner, and G.B. Cohen, "Progress in the Mechanical Simulation of Human Head - Neck Response", Human Impact Response, edited by W.F. King, and H.J. Mertz, Plenum Press, 1973, pp 289-320.
77. G.S. Nusholtz, J.W. Melvin, and N.M. Alem, "Head Impact Response Comparisons of Human Surrogates", SAE Paper No. 791020, Proceedings of the Twenty-Third Stapp Car Crash Conference, October 1979.
78. S.A. Shatsky, "Flash X-Ray Cinematography During Impact Injury", SAE Paper No. 730978, Proceedings of the Seventeenth Stapp Car Crash Conference, November 1973.
79. S.A. Shatsky, W.A. Alter III, D.E. Evans, V. Armbrustmacher, and G. Clark, "Traumatic Distortions of the Primate Head and Chest: Correlation of Biomechanical, Radiological and Pathological Data", SAE Paper No. 741186, Proceedings of the Eighteenth Stapp Car Crash Conference, December 1974.

80. C. Got, A. Patel, A. Fayon, C. Tarriere, and G. Walfisch, "Results of Experimental Head Impacts on Cadavers - The Various Data Obtained and Their Relations to Some Measured Physical Parameters", SAE Paper No. 780887, Proceedings of the Twenty-Second Stapp Car Crash Conference, October 1978.
81. J.D. States, H.A. Fenner, Jr., E.E. Flamboe, W.D. Nelson, and L.N. Hames, "Field Application and Research Development of the Abbreviated Injury Scale", SAE Paper No. 710873, Proceedings of the Fifteenth Stapp Car Crash Conference, November 1971.
82. A.N. Mucciardi, J.D. Sanders, and R.H. Eppinger, "Prediction of Brain Injury Measures from Head Motion Parameters", SAE Paper No. 770923, Proceedings of the Twenty-First Stapp Car Crash Conference, October 1977.
83. S. Baker, and B. O'Neill, "The Injury Severity Score: An Update", Volume 16, No. 882, Journal of Trauma, 1976.
84. D.C. Viano, and C.W. Gadd, "Significance of Rate of Onset in Impact Injury Evaluation", SAE Paper No. 751169, Proceedings of the Nineteenth Stapp Car Crash Conference, November 1975.
85. R.L. Stalnaker, J.W. Melvin, G.S. Nusholtz, N.M. Alem, and J.B. Benson, "Head Impact Response", SAE Paper No. 770921, Proceedings of the Twenty-First Stapp Car Crash Conference, October 1977.
86. Baggaley, "The Variation of Human Tolerance to Impact and Its Effect on the Design and Testing of Automotive Impact Performance", SAE Paper No. 780885, Proceedings of the Twenty-Second Stapp Car Crash Conference, October 1978.
87. R. Mattern, J. Barz, F. Schulz, D. Kallieris, and G. Schmidt, "Problems Arising When Using Injury Scales in Biomechanical Investigation with Special Consideration of the Age Influence", Fourth International IRCOBI Conference, Goteborg, Sweden, September 1979.
88. V.R. Hodgson, and L.M. Thomas, "Acceleration Induced Shear Strains in Monkey Brain Hemisection", SAE Paper No. 7910 23, Proceedings of the Twenty-Third Stapp Car Crash Conference, October 1979.
89. L.M. Patrick, "Comparison of Dynamic Response of Humans and Test Devices (Dummies)", Human Impact Response, Edited by W.F. King, and H.J. Mertz,; Plenum Press, 1973, pp 17-34.
90. J.P. Stapp, "Quantitative Correlation of Impact and Its Effects on the Living Body and its Surrogates", Proceedings of the Fifteenth Stapp Car Crash Conference, November 1971.
91. P.I. Mate, and L.E. Popp, "Third Generation of Automotive Test Dummies", SAE Paper No. 700908, Proceedings of the Fourteenth Stapp Car Crash Conference, November 1970.
92. J.F. Sprouffske, W.H. Muzzy, E.M. Trout, T.D. Clarke, and CD. Gragg, "The Effect on Data Reproducibility of Dummy Modification", SAE Paper No. 710847, Proceedings of the Fifteenth Stapp Car Crash Conference, November 1971.
93. H.T. McAdams, "The Repeatability of Dummy Performance", Human Impact Response, Edited by King, W.R., and Mertz, H.J., Plenum Press, 1973, pp 35-68.
94. R.P. Daniel, R. Trosien, and B.O. Yound, "The Impact Behavior of the Hybrid II Dummy", SAE Paper No. 751145, Proceedings of the Nineteenth Stapp Car Crash Conference, November 1975.

95. V.S. Gersbach, and P.M. Musseler, "Dummy Design and Reaction at Impact Simulation", SAE Paper No. 770262, International Automotive Engineering Congress and Exposition, Feb 28 - Mar 4, 1977.
96. U.W. Seiffert, H.K. Leyer, "Dynamic Dummy Behavior Under Different Temperature Influence", SAE Paper No. 760804, Proceedings of the Twentieth Stapp Car Crash Conference, October, 1974.
97. M. Dejeammes, and R. Quincy, "Efficiency Comparison Between Three-Point Belt and Air Bag in a Subcompact Vehicle", SAE Paper No. 751142, Proceedings of the Nineteenth Stapp Car Crash Conference, November 1975.
98. J. Harris, "The Design and Use of the TRRL Side Impact Dummy", SAE Paper No. 760802, Proceedings of the Twentieth Stapp Car Crash Conference, October 1976.
99. O.G.G. O'Connell, and R. Almqvist, "A Survey Concerning the Quality of Part 572 Hybrid II Dummies as Measuring Instruments for Crash Testing", SAE Paper No. 770263, International Automotive Engineering Congress and Exposition, Feb 28, March 4, 1977.
100. S.W. Alderson, "A New Concept in Anthropomorphic Test Dummies for Lateral Impact", SAE Paper No 790748, Passenger Car Meeting, June 11-15, 1979.
101. R.L. Stalnaker, C. Tarriere, A. Fayon, G. Walfisch, M. Balthazard, J. Masset, C. Got, and A. Patel, "Modification of Part 572 Dummy for Lateral Impact According to Biomechanical Data", SAE Paper No. 791031, Proceedings of the Twenty-Third Stapp Car Crash Conference, October 1979.
102. R.W. Lowne, S.P.F. Petty, J. Harris, and C.A. Hobbs, "The Need for a Force Measuring Dummy in Side Impact Testing", SAE Paper No. 790750, Passenger Car Meeting, June 11-15, 1979.
103. J.W. Melvin, J.H McElhaney, and V.L. Roberts, "Development of a Mechanical Model of the Human Head - Determination of Tissue Properties and Synthetic Substitute Materials", SAE Paper No. 700903, Proceedings of the Fourteenth Stapp Car Crash Conference, November 1970.
104. J.w. Melvin, and F.,G. Evans, "A Strain Energy Approach to the Mechanics of Skull Fracture", SAE Paper No. 710871, Proceedings of the Fifteenth Stapp Car Crash Conference, November 1971.
105. B.G. Master, K.J. Saczalski, "Anthropomorphic Headform Development and Simplified Technique for Impact Evaluation of Protective Headgear", ASME Paper No. 72-WA/8DHF-7, 1972.
106. R.C. Haut, C.W. Gadd, and R.G. Madeira, "Nonlinear Viscoelastic Model for Head Impact Injury Hazard", SAE Paper No. 720963, Proceedings of the Sixteenth Stapp Car Crash Conference, November 1972.
107. A. Slattenscheck, W. Tauffkirchen, and G. Benedikter, "The Quantification of Internal Head Injury by Means of the Phantom Head and the Impact Assessment Methods", SAE Paper No. 710879, Proceedings of the Fifteenth Stapp Car Crash Conference, November 1971.
108. V.R. Hodgson, M.W. Mason, and L.M. Thomas, "Head Model for Impact", SAE Paper No. 720969, Proceedings of the Sixteenth Stapp Car Crash Conference, November 1972.
109. V.R. Hodgson, "Head Model for Impact Tolerance", Human Impact Response, Edited by W.F. King, and H.J. Mertz, Plenum Press, 1973, pp 113-128.

110. National Operating Committee on Standards for Athletic Equipment, Inc., NOCSAE; "Standard Methods for Impact Test and Performance Requirements for Football Helmets", September 1973.
111. E.B. Becker, "Measurement of Mass Distribution Parameters of Anatomical Segments", SAE Paper No. 720954, Proceedings of the Sixteenth Stapp Car Crash Conference, November 1972.
112. L.B. Walker Jr., E.H. Harris, and U.R. Pontius, "Mass, Volume, Center of Mass, and Mass Movement of Inertia of Head and Head and Neck of Human Body", SAE Paper No. 730985, Proceedings of the Seventeenth Stapp Car Crash Conference, November 1973.
113. V.R. Hodgson, and L.M. Thomas, "Comparison of Head Acceleration Injury Indices in Cadaver Skull Fracture", SAE Paper No. 710854, Proceedings of the Fifteenth Stapp Car Conference, November 1971.
114. G.D. Webster, and J.A. Newman, "A Comparison of the Impact Response of Cadaver Heads and Anthropometric Headforms", Proceedings of the 20th Conference of the American Association for Automotive Medicine, Atlanta, November, 1976.
115. P.C. Begeman, A.I. King, P. Weigt, and L.M. Patrick, "Safety Performance of Asymmetric Windshields", SAE Paper No. 780900, Proceedings of the Twenty-Second Stapp Car Crash Conference, October 1978.
116. European Standard prEN 1317-2, Road Restraint Systems – Part 2: Safety barriers –Performance classes, impact test acceptance criteria and test methods, Brussels November 1995.
117. European Standard prEN 1317-1, Road Restraint Systems – Part 1: Terminology and general criteria for test methods, Brussels March 1995
118. 18th Conference of the American Association for Automotive Medicine, Revision of the Abbreviated Injury Scale (AIS)
119. NCHRP Report 350, Recommended Procedures for the Safety Performance Evaluation of Highway Features, Washington DC, 1993
120. Shojaati M. and Schueler W., ASI Measuring Method, IVT, ETH Zurich, December 2000.
121. Prasad P. and Mertz H., The Position of the United States Delegation to the ISO working group 6 on the use of HIC in the Automotive Environment, SAE technical Paper Series, 1985.
122. Gina Rablau, "Calculus in Crash Safety Tests: The Head Injury Criterion (HIC) Number, 3-22-2016.
123. Dalong Gao, and C.W. Wampler. "Head injury criterion." Robotics & Automation Magazine, IEEE 16.4 (2009): 71-74. ©2009 Institute of Electrical and Electronics Engineers.
124. Dr. M. Shojaati, IVT, ETH Zurich, "Correlation between injury risk and impact severity index ASI", STRC 03 Conference Paper Session Safety, 3rd Swiss Transport Research Conference Monte Verità / Ascona, March 19 -21, 2003.
125. Douglas Gabauer, Hampton C. Gabler, "Evaluation of the Acceleration Severity Index Threshold Values Utilizing Event Data Recorder Technology", TRB-05-2220.
126. Brian G. McHenry, "Head Injury Criterion and the ATB", 2004.
127. E/ECE/324/Rev.1/Add.42/Rev.3–E/ECE/TRANS/505/Rev.1/Add.42/Rev.3, 29 August 2012

129. DJ Searson, RWG Anderson, G Ponte, AL van den Berg, "Headform impact test performance of vehicles under the GTR on pedestrian safety", CASR REPORT SERIES CASR072, December 2009.
130. <http://www.eurailsafe.net/subsites/operas/HTML/Section3/Page3.3.1.3.htm>
131. Greenwald RM1, Gwin JT, Chu JJ, Crisco JJ., "Head impact severity measures for evaluating mild traumatic brain injury risk exposure.", *Neurosurgery*. 2008 Apr;62(4):789-98; discussion 798. doi: 10.1227/01.neu.0000318162.67472.ad.
132. Gaetano Bellavia, Gabriele Virzì Mariotti, "Development of an anthropomorphic model for vehicle-pedestrian crash test", 23-25 April, Serbia.
133. Carlos Roque, João Lourenço Cardoso, "Observations on the relationship between European standards for safety barrier impact severity and the degree of injury sustained", Portugal, 23 May 2013.
134. Akihiko Akiyama, Masayoshi Okamoto, N. Rangarajan, "Development and application of the new pedestrian dummy", Paper Number 463.
135. P. F. Gloyns Ph. D., S. J. Rattenbury Ph. D., R. O. Weller M. D., Ph. D., FRCPath., D. C. Lestina B. S., "Mechanism and patterns of head injuries in fatal frontal and side impact crashes".
136. John W. Melvin and Kathleen Weber, "Review of biomedical impact response and injury in the automotive environment", March 1085.
137. Andrew Post and T Blaine Hoshizaki, "Mechanisms of brain impact injuries and their prediction: A review", Jun 14, 2012.
138. Blaine Hoshizaki, Andrew Post, Marshall Kendall, Clara Karton and Susan Brien, "The Relationship between Head Impact Characteristics and Brain Trauma", 2013.
139. Sten Lindgren, "Modern concepts in neurotraumatology", Springer-Verlag Wien New York, May 20-23 1989, DOL: 10.1007/978-3-7091-8859-0.
140. Mellander H., HIC-the head injury criterion. Practical significance for the automotive industry, 1986.
141. Sven Kleiven, Why Most Traumatic Brain Injuries are Not Caused by Linear Acceleration but Skull Fractures are, 2013.

# 7 APPENDIX

---

## 7.1 MATLAB COMPUTATION CODE

```

clear all
close all
clc

%DATA
m=10.2; %kg
g=9.81; %m/s^2;
h=1.5; %m

%DATA READ FROM EXCEL
t=xlsread('sample_1',1,'A4:A364');
a_z_t=xlsread('sample_1',1,'B4:B364');
a_y_t=xlsread('sample_1',1,'C4:C364');
a_x_t=xlsread('sample_1',1,'D4:D364');

%RESULTING DECELERATION
a_tot=sqrt((a_x_t).^2+(a_y_t).^2+(a_z_t).^2);

%THEORETICAL IMPACT_VELOCITY CALCULATION
THEOR_IMP_VEL=sqrt(2*g*h); %m/s

%MAX g
Max_g=(max(a_tot));

%ALLOCATE NAN TO ALL CELLS OF MATRIX
HIC = nan(length(a_tot));

%SCALE FACTOR TO USE INDEXES AS A NUMBER
s_f = 0.0001;

%HEAD IMPACT FORCE
F = m*a_tot;

% HIC COMPUTATION
for i = 1:length(t)
    for j = 1:length(t)
        HIC(i,j)=(((trapz(a_tot(i:j)))/(j-i+1)))^2.5).*(((j-i+1)*s_f));
    end
end
[HIC_max,I]=max(HIC(:));

```

```

[T_1,T_2]=(ind2sub(size(HIC),I));
T1=T_1*(s_f*1000); %millisecondi
T2=T_2*(s_f*1000); %millisecondi
dt_HIC_max=(T2-T1); %millisecondi

%CALCULATE HIC 15
for i = 1:length(t)
    for j = 1:length(t)
        if (j-i+1)==150
            HIC_15(i,j)=HIC(i,j);
        end
    end
end
HIC_max_15=max(HIC_15);
[HIC_max_15,I]=max(HIC_15(:));
[T1_15,T2_15]=ind2sub(size(HIC_15),I);
T1_15=T1_15*(s_f*1000);%millisecondi
T2_15=T2_15*(s_f*1000);%millisecondi

%CONSTRAIN AND CONDITIONS
%a_x_t constrain
for i=1:length(t)
    if ((a_x_t(i))/10)<a_z_t(i)
        disp(['The acceleration components along X axis respect the constrain']);
    else
        disp(['The acceleration components along X axis NOT respect the constrain']);
    end
end

%a_y_t constrain
for i=1:length(t)
    if ((a_y_t(i))/10)<a_z_t(i)
        disp(['The acceleration components along Y axis respect the constrain']);
    else
        disp(['The acceleration components along Y axis NOT respect the constrain']);
    end
end

% Outputs
disp(['HIC max: ', num2str(HIC_max)])
disp(['Delta-t HIC max: ', num2str(dt_HIC_max),' ms'])
disp(['T1 HIC MAX: ',num2str(T1), ' ms'])
disp(['T2 HIC MAX: ',num2str(T2), ' ms'])
disp(['HIC 15: ',num2str(HIC_max_15)])
disp(['T1 15: ',num2str(T1_15), ' ms'])
disp(['T2 15: ',num2str(T2_15), ' ms'])
disp(['Max g: ', num2str(Max_g), ' g'])

```

```
disp(['Impact_velocity: ',num2str(THEOR_IMP_VEL),' m/s'])
```

```
%PLOTS
```

```
%Deceleration curve along x axis
```

```
figure(1)
plot(a_x_t,'LineWidth',1);
hold on
grid;
title('Deceleration curve along x axis');
xlabel('Time [0.1 ms]');
ylabel('Deceleration in g');
hold off
```

```
%Deceleration curve along y axis
```

```
figure(2)
plot(a_y_t,'LineWidth',1);
hold on
grid;
title('Deceleration curve along y axis');
xlabel('Time [0.1 ms]');
ylabel('Deceleration in g');
hold off
```

```
%Deceleration curve along z axis
```

```
figure(3)
plot(a_z_t,'LineWidth',1);
hold on
grid;
title('Deceleration curve along z axis');
xlabel('Time [0.1 ms]');
ylabel('Deceleration in g');
hold off
```

```
%Total resultant deceleration
```

```
figure(4)
plot(a_tot,'LineWidth',1);
hold on
grid;
title('Total resultant deceleration curve');
xlabel('Time [0.1 ms]');
ylabel('Deceleration in g');
hold off
```

```
%Head impact force
```

```
figure(5)
plot(F,'LineWidth',1);
hold on
```

```
grid;  
title('Head impact force');  
xlabel('Time [0.1 ms]');  
ylabel('Head impact force');  
hold off  
  
%HIC vs (t2-t1)  
figure(6)  
plot(HIC, 'LineWidth',1);  
hold on  
grid;  
title('HIC vs (t2-t1)');  
xlabel('(t2-t1) [0.1 ms]');  
ylabel('HIC');  
hold off  
  
% 3D hic surface  
figure(7)  
surf(HIC), shading interp, lighting gouraud  
view([-350 40])  
colorbar  
hold on  
title('HIC surface');  
xlabel('Time [0.1 ms]');  
ylabel('(t2-t1) [0.1 ms]');  
zlabel('HIC');  
hold off
```

## 7.2 TECHNICAL CHARACTERISTIC OF THE PCB ACCELEROMETER USED IN THE TESTS

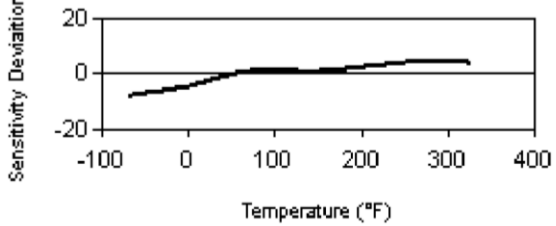
<b>Performance</b>	<b>ENGLISH</b>	<b>SI</b>	
Sensitivity(± 20 %)	1.0 mV/g	0.1 mV/(m/s <sup>2</sup> )	
Measurement Range	± 5000 g pk	± 49,050 m/s <sup>2</sup> pk	
Frequency Range(± 5 %)(y or z axis)	2 to 10,000 Hz	2 to 10,000 Hz	
Frequency Range(± 5 %)(x axis)	2 to 7000 Hz	2 to 7000 Hz	
Resonant Frequency	≥ 55 kHz	≥ 55 kHz	
Broadband Resolution(1 to 10,000 Hz)	0.03 g rms	0.29 m/s <sup>2</sup> rms	[1]
Non-Linearity	≤ 2.5 %	≤ 2.5 %	[3]
Transverse Sensitivity	≤ 5 %	≤ 5 %	
<b>Environmental</b>			
Overload Limit(Shock)	± 7000 g pk	± 68,600 m/s <sup>2</sup> pk	
Temperature Range(Operating)	-65 to +250 °F	-54 to +121 °C	[2]
Temperature Response	See Graph	See Graph	[1][2]
<b>Electrical</b>			
Excitation Voltage	18 to 30 VDC	18 to 30 VDC	
Constant Current Excitation	2 to 20 mA	2 to 20 mA	
Output Impedance	≤ 200 Ohm	≤ 200 Ohm	
Output Bias Voltage	7 to 12 VDC	7 to 12 VDC	
Discharge Time Constant	1.5 to 3.0 sec	1.5 to 3.0 sec	
Settling Time(within 10% of bias)	<10 sec	<10 sec	
Spectral Noise(1 Hz)	9000 µg/√Hz	88,290 (µm/sec <sup>2</sup> )/√Hz	[1]
Spectral Noise(10 Hz)	2500 µg/√Hz	24,525 (µm/sec <sup>2</sup> )/√Hz	[1]
Spectral Noise(100 Hz)	800 µg/√Hz	7848 (µm/sec <sup>2</sup> )/√Hz	[1]
Spectral Noise(1 kHz)	250 µg/√Hz	2453 (µm/sec <sup>2</sup> )/√Hz	[1]
<b>Physical</b>			
Sensing Element	Ceramic	Ceramic	
Sensing Geometry	Shear	Shear	
Housing Material	Titanium	Titanium	
Sealing	Hermetic	Hermetic	
Size (Height x Length x Width)	0.4 in x 0.4 in x 0.4 in	10.2 mm x 10.2 mm x 10.2 mm	
Weight	0.14 oz	4 gm	[1]
Electrical Connector	8-36 4-Pin	8-36 4-Pin	
Electrical Connection Position	Side	Side	
Mounting Thread	5-40 Female	5-40 Female	
Mounting Torque	4 to 5 in-lb	45 to 56 N-cm	



[4]

Typical Sensitivity Deviation vs Temperature



Sensitivity Deviation(%)

Temperature (°F)

*All specifications are at room temperature unless otherwise specified.  
In the interest of constant product improvement, we reserve the right to change specifications without notice.*

ICP® is a registered trademark of PCB Group, Inc.

Table 10: Technical characteristic of the PCB accelerometer used in the tests

<b>OPTIONAL VERSIONS</b>				
Optional versions have identical specifications and accessories as listed for the standard model except where noted below. More than one option may be used.				
<b>HT</b> - High temperature, extends normal operation temperatures				
Temperature Range(Operating)	-65 to +325 °F		-54 to +163 °C	
<b>J</b> - Ground Isolated				
Frequency Range(+5 %)	7 kHz		7	
Electrical Isolation(Base)	>10 <sup>8</sup> Ohm		>10 <sup>8</sup> Ohm	
Size - Height x Length x Width	0.44 in x 0.40 in x 0.44 in		11.2 mm x 10.2 mm x 11.2 mm	
Weight	0.16 oz		4.5 gm	
Mounting	Adhesive		Adhesive	
Resonant Frequency	≥ 50 kHz		≥ 50	
Supplied Accessory : Model 080A109 Petro Wax (1)				
Supplied Accessory : Model 080A90 Quick Bonding Gel (1)				
<b>NOTES:</b>				
[1] Typical.				
[2] 250° F to 325° F data valid with HT option only.				
[3] Zero-based, least-squares, straight line method.				
[4] See PCB Declaration of Conformance PS023 for details.				
<b>SUPPLIED ACCESSORIES:</b>				
Model 034K10 Cable 10FT Mini 4 Pin To (3) BNC (1)				
Model 080A Adhesive Mounting Base (1)				
Model 080A109 Petro Wax (1)				
Model 081A27 Mounting Stud (5-40 to 5-40) (1)				
Model 081A90 Mounting stud, 10-32 to 5-40 (1)				
Model ACS-1T NIST traceable triaxial amplitude response, 10 Hz to upper 5% frequency. (1)				
Model M081A27 Metric mounting stud, 5-40 to M3 x 0.50 long (1)				
Entered: AP	Engineer: JJB	Sales: WDC	Approved: JJB	Spec Number:
Date: 11/8/2013	Date: 11/8/2013	Date: 11/8/2013	Date: 11/8/2013	<b>20510</b>
 3425 Walden Avenue, Depew, NY 14043			<b>Phone: 716-684-0001</b> <b>Fax: 716-684-0987</b> <b>E-Mail: info@pcb.com</b>	

Table 11: Technical characteristic of the PCB accelerometer used in the tests

REV. DESCRIPTION		REV. DESCRIPTION		REV. DESCRIPTION		REV. DESCRIPTION		REV. DESCRIPTION		REV. DESCRIPTION		REV. DESCRIPTION		REV. DESCRIPTION		REV. DESCRIPTION		REV. DESCRIPTION																					
REV.	P.	REV.	P.	REV.	P.	REV.	P.	REV.	P.	REV.	P.	REV.	P.	REV.	P.	REV.	P.	REV.	P.																				
<p>FOR BEST RESULTS, PLACE A THIN LAYER OF SILICONE GREASE (OR EQUIVALENT) ON INTERFACE PRIOR TO MOUNTING.</p> <p>MOUNTING SURFACE SHOULD BE FLAT TO WITHIN .001 (0.003) TIR OVER DIM 'A' WITH A <math>63 \pm 1.61^\circ</math> OR BETTER FINISH FOR BEST RESULTS.</p> <p>MOUNTING SURFACE SHOULD BE FLAT TO WITHIN .001 (0.003) TIR OVER DIM 'A' WITH A <math>63 \pm 1.61^\circ</math> OR BETTER FINISH FOR BEST RESULTS.</p> <p>DRILL PERPENDICULAR TO MOUNTING SURFACE TO WITHIN <math>\pm 1^\circ</math>.</p>																																							
<p>UNLESS OTHERWISE SPECIFIED TOLERANCES ARE:</p> <table border="1"> <tr> <th colspan="2">DIMENSIONS IN INCHES</th> <th colspan="2">DIMENSIONS IN MILLIMETERS</th> </tr> <tr> <td>DECIMALS</td> <td>XX ± .01</td> <td>DECIMALS</td> <td>XX ± 0.3</td> </tr> <tr> <td>ANGLES</td> <td>± .005</td> <td>ANGLES</td> <td>± 5.0</td> </tr> <tr> <td colspan="2">FILLET AND RADI</td> <td colspan="2">FILLET AND RADI</td> </tr> <tr> <td colspan="2">.003 - .005</td> <td colspan="2">0.07 - 0.13</td> </tr> </table>																				DIMENSIONS IN INCHES		DIMENSIONS IN MILLIMETERS		DECIMALS	XX ± .01	DECIMALS	XX ± 0.3	ANGLES	± .005	ANGLES	± 5.0	FILLET AND RADI		FILLET AND RADI		.003 - .005		0.07 - 0.13	
DIMENSIONS IN INCHES		DIMENSIONS IN MILLIMETERS																																					
DECIMALS	XX ± .01	DECIMALS	XX ± 0.3																																				
ANGLES	± .005	ANGLES	± 5.0																																				
FILLET AND RADI		FILLET AND RADI																																					
.003 - .005		0.07 - 0.13																																					
<p>PCB PIEZOTRONICS 3425 WALDEN AVE, DEPEW, NY 14043 (716) 684-0001 E-MAIL: sales@pcb.com</p> <p>PCB PIEZOTRONICS 3425 WALDEN AVE, DEPEW, NY 14043 (716) 684-0001 E-MAIL: sales@pcb.com</p> <p>PCB PIEZOTRONICS 3425 WALDEN AVE, DEPEW, NY 14043 (716) 684-0001 E-MAIL: sales@pcb.com</p> <p>PCB PIEZOTRONICS 3425 WALDEN AVE, DEPEW, NY 14043 (716) 684-0001 E-MAIL: sales@pcb.com</p>																																							
<p>INSTALLATION DRAWING FOR STANDARD 081 SERIES MOUNTING</p> <p>DWG. NO. 081-XXXX-90 PART NO. 9281 SCALE: N.T.S. SHEET 1 OF 1</p>																																							
<p>ENGINEER: JBD 3/19/07 CHECKED: ECA 3/19/07 DRAWN: JDM 3/19/07</p>																																							
<p>06-XXXX-180</p>																																							
<p>STANDARD STUD MOUNT</p> <p>SENSOR MOUNTING THREAD SENSOR THREAD</p> <table border="1"> <tr> <th>MOUNTING THREAD</th> <th>SEE DRAWING</th> </tr> <tr> <td>A</td> <td>5-40</td> </tr> <tr> <td>B</td> <td>M3 X 0.50</td> </tr> <tr> <td>C</td> <td>10-32</td> </tr> <tr> <td>D</td> <td>M5 X 0.80</td> </tr> <tr> <td>E</td> <td>1/4-28</td> </tr> <tr> <td>F</td> <td>M6 X 1.00</td> </tr> </table>																				MOUNTING THREAD	SEE DRAWING	A	5-40	B	M3 X 0.50	C	10-32	D	M5 X 0.80	E	1/4-28	F	M6 X 1.00						
MOUNTING THREAD	SEE DRAWING																																						
A	5-40																																						
B	M3 X 0.50																																						
C	10-32																																						
D	M5 X 0.80																																						
E	1/4-28																																						
F	M6 X 1.00																																						
<p>"A" 5-40 MOUNTING INSTRUCTIONS (ENGLISH DIMENSIONS IN BRACKETS)</p> <p>MOUNTING HOLE PREPARATION: Ø 2.01 (Ø 2.57) X .205 (1.17) MIN. 5-40 UNC-2B X .153 (Ø 1.17) MIN.</p> <p>4.) RECOMMENDED MOUNTING TORQUE: 4-5 INCH POUNDS (45-55 NEWTON CENTIMETERS)</p>																																							
<p>"B" M3 X 0.50 MOUNTING INSTRUCTIONS (ENGLISH DIMENSIONS IN BRACKETS)</p> <p>MOUNTING HOLE PREPARATION: Ø 2.2 (Ø 2.09) X 4.6 (1.81) MIN. M3 X 0.50-6H X 3.3 (1.31) MIN.</p> <p>4.) RECOMMENDED MOUNTING TORQUE: 45-55 NEWTON CENTIMETERS (4-5 INCH POUNDS)</p>																																							
<p>"C" 10-32 MOUNTING INSTRUCTIONS (METRIC DIMENSIONS IN BRACKETS)</p> <p>MOUNTING HOLE PREPARATION: Ø 1.99 (Ø 4.04) X .23 (5.81) MIN. 10-32 UNF-2B X .15 (3.81) MIN.</p> <p>4.) RECOMMENDED MOUNTING TORQUE: 10-20 INCH POUNDS (113-225 NEWTON CENTIMETERS)</p>																																							
<p>"D" M5 X 0.80 MOUNTING INSTRUCTIONS (ENGLISH DIMENSIONS IN BRACKETS)</p> <p>MOUNTING HOLE PREPARATION: Ø 4.22 (Ø 1.68) X 7.43 (1.90) MIN. M5 X 0.8-6H X 5.08 (1.29) MIN.</p> <p>4.) RECOMMENDED MOUNTING TORQUE: 113-225 NEWTON CENTIMETERS (10-20 INCH POUNDS)</p>																																							
<p>"E" 1/4-28 MOUNTING INSTRUCTIONS (METRIC DIMENSIONS IN BRACKETS)</p> <p>MOUNTING HOLE PREPARATION: Ø 2.18 (Ø 5.54) X .300 (7.62) MIN. 1/4-28 UNF-2B X .200 (5.08) MIN.</p> <p>4.) RECOMMENDED MOUNTING TORQUE: 2-5 FOOT POUNDS (3-7 NEWTON METERS)</p>																																							
<p>"F" M6 X 0.75, M6 X 1.00, M8 X 1.25 MOUNTING INSTRUCTIONS (ENGLISH DIMENSIONS IN BRACKETS)</p> <p>M6 X 0.75 MOUNTING HOLE PREPARATION: Ø 5.31 (Ø 2.09) X 7.62 (1.90) MIN. M6 X 0.75-6H X 5.08 (1.29) MIN.</p> <p>M6 X 1.00 MOUNTING HOLE PREPARATION: Ø 6.5 (Ø 1.99) X 8.10 (2.03) MIN. M6 X 1.0-6H X 6.35 (2.50) MIN.</p> <p>M8 X 1.25 MOUNTING HOLE PREPARATION: Ø 8.75 (Ø 2.68) X 10.16 (2.57) MIN. M8 X 1.25-6H X 8.00 (1.97) MIN.</p> <p>4.) RECOMMENDED MOUNTING TORQUE: 3-7 NEWTON METERS (2-5 FT POUNDS)</p>																																							
<p>"G" MOUNTING INSTRUCTIONS FOR SPECIAL THREAD LENGTHS (METRIC DIMENSIONS IN BRACKETS)</p> <p>MOUNTING HOLE PREPARATION: Ø DRILL DIA. X C + Y MIN. X B + Y MIN. TAP X C + Y MIN. X B + Y MIN.</p> <p>1) THREAD PITCH SHOWN</p> <p>THREAD DEPTH: B = X + 1 THREAD PITCH DRILL DEPTH: C = B + 3 THREAD PITCH SEE A-F FOR APPROPRIATE DRILL AND TAP THREAD PITCH: 1/PI [P]</p>																																							
<p>"THRU-BOLT" STUD MOUNT</p> <p>THRU-BOLT SENSOR MOUNTING THREAD SENSOR THREAD</p> <table border="1"> <tr> <th>BOLT THREAD</th> <th>SEE DRAWING</th> </tr> <tr> <td>A</td> <td>M5 X 0.80</td> </tr> <tr> <td>B</td> <td>1/4-28</td> </tr> <tr> <td>C</td> <td>M6 X 1.00</td> </tr> <tr> <td>D</td> <td>M8 X 1.25</td> </tr> <tr> <td>E</td> <td></td> </tr> <tr> <td>F</td> <td></td> </tr> </table>																				BOLT THREAD	SEE DRAWING	A	M5 X 0.80	B	1/4-28	C	M6 X 1.00	D	M8 X 1.25	E		F							
BOLT THREAD	SEE DRAWING																																						
A	M5 X 0.80																																						
B	1/4-28																																						
C	M6 X 1.00																																						
D	M8 X 1.25																																						
E																																							
F																																							
<p>INTEGRAL STUD MOUNT</p> <p>INTEGRAL MOUNTING STUD</p> <table border="1"> <tr> <th>MOUNTING THREAD</th> <th>SEE DRAWING</th> </tr> <tr> <td>A</td> <td>M3 X 0.50</td> </tr> <tr> <td>B</td> <td>10-32</td> </tr> <tr> <td>C</td> <td>M5 X 0.80</td> </tr> <tr> <td>D</td> <td>1/4-28</td> </tr> <tr> <td>E</td> <td></td> </tr> <tr> <td>F</td> <td>M6 X 1.00</td> </tr> </table>																				MOUNTING THREAD	SEE DRAWING	A	M3 X 0.50	B	10-32	C	M5 X 0.80	D	1/4-28	E		F	M6 X 1.00						
MOUNTING THREAD	SEE DRAWING																																						
A	M3 X 0.50																																						
B	10-32																																						
C	M5 X 0.80																																						
D	1/4-28																																						
E																																							
F	M6 X 1.00																																						

Table 12: Technical characteristic of the PCB accelerometer used in the tests

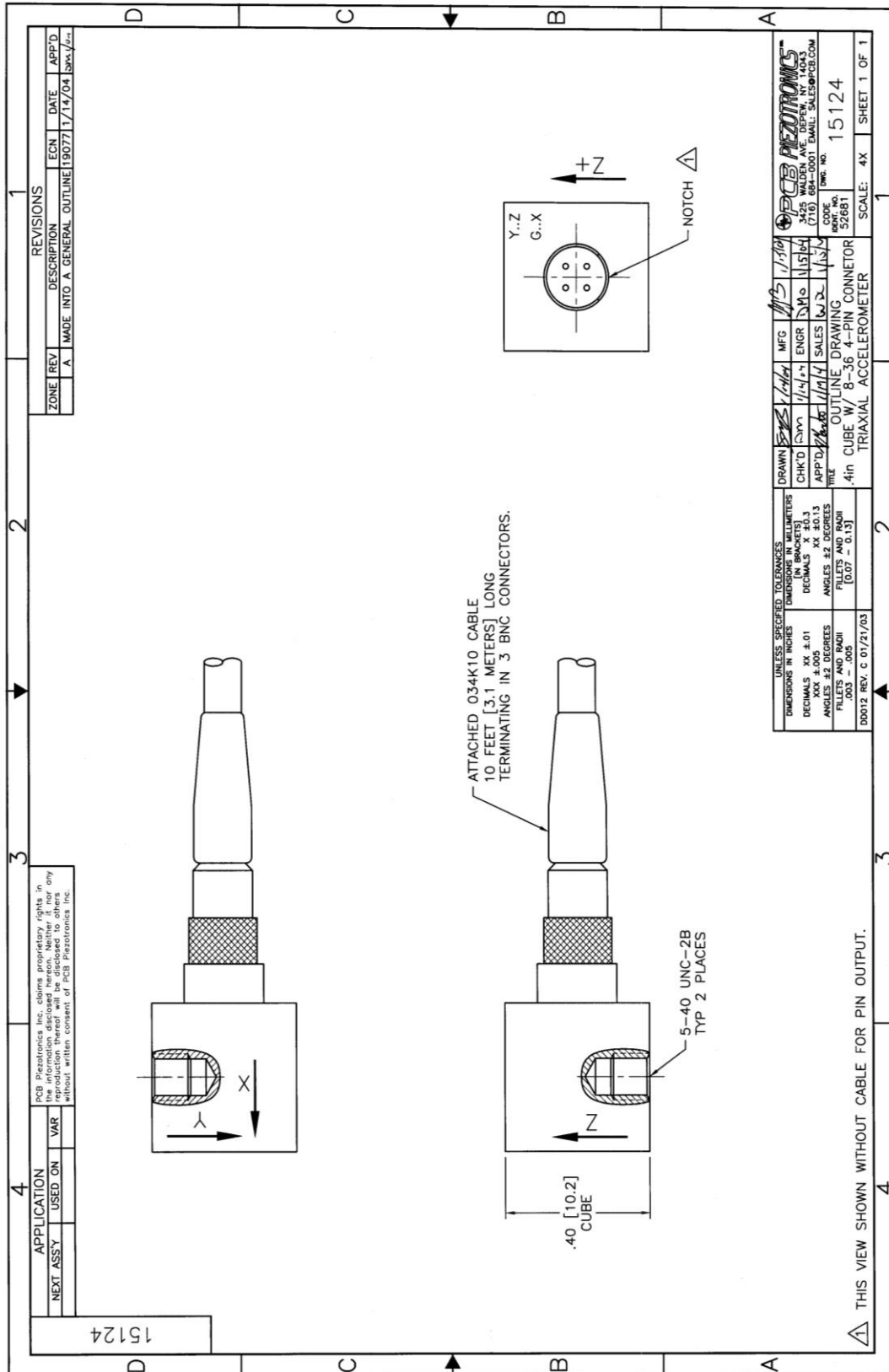


Table 13: Technical characteristic of the PCB accelerometer used in the tests